DEGRADATION OF TRICLOSAN IN WATER BY HETEROGENEOUS ADVANCED OXIDATION PROCESS ACTIVATED BY MAGNETIC NANOPARTICLES

LIN KOON YEE

Ph.D

The Hong Kong Polytechnic University

2017

The Hong Kong Polytechnic University

Department of Civil and Environmental Engineering

DEGRADATION OF TRICLOSAN IN WATER BY HETEROGENEOUS ADVANCED OXIDATION PROCESS ACTIVATED BY MAGNETIC NANOPARTICLES

LIN KOON YEE

A thesis submitted in partial fulfilment of the requirements for the degree of Doctor of Philosophy

September 2015

CERTIFICATE OF ORIGINALITY

I hereby declare that this thesis is my own work and that, to the best of my knowledge and belief, it reproduces no material previously published or written, nor material that has been accepted for the award of any other degree or diploma, except where due acknowledgement has been made in the text.

_____

LIN KOON YEE

ABSTRACT

The major aim of this dissertation is to investigate the degradation of a pharmaceutical and personal care product (PPCP) and endocrine disrupting chemical (EDC), triclosan (TCS), by an advanced oxidation process (AOP) using magnetic nanoparticles, Fe_3O_4 and $MnFe_2O_4$, especially their performance in activation of oxidants, hydrogen peroxide, peroxymonosulfate (PMS) and persulfate (PS).

Effect of different experimental parameters including pH and dosage on the TCS adsorption and degradation by Fe_3O_4 was studied. The adsorption of TCS onto Fe_3O_4 was affected by the pH of the system and the Fe_3O_4 dosage. Maximum TCS adsorption capability was observed at pH 2-6. Increase in Fe_3O_4 dosage led to increase in TCS adsorption. Fe_3O_4/PMS was found to be superior in terms of TCS degradation efficiency than Fe_3O_4/PS or Fe_3O_4/H_2O_2 especially in neutral pH range and thus become the focus of the investigation. At pH 2, both Fe(II) and Fe(III) were detected in the solution throughout the reaction, suggesting the reaction mainly proceeds through homogenous mechanism. However, no iron species were detected in the solution for the other cases with pH level above 2, and optimum treatment performances were found to be in the neutral pH range (6-9). Under these circumstances, the reactions mainly occur on or nearby the surface of Fe_3O_4 through the heterogeneous mechanism. Optimal TCS to PMS dosage was 1:25.

$MnFe_2O_4$ system was more complex than Fe_3O_4 system as $MnFe_2O_4$ alone can oxidize TCS at pH 3.3 or below likely through non-radical pathway involving the complexation

of TCS with Mn(III) on the surface of $MnFe_2O_4$ and subsequent electron transfer. The addition of PMS or PS further enhances the removal efficiency of TCS at all pH levels tested but H_2O_2 inhibits it. PMS produced the most significant improvement with the reaction time cut from 4 hours to less than 20 minutes. Effect of pH and dosages and their kinetics were studied in detail for the degradation of TCS by $MnFe_2O_4$/PS and $MnFe_2O_4$/PMS.

Optimal reaction pH for $MnFe_2O_4$/PS was 3.3 while optimum PMS and $MnFe_2O_4$ dosages were at 0.5 mM and 0.5 g/L respectively. Reaction rate decreased as pH increased. Autocatalysis was observed in $MnFe_2O_4$/PS system at pH 4.0 and above and a mathematical model was developed for pH 4.0. For $MnFe_2O_4$ /PMS system, optimal performance were at pH 5-9, and 0.5 mM PMS and 0.75 g/L $MnFe_2O_4$.

As the most efficient system in this study, $MnFe_2O_4$/PMS was also evaluated for practical application. $MnFe_2O_4$ exhibited good recyclability with improvement in degradation efficiency in the second and third cycle before stabilizing for the fourth and fifth. Besides, $MnFe_2O_4$ retained TCS degradation capability even without addition of PMS in the second cycle. Degradation of TCS was slower in secondary effluent than in distilled and deionized water (DDW).

Toxicity assessment was performed on TCS degradation by $MnFe_2O_4$ at pH 3.3 and $MnFe_2O_4$/PMS at pH 7.0. The treatment with $MnFe_2O_4$ alone at pH 3.3 exhibited lower toxicity for brine shrimp than $MnFe_2O_4$/PMS at pH 7.0. A new experimental approach was explored to eliminate the use of *in situ* oxidants to lower toxicity and take advantage of PMS superior power in TCS degradation at the same time. $MnFe_2O_4$ pre-activated by acid, PMS and PS can remove TCS at neutral pH without any *in situ* oxidants. The major degradation pathway is believed to be non-radical reactions while oxidation by sulfate radicals is considered to be the minor pathway.

ACKNOWLEDGEMENTS

I would like to express my gratitude to my thesis supervisor, Prof. Wei Chu, for his support and guidance.

I am greatly indebted to the technicians in Waters and Waste Laboratory, Mr. Wai-Shung Lam, Mr. Chi-wai Lau, Ms. Chloe Tang, and Ms. Celine Che for their technical support.

I would also like to thank Ms. Han Gong for her assistance in toxicology assessment and the following people for their generosity and assistance in instrumentation or characterization of materials:

Prof. Xiang Dong Li, Department of Civil and Environmental Engineering, The Hong Kong Polytechnic University

Ms. Carmen Ip, Department of Civil and Environmental Engineering, The Hong Kong Polytechnic University

Dr. Chi Wah Leung, Department of Applied Physics, The Hong Kong Polytechnic University

Dr. Hardy Lui, Materials Research Centre, The Hong Kong Polytechnic University

Mr. Nick K.C. Ho, Material Characterization and Preparation Facility, The Hong Kong University of Science and Technology

Finally, I am also grateful for the financial support of a research grant from the Hong Kong Polytechnic University (project no. RPTB and G-YJ95).

TABLE OF CONTENTS

Chapter One Introduction

Clean fresh water is one of the most stressed resources in the world. Many countries face water scarcity and wars are fought over the precious resources. However, in recent years, it has come to our awareness that PPCPs have made their way into natural water bodies all over the world and become emerging pollutants that could potentially threatened our delicate fresh water sources that have already been weakened due to global warming.

PPCPs refer to a wide range of products used by the public including all the veterinary and human drugs, shampoo, sunscreen, fragrance, cosmetics etc. They have been used in copious amount in everyday life for years. Only recent advances in technology makes detection of these chemicals in low or biologically-active concentration possible. Reports of their occurrence in rivers, lakes, groundwater and sediments becoming alarming. It becomes clear that conventional wastewater treatment processes are not equipped to properly treat them.

Due to their persistence through the wastewater treatment process, these contaminants often enter the environment upon discharge or sludge disposal. Some of them are directly released into water bodies through illegal discharge from factories or illicit drugs production, and runoff of pest control agents.

The presence of PPCPs in the environment is a concern for various reasons. Some of the PPCPs are acutely toxic to aquatic species and some have been found to be

endocrine disruptors. In the environment, they might be persistent or further go through biotransformation or phototransformation, sometimes into more toxic compounds, and biomagnify up the food chain. Recent studies have also shown that exposure of many organic compounds to chlorine disinfection in water treatment system can result in more toxic chlorinated disinfection by-product.

AOP has been developed to cope with the challenges posed by these recalcitrant chemicals to traditional wastewater treatment process and to safeguard our drinking water supplies. Fenton process is one of the earliest developed and studied AOPs; however, its practical application is limited due to drawbacks like pH restriction and the requirement of post-treatment. Some other AOPs such as electro-Fenton relies heavily on energy input and thus deemed far from ideal for its cost and carbon footprint. The need for better AOP and a better understanding of the transformation of PPCPs during the process is immense.

In recent years, sulfate-radical based advanced oxidation process (SR-AOP) and the use of heterogeneous catalysts has gained attention as a substitute for traditional Fenton-process. In this thesis, the degradation of a PPCP, namely Triclosan, by SR-AOP activated by magnetic particles, Fe_3O_4 and $MnFe_2O_4$, was studied. In short, the kinetics of degradation, and influence of a variety of engineering-relevant parameters such as pH and dosage was investigated.

The rationale of choosing TCS as probe compound in this study and the use of magnetic particles will be laid out in chapter two, along with the background information for TCS, literature on SR-AOP and heterogeneous catalysts.

The experimental design will be detailed in chapter three whereas the experimental results will be discussed in chapter four and five.

Chapter Two Literature Review

2.1 Probe compound – Triclosan

TCS was chosen as the probe compound in this study mainly because of its widespread use in many personal care products and it is ubiquitous in the natural environment. Its transformation in wastewater treatment facilities and natural environment is also a major concern. In recent years, studies have shown that TCS is an endocrine disrupting chemical. This section will detail the research findings regarding TCS including its occurrence and environmental fate, the health risk resulting from exposure to it or its transformation products, and effectiveness of treatment by some AOPs.

2.1.1 Basic information

TCS has anti-bacterial activity against most gram-positive and gram-negative bacteria. It inhibits the enzyme, enoyl-acyl carrier protein reductase, which is responsible for biosynthesis of fatty acid in bacteria [1]. At low concentration it is bacteriostatic, meaning it slows the growth of bacteria while at high concentration, it is bactericidal, killing the bacteria. Some properties of TCS is listed in Table 2-1.

Table 2-1: Properties of Triclosan

Formula	$C_{12}H_7Cl_3O_2$
CAS #	3380-34-5
Other names	5-Chloro-2-(2,4-dichlorophenoxy)phenol 2,4,4'-trichloro-2'-hydroxydiphenyl ether
Molecular weight	289.54 g/mol
Melting point / Boiling point	55-57°C / 180°C
Solubility in water	0.01 g/L
pKa	7.9
Octanol-water partitioning coefficient (log K_{ow})	4.8 [2]
Organic carbon-water partitioning coefficient (log K_{oc})	3.8 – 4.0
Vapor pressure	4 x 10^{-6} mmHg at 20°C
Half-life in soil	18-58 days
Half-life in aerobic condition	2.5 -35 days

2.1.2 Human Exposure

TCS is widely used in PPCPs such as toothpaste, mouthwash, deodorants, and hand sanitizer, textiles and even food packaging. It can also be found in medical devices such as sutures. Due to its widespread use, the general population can be exposed to TCS directly: through dermal contact with or direct ingestion of consumer products containing TCS; or indirectly: through the consumption of food or water that is contaminated by TCS.

TCS has been detected in 71% of the 100 urine samples collected from Athens, Greece, ranging from <0.5 – 2580 ng mL^{-1} [3]. In a study in China, TCS was also detected in 93% of the urine samples of 289 children and students [4]. And Calafat et al. (2008) detected TCS in 74.6% of the urine samples collected from U.S., concentration ranging

from 2.4 – 3790 ng mL^{-1} [5]. It was also found that TCS was present in the plasma and milk of Swedish nursing mothers, whether or not they use TCS-containing products in their daily life, with the concentration higher in mothers who used products containing TCS, which indicates that TCS is ubiquitous and direct contact is not the only exposure route [6]. In Australia, the concentration of TCS detected in the blood samples were found to be a factor of two higher than those in Sweden, and TCS was detected in 141 out of 151 human milk samples [7].

2.1.3 Potential health concern for humans and other organisms

There is increasing evidence of cellular, metabolic, hormonal and teratogenic effect of TCS from both in vitro and in vivo tests [8-14]. The lipophilic nature of TCS makes it likely to bioacculmuate in the lipid rich tissues in human. TCS has been found in human adipose tissue, liver and to a smaller extent, the brain [15].

Various studies have found TCS to be an endocrine disrupting compounds. TCS has been shown to be an endocrine disruptor to the thyroid system in amphibians [14] and mammals [16] at environmentally relevant concentrations. Another study by the USEPA also shows that TCS significantly affects the thyroid hormones concentration in male juvenile rats [17]. As for female pubertal and weanling rats, TCS was found to affect estrogen-mediated responses [18].

Studies found that TCS at everyday human exposure concentration can hinder cardiac and skeletal muscular contractions at cellular level [19] resulting in the impairment of swimming behavior in fathead minnow [20].

TCS has also been linked to a variety of negative health effects including interference of immune system with a positive association with allergy and hay fever [21]

2.1.4 Occurrence of Triclosan

TCS is among one of the most commonly detected PPCPs in the influent and effluent samples of sewage treatment plants (STPs), surface water, sediments, ground water and sometimes tap water around the world in recent years. Among the countries where the samples were collected and analyzed are Australia [22], Canada [23, 24], China [25-29], France [30], Greece [31-34], Japan [35, 36], Korea [37, 38], Spain [39-41],Taiwan [42], UK [43], US [44-48], Switzerland [49, 50], and other European Union countries [51].

2.1.4.1 Removal and Transformation of TCS in Wastewater Treatment Process

The reported removal efficiency of TCS during conventional sewage treatment process varied, ranging from 17.4% to 99% [22, 27, 33, 34, 46, 52-54].

Although high removal efficiency of TCS has been recorded in many wastewater treatment plants, the majority of TCS is far from truly removed. Due to its low water solubility and high octanol-water partitioning coefficient and high organic carbon-water coefficient, TCS is likely to be accumulated onto biosolids during wastewater treatment process. A study of a German STP showed that of the 1000 ng L^{-1} TCS in the influent, about 5% is dissolved in the effluent, 30% is adsorbed onto the sludge through weak bonds and a small amount is sorbed as bound residues. 50% is either transformed into unknown metabolites or strongly bonded to the sludge [52]. Similar fate for TCS was observed in STPs in the US. Heidler and Halden (2007) found that 50% of TCS in the influent could be detected in the sludge and 48% biotransformed or underwent unknown mechanism [46]. Lozano et al. (2013) reported that although over 97% of the TCS in the influent was removed, 64% was in fact transferred to the solids, with the majority removed during primary treatment [54].

TCS was therefore often found in high concentration in biosolids. In the U.S., the Targeted National Sewage Sludge Survey revealed TCS concentration in sludge to be 344 to 133,000 µg/kg in dry weight in samples randomly collected from 74 STPs in 35 states between 2006 and 2007 [55], and Andrade et al. (2015) found a mean TCS concentration of 16,600 µg/kg d.w. in the biosolids in a mid-Atlantic STP from 2005 to 2011 [45]. TCS was also detected in biosolids in STPs in Australia with a median of 2320 µg/kg d.w. [22], Canada – a median of 6800 µg/kg d.w. [53] and in Europe but in lower amount – 0.46 µg/kg d.w. in Greece [31], and 2469 ±132 µg/kg in UK [43].

Activated sludge process (Secondary treatment) is one of the most widely used wastewater treatment processes in STPs worldwide. During activated sludge process, Chen et al. (2015) shows that TCS is transformed to 4-chlorocatechol, 2,4-dichlorophenol (2,4-DCP), methyl-TCS, 5-hydroxy-TCS, dihydroxy-TCS and TCS-O-sulfate [56]. Among the detected intermediates, TCS-O-sulfate was found to be the most persistent in conditions carrying out the activated sludge process [56] while 2,4-DCP is one of the priority toxic pollutants listed by the USEPA in the Clean Water Act and it has been proven to be one of the dioxin precursors [57].

TCS was found to be transformed to chlorinated triclosan derivatives (CTDs) in STPs that use chlorine as disinfectant [58, 59]. Sodium Hypochlorite, which is one of the most commonly used chlorine disinfectants, is known to add chlorine to the phenol ring of TCS at the ortho- and or para- positions [60-62]. 4,5-dichloro-2-(2,4-dichlorophenoxy)phenol (4-Cl-TCS), 5,6-dichloro-2-(2,4- dichlorophenoxy)phenol (6-Cl-TCS), and 4,5,6-dichloro-2-(2,4- dichlorophenoxy)phenol (4,6-Cl-TCS) have been detected in the effluent of STPs [63] and their bio-methylated analogues were found in the carp of a bay area with heavy wastewater effluent input [64].

These CTDs are of concern mainly for two reasons:

1. Comparing to TCS, they may possess enhanced levels of antimicrobial and endocrine-disrupting properties [59];
2. In natural water, study has shown that they undergo photolysis to form respective dioxins - (2,3,7-trichlorodibenzo-p-dioxin (2,3,7-TriCDD), 1,2,8-trichlorodibenzo-p-dioxin (1,2,8-TriCDD) , and 1,2,3,8-trichlorodibenzo-p-dioxin (1,2,3,8-TriCDD)) [65, 66]. Their toxicity was estimated to be ten times higher than 2,8-

dichlorodibenzo-*p*-dioxin (2,8-DCDD), the photo-transformation product of TCS since it was believed that the toxicity of dioxin generally increases with chlorine substitution at the lateral positions.

Recent study shows that TCS goes through rapid halogenation in chlorinated waters containing halogens such as iodide and bromide. The authors found that the halogenation of TCS during chlorination by either chlorine, bromine or iodine occurs much faster in the presence of even a low level of iodide or bromide. This is a concern because (1) iodide or bromide is common electrolytes in natural water and they are likely present during the chlorination of wastewater or drinking water (2) iodinated or brominated disinfection by-products are often much more toxic than their chlorinated analogues [67, 68]. The formation of iodinated intermediates or products of TCS in the presence of both iodide and free chlorine was also reported [68].

2.1.4.2 Environmental Fate

TCS was often detected in freshwater environment and rivers receiving effluents and field soils that receives sewage sludge around the world: Canada [24] China [28, 29, 69-71], Germany [72], Hong Kong [73], Japan [35], Korea [38], Spain [41], and Switzerland [50], US [74].

Effluent

Photochemical transformation

After leaving the STPs, the TCS remained in the liquid phase is discharged into natural waters. It is believed that direct photolysis is the main degradation pathway of TCS in natural waters [50, 75]. TCS is photolytically transformed to 2,8-DCDD when exposed to natural sunlight [76, 77], with half-lives ranging from 2 - 2000 days [65, 75]. Such transformation was also observed in seawater [65]. TCS has a *pka* of about 8, and its phenolate form degrades much faster than the phenol form due to their respective UV absorbance. The phenol form does not absorb light >300 nm and sunlight emits only little below 300 nm. Thus, under the direct sunlight exposure and at pH 8, TCS is photochemically transformed to 2,8-DCDD and 2,4-DCP rapidly with half-lives of just a few hours [78].

Surfactants coexists with TCS in many PPCPs and can affect its degradation in natural environment. Study shows that the presence of cationic surfactant, cetyl trimethylammonium bromide (CTAB), was found to lower the *pKa* of TCS and thus accelerate the transformation of TCS to 2,8-DCDD under natural sunlight irradiation [79].

Computer model calculations suggest that indirect photochemical pathway may also play a role in the transformation of TCS. Besides direct photolysis, TCS may react with $OH^{\bullet}$ and triplet states of chromophoric dissolved organic matter (CDOM). Computer modelling predicted that most of the TCS in the protonated form are degraded through indirect photochemical pathway, by reacting with $OH^{\bullet}$ in low dissolved organic carbon

(DOC) water bodies and triplet states of CDOM in high DOC water bodies. As for the deprotonated form of TCS, transformation by triplet states CDOM produces higher yield of DCDD than direct photolysis. This pathway may be significant in deep water bodies with high DOC [78, 80].

Besides dioxins, Latch et al. (2005) also found that some of the TCS may have formed photocoupled products – small oligomers and polymers with TCS itself or other dissolved organic matters [78].

In natural aquatic environment, many factors such as minerals could influence the degradation of TCS. In a study carried out under simulated sunlight, the presence of Fe(III) and a basic pH were found to favor the photodegradation of TCS, and humic acids (HA), which was ubiquitous in natural waters, slow it [81].

Bioaccumulation in aquatic organisms

Bioaccumulation of TCS or its transformation products in aquatic organisms was observed in various natural water environment. TCS was found to bioaccumulate in algae in a stream that receives effluent from STPs in Texas, USA. In the samples that were taken from various sites along the stream, the algal bioaccumulation factors (BAFs) for TCS range from 900 to 2100 and for methyl-TCS 700 to 1000 [82]. Another study collected samples from various lakes in Switzerland and confirmed bioaccumulation of methyl-TCS in fish with tissue concentration ranging from 165 to 300 ng g^{-1} lipid when compared to 0.8 to 1.2 ng L^{-1} lake water [83].

Sludge

TCS sorbed onto the sludge can enter the environment via the following pathways:

1. Biosolid application

In a study of biosolids land application in Virginia, USA, significant concentration of TCS was measured in biosolids-treated agricultural soils in the year after application, between 23.6 and 66.6 ng g^{-1} [84]. Ying et al. (2007) found that TCS does not degrade fast in soil. A half-life of 108 days was recorded in aerobic condition but in anaerobic condition, it was found to be highly resistant to biodegradation [85]. Bioaccumulation of TCS in earthworm was observed [86].

Although the level of TCS decreased in field soils that received sewage sludge over time, most of it could be recovered as methyl-TCS, biotransformation products of TCS [87].

Besides being biotransformed, TCS in sludge can undergo other transformation through non-biological pathway. Ding et al. (2015) found that under near dry condition, TCS reacts with goethite and manganese oxides (MnOx), which are naturally occurring in soils and sediments, to form 2,8-DCDD, 2,4-DCP, 4-chlorobenzene-1,2-diol, 2-chloro-5-(2,4-dichlorophenoxy)benzene-1,4-diol, and 2-chloro-5-(2,4-dichlorophenoxy)-1,4-benzoquinone, whereas the presence of water inhibits the formation of 2,8-DCDD [88].

2. Disposed of at the landfills

Sludge containing TCS can end up in the leachate in landfill and contaminate ground or surface water in the vicinity. In a study in mainland China, TCS is among one of the most frequently detected PPCPs in the groundwater and reservoirs near two municipal landfills in Guangzhou [89]. TCS was also detected in wells downgradient of landfills in Indiana USA [90]. In areas where groundwater is used as drinking water, the contamination could pose direct threats to human health.

3. Incineration

Combustion of products containing TCS was found to form polychlorinated dibenzo-p-dioxins [91], which raise concerns over environmental pollution and adverse health effect resulting from the incineration of TCS-containing products.

2.1.5 Previous studies on TCS degradation

Many AOPs have been employed to more efficiently remove TCS without generating dioxins in the process, which include homogenous and heterogeneous Fenton-like process or enhanced ones that coupled with UV or electricity, ozonation, sonochemical, sonoelectrochemical processes [92-100]. 2,4-DCP, quinone and hydroquinone of TCS were among the most commonly identified intermediates during these treatment. There were also a few studies attempting to dechlorinate TCS through reduction but degradation of TCS was often followed by polymerization of intermediates. In most cases, mineralization was rarely achieved [101, 102].

Oxidation of TCS

Fenton-like process utilizing Fe^{3+} and H_2O_2 has been employed to breakdown TCS. Like traditional Fenton process, an acidic medium is required for the reaction. The detected intermediates include p-hydroquinone and p-quinone of TCS, 2,4-DCP, 4-chlorocatechol, 4,6-dichloro-1,2-benzenediol and 4,6-dichloro-1,3-benzenediol [92].

Another Fenton-like process employing $BiFeO_3$ and H_2O_2 was attempted by Song et al. (2012) to degrade TCS. About 80% removal was achieved in 180 mins and addition of the ligand EDTA further enhanced the reaction [93].

Besides the more traditional hydroxyl radical, sulfate radical generated using metal and PMS and PS was also used to decompose TCS. Regardless of metal, PMS was found to decompose TCS faster than PS [94].

Electro-Fenton using electrolytic cells for in-situ generation of OH radical to react with added Fe^{3+} as catalyst completely removed TCS in 60 mins, but a low pH was also required as in traditional Fenton process [95].

Photo-Fenton-like reaction such as Fe^{2+} and UVC has been attempted on the removal of TCS. TCS was completely degraded after 30 minutes in the combined reaction. Oxidation of C-Cl bonds was found to be the limiting factor for mineralization of TCS. The advantages of the method include not needing to add expensive H_2O_2 and reaction is sustainable in the neutral pH range [96].

TiO_2 combined with UV light was used to degrade to TCS and 2,4-DCP, quinone of TCS and hydroquinone of TCS were detected as intermediates. The addition of H_2O_2 enhances the process [97].

Ozonation treatment of TCS generates 2,4-DCP, 4-Chlorocatechol, 4-chlorororesorcinol (4-chloro-1,3-dihydroxybenzene), monohydroxy-TCS and dihydroxy-TCS. Complete removal of TCS was achieved at a TCS:ozone ratio of 1 to 5. 2,4-DCP was found to be less genotoxic than TCS [98].

Low frequency sonochemical method was employed to remove TCS in water, wastewater and seawater. TCS was degraded fastest in seawater and slowest in domestic wastewater influent. Although chloride ions are present, no formation of chlorinated and other toxic by-products. Such method leads to the thermal decomposition of TCS [99].

The combined use of sonochemical and electrochemical method, sonoelectrochemical method has also been applied in the degradation of TCS. More than 90% removal of TCS can be achieved in 15 minutes in acidic medium using Diamond coated niobium electrode. It was found that acidic condition favors the sonoelectrochemical degradation of TCS as in its molecular form, it can diffuse to the hydrophobic interfacial region of cavitation bubbles where OH radical is more concentrated than in the bulk solution more easily than its phenolate form [100].

High oxidation state molecules including ferrate (Fe(VI)) and permanganate were also used to oxidize TCS. The use of ferrate to oxidize TCS was carried out by Yang et al. (2011). The author proposed that the degradation of TCS proceeds through the scission of the ether bond and phenoxy radical addition reaction, forming chlorophenols, quinone and hydroquinone of TCS. It is also suspected that coupling reactions occur in the process and form polymeric products [103].

Jiang et al. (2009) oxidized TCS with permanganate. They found that in slightly acidic condition, MnO_2 were formed in the reaction solution, which accelerate the oxidation of TCS by Mn(VII). The phenolic moieties of TCS form a complex with Mn(IV) on the surface of MnO_2 and was quickly oxide by Mn(VII). The presence of phosphate buffer and other ligands (i.e. pyrophosphate, EDTA, and citrate) also enhanced the process. It was speculated that the ligands can stabilize reactive aqueous manganese intermediates ($Mn(INT)_{aq}$) species, which includes Mn(VI), Mn(V) and Mn(III) [104].

Besides soluble Mn, manganese oxides were also utilized for the oxidation of TCS. Just as described earlier, the formation of a precursor complex between TCS and the Mn(IV) of the MnO_2 is necessary for the electron transfer. 2,4-DCP, quinone and hydroquinone of TCS were identified as intermediates. The oxidation of 2,4-DCP was also studied and found that a dimeric product, 2-chloro-6-(2,4-dichlorophenoxy)-[1,4]benzoquinone, was formed. Acidic condition was found to be ideal for the process [105].

Reductive Dechlorination of TCS

Since 2,4-DCP, quinone and hydroquinone are the most common intermediates found in the oxidation of TCS, attempts have been made to reduce TCS in an effort to dechlorinate TCS. Bokare et al. employed an integrated nano-bio redox process to treat TCS by first reducing TCS with Pd/nFe to 2-phenoxyphenol and then use an isolated fungal enzyme, laccase, along with an redox mediator, syringaldehyde, to further breakdown 2-phenoxyphenol to phenol and catechol, which further coupled to form dimer or trimer, or polyermerized to form long chains [101].

Another attempt to reduce TCS was done by Zhang et al. (2015), employing hydrated electron generated by electron beam and a lower energy consumption counterpart, ferrocyanide ($K_4Fe(CN)_6$) activated by simulated sunlight irradiation. Although dechlorination was detected, the intermediates polymerize to form biphenyls. In addition, in the case of using simulated sunlight irradiation, direct photolysis leading to the formation of dioxins is unavoidable [102].

2.2 Advanced oxidation processes

2.2.1 Sulfate radical based advanced oxidation process (SR-AOP)

Besides the traditional Fenton reagent using H_2O_2 as the source to generate hydroxyl radicals, PMS and PS have also been used in producing sulfate radicals for the degradation of organic pollutants. Sulfate radicals have gained popularity due to several advantages over hydroxyl radicals. First, sulfate radicals are considered to demonstrate

higher oxidation potential (2.5－3.1 V vs normal hydrogen electrode (NHE)) than hydroxyl radicals (1.8 – 2.7 V vs NHE) [106]. They are also more selective for oxidation than hydroxyl radicals. They react more selectively towards organic compounds with unsaturated carbon bonds through electron transfer while hydroxyl radical might also react with a wide range of compounds through mechanisms like hydrogen abstraction or electrophilic additions [107, 108]. Third, sulfate radicals with a half-life of 30 – 40 μs were found to be more long-lasting than hydroxyl radical, which lasts for less than 1μs [109, 110] .

PMS is a component of the triple salt $2KHSO_5 \bullet KHSO_4 \bullet K_2SO_4$, which is trademarked Oxone®. PMS and PS can be activated by UV radiation [111], heat [112, 113], sonolysis [114], photolysis [108, 115, 116], metallic ions [117-121], heterogeneous catalysts such as metal oxides [122-130], and natural occurring minerals [131, 132] and other chemicals like phenols [133, 134] to form sulfate radical.

Decomposition of PMS by cobalt (II) and molybdenum (VI) as catalysts was first reported in 1958 [135]. Since then, other metallic ions have been shown to be able to activate PMS or PS as well with Co(II) and Ru(II) being the best catalyst for PMS and Ag(I) for PS [117].

2.2.2 Magnetic particles as heterogeneous catalysts for AOP

In recent years, heterogeneous catalysts have been developed to compensate the drawback of traditional Fenton process using Fe^{2+}/H_2O_2 such as the pH restriction and the requirement of post-treatment. Among them, magnetic particles, in particular, ferrites, have received a lot of attentions due to their ease of recovery and reusability.

Magnetite, Fe_3O_4, has been studied for its application in AOPs [136-140]. Zhang et al. investigated the degradation of aniline and phenol by Fe_3O_4 nanoparticles. They were completely removed after 6 hours at 308 K using Fe_3O_4 and H_2O_2 [138]. Magnetite has an inverse spinel structure and thus exhibits unique electric and magnetic properties based on the transfer of electrons between ferrous ions and ferric ions in the octahedral sites [141]. Lin and Gurol (1998) proposed that the activation of H_2O_2 on Fe_3O_4 takes place on the surface hydroxyl group, i.e. $\equiv Fe^{III}$-OH sites [142]. Yang et al. suggested a similar activation mechanism with PMS [123].

Spinel ferrites are usually represented by the formula of MFe_2O_4 where M is a metal cation, and have cubic crystal structure usually with M^{2+} occupying the tetrahedral sites and Fe^{3+} the octahedral sites. Fe_3O_4, and other ferrites especially $CoFe_2O_4$ and $CuFe_2O_4$ have been investigated for their oxidant activating efficiency and found that many can activate H_2O_2, PMS, or PS to generate hydroxyl and/or sulfate radical [123, 128, 138, 143-146]. Co^{2+} has been established as an excellent activator for PMS and thus quite a few studies investigated the performance of $CoFe_2O_4$. However, concerns over the adverse health effects of leached cobalt were repeatedly expressed. Therefore,

increasing number of studies turned to $CuFe_2O_4$ instead for the activation of PMS [125-127] or H_2O_2 [124]. Generation of hydroxyl or sulfate radicals or both were reported in such systems.

Nickel and Zinc ferrites have also been occasionally studied but their performance was usually reported to be inferior to cobalt and copper ferrite [143]. Only few studies utilized $MnFe_2O_4$, a spinel ferrite, as magnetic heterogeneous catalyst for the activation of oxidants. However, the results vary greatly from study to study. Zhang and Wu (2013) synthesized $MnFe_2O_4$ with sol-gel method and found that it could completely remove Methyl orange in four hours when H_2O_2 is added [147] and Ren et al. (2015) have reported that $MnFe_2O_4$ can induce the generation of sulfate radical from PMS for the degradation of di-n-butyl phthalate [143]. On the other hand, Zhang et al. (2013) suggest that $MnFe_2O_4$ cannot activate PMS and has no observable effect in the degradation of Iopromide [127].

Different researchers have debated over the activation mechanism of PMS by MFe_2O_4. Some have suggested the involvement of redox reaction of both M^{2+} and Fe^{3+} [124, 126] while others proposed the key role of surface hydroxyl group in the activation of PMS with Fe^{3+} too weak to participate [127].

2.2.3 Oxidation of phenolic compounds by Manganese-containing oxides

Both iron and manganese are widely distributed in surface water, soil and sediments. In nature, it was found that manganese oxides existing in Mn^{3+} and Mn^{4+} can be reduced by organic compounds and release Mn^{2+}. Stone (1987) reported the reduction and dissolution of Mn(III/IV) oxides by substituted phenols and found that the rate was enhanced by the decrease in pH [148]. In that study, he proposed a reaction mechanism that involves the formation of precursor complex between Mn and phenolic compounds followed by the electron transfer and the release of phenoxy radical and Mn(II) ions.

Zhang and Huang (2003) reported that manganese oxides can oxidize TCS through the formation of a precursor complex between Mn(IV) and TCS. The adsorption of TCS to MnO_2 and the subsequent transformation increases with decreasing pH [105].

Chapter Three Materials and Methodology

3.1 Chemicals and reagents

The magnetic nanoparticles Fe_3O_4 (<50 nm) and $MnFe_2O_4$ (60 nm) were purchased from International Laboratory USA and US Research Nanomaterials, Inc. respectively. Other chemicals used in this study is listed in Table 3-1. All chemicals were used as received without further purification. Solvents used for high performance liquid chromatography (HPLC) were of HPLC grade. DDW prepared from a Millipore Waters Milli-Q water purification system with resistivity of 18.3 MΩ·cm was used in this study. Acetonitrile (ACN) (≥ 99.9%) of HPLC grade was filtered by 0.22 μm membrane and degassed before use. Solutions of hydrochloric acid and sodium hydroxide were used for pH adjustment.

The algae Isochrysis galbana and dehydrated cysts of the brine shrimp A. salina used in Chapter 5 were purchased from Biotech Company of Jiangmen, China. I.galbana was cultured in artificial seawater (filtered through a 0.22 μm mixed cellulose esters (MCE) membrane filter and sterilized) prepared by the method modified from Kester et al. [149]. The cysts of brine shrimps were allowed to hatch in aerated seawater at 28°C with continuous illumination. After 24 h, newly hatched nauplii (Instar I stage larvae) were separated for the experimental use.

Secondary effluent was collected from Tai Po Sewage Treatment Works, Hong Kong on 30th August, 2013. It was filtered with 1 μm glass fiber filters and stored below 4°C

before use and were used within 48 hours of collection. The characteristics of the collected effluent were provided in Table 3-2.

Table 3-1 List of chemicals and reagents used in this study

Chemical name	Purity (%)	CAS No.	Molecular Weight ($g \cdot mol^{-1}$)	Formula	Manufacturer
Triclosan	99	3380-34-5	289.55	$C_{12}H_7Cl_3O_2$	ABCR
Hydrogen peroxide	35	7722-84-1	34.01	H_2O_2	Sigma Aldrich Inc.
Oxone®	99	70693-62-8	307.38	$KHSO_5 \cdot 0.5KHSO_4 \cdot 0.5K_2SO_4$	Sigma Aldrich Inc.
Sodium persulfate	99.5	7775-27-1	238.10	$Na_2S_2O_8$	International Laboratory USA
Ferrous sulfate heptahydrate	≥ 99.0	7720-78-7	278.05	$FeSO_4 \cdot 7H_2O$	Sigma Aldrich Inc.
Manganese sulfate monohydrate	98	10034-96-5	169.02	$MnSO_4 \cdot H_2O$	BDH Chemicals
1, 10-phenanthroline	≥ 99.5	5144-89-8	198.22	$C_{12}H_{10}N_2O$	Riedel-de Haën
Titanium (IV) oxide sulfate hydrate	93.0	13825-74-6	159.94	$TiOSO_4 \cdot xH_2O$	International Laboratory USA
Ethanol	Analytical grade	64-17-5	46.07	C_2H_6O	AppliChem Panreac
tert-Butanol	99.5	75-65-0	74.12	C_4H_9OH	Sigma Aldrich Inc.
Sodium chloride	≥99.0	7647-14-5	58.44	NaCl	Sigma Aldrich Inc.
Sodium nitrite	> 99.0	7632-00-0	69.00	$NaNO_2$	UNI-chemicals Ltd.

Table 3-2 Characteristics of secondary effluent collected

pH	6.65
Conductivity (mS)	17.62
Alkalinity (mg/L)	86
BOD_5 (mg/L)	3.6
COD (mg/L)	47
SO_4^{2-} (mg/L)	420
NO_2^- (mg/L)	0.034
NO_3^- (mg/L)	4.5
PO_4^{3-} (mg/L)	8.2
NH3-N (mg/L)	0.17
Cl^- (mg/L)	4590

3.2 Analytical Methods

TCS concentration was determined using HPLC (Waters) consisted of a Waters 515 HPLC pump, a Waters 2489 UV/Visible Detector and a Water 717 plus Autosampler. The chromatographic separations were performed on a Pinnacle DB C18 reversed phase column (250 mm × 4.6 mm with i.d. of 5 μm) from RESTEK. The mobile phase was composed of 80% ACN and 20% water (V/V). The flow rate was 1 mL min^{-1} and injection volumes were 10 μL. Retention time for TCS was observed at 5.7 min under the above conditions. The UV/Visible Detector was set at 280 nm.

The UV absorption spectra of the target compound were obtained using a Biochrom Libra S35 UV-visible spectrophotometer. X-ray photoelectron spectroscopy (XPS) was performed on a Physical Electronics 5600 multi-technique system. Magnetic characteristics of Fe_3O_4 and $MnFe_2O_4$ at room temperature was measured by LakeShore

7407 Vibrating Sample Magnetometer (VMS). The concentration of manganese and iron in the aqueous phase was measured by ICP-AES (Perkin Elmer Optima 3300DV) after digestion of samples. Total Organic Carbon (TOC) measurement was conducted by Shimadzu TOC-L analyzer. pH_{pzc} of $MnFe_2O_4$ was determined by acid-base titration method.

The quantification of Fe(II) was monitored by spectrophotometric method at 510 nm after adding 1,10-phenanthroline to form the reddish Fe(II)–phenanthroline complexes. The detection limit of this approach for Fe(II) was determined to around 1.8×10^{-4} mM. Ascorbic acid was added to reduce Fe(III) to Fe(II) for the quantification of total soluble iron.

The concentration of remaining PMS was analyzed using iodometric procedure described by Kolthoff and Carr [150], in which 20 mL sample was transferred to a 50 mL conical flask containing 4 g potassium iodide dissolved in 10 mL water. The flask was then sealed with paraffin and left in the dark for 30 minutes. Then 2 mL glacial acetic acid (36%) was added to the flask and the amount of evolved iodine was determined by titration with sodium thiosulfate solution. Starch indicator was used for a clear end point in the titration.

3.3 Experimental Procedures

TCS Degradation Studies

Chapter 4 (Fe_3O_4)

200 mL of TCS at 0.03 mM was premixed with a known quantity of catalyst. The mixtures were immersed in ultrasound for 30 minutes for dispersing the catalyst and allowing the adsorption reaches equilibrium between TCS and catalyst. Oxidants (H_2O_2, PMS or PS) and acid/base (for pH adjustment) were then added simultaneously to the mixture to initiate the reaction. An aliquot of the sample taken at predetermined time were then filtered through 0.22 µm filter (PTFE) for further analysis.

Chapter 5 ($MnFe_2O_4$)

Oxidants (H_2O_2, PMS or PS) were first added to TCS before pH is adjusted as some oxidant might change the pH of TCS solution. The pH-adjusted solution was then added to $MnFe_2O_4$ to initiate the reaction (In the case of studying the degradation of TCS by $MnFe_2O_4$, no oxidant is added). An aliquot of sample is then taken at predetermined time and $MnFe_2O_4$ was magnetically separated. The aqueous phase is subjected to further analysis.

Recyclability test After the first cycle, $MnFe_2O_4$ was magnetically separated and the solution was discarded. $MnFe_2O_4$ was then washed until pH is neutral. Fresh TCS was

added to the used catalyst for the subsequent cycle. Lost catalysts were compensated with fresh catalysts. Five cycles were performed.

Pre-activation of $MnFe_2O_4$ 0.025 g $MnFe_2O_4$ is pre-activated by mechanically stirred in 100 mL DDW, 1 mM PS, or 1 mM PMS, with pH adjusted to 3.0 or 7.0, for 30 minutes. Then, $MnFe_2O_4$ is magnetically separated and washed until pH is neutral. The pretreated $MnFe_2O_4$ is then added to 100 mL 0.03 mM TCS. An aliquot of sample was removed at predetermined time from the reactor and subjected to HPLC analysis.

N_2 protected experiment pH-adjusted TCS was purged with nitrogen for 1 hour before adding to $MnFe_2O_4$. The mixture is continuously purged with nitrogen during the reaction.

Toxicity Assessment Samples collected from TCS degradation experiments at predetermined time were subjected to toxicity test utilizing the mortality and vitality of A. salina. to evaluate the toxicity of TCS and degradation products. All experiments were performed in triplicate at 20 ±0.5°C and pH 7.0±0.2 in a 24-well polystyrene plate with 1 mL test solution. The test solution was diluted with 50 µL double concentrated seawater to guarantee the suitable salinity environment for the brine shrimp. Ten healthy and vivacious larvae were introduced randomly to each well of the plate. 50 µL algae I. galbana were added as diets. The number of motionless but alive larvae (motionless unless poked), swimming larvae and dead brine shrimps (completely motionless) in each well was determined under a stereomicroscope. The percentages of survival and swimming larvae were then calculated.

Chapter Four Heterogeneous activation of Peroxymonosulfate by Fe_3O_4 nanoparticles for the removal of Triclosan

4.1 Effect of three different oxidants on the degradation of TCS

Three oxidants, H_2O_2, PMS and PS were tested for their effectiveness to remove TCS using commercial Fe_3O_4 nanoparticles as catalyst. Fe_3O_4 were immersed in TCS solution and ultrasonicated for 30 minutes for better dispersal of the nanoparticles and to ensure equilibrium of TCS in between homogeneous and heterogeneous phases before the addition of oxidants. The moment of adding oxidants was defined as the time zero to initiate the reaction as shown in all the figures. The adsorptive property of Fe_3O_4 has been quantified in this process , as shown in Figure 4-1, where about 30 – 34% TCS was adsorbed by Fe_3O_4 after 30-minute of sonication. There is no significant removal and/or oxidation of TCS in Fe_3O_4/H_2O_2 and Fe_3O_4/PS processes besides adsorption, where the observed fluctuation is likely due to the continuing adsorption, desorption and competition of adsorption sites among the TCS and oxidants in the system. Upon the use of PMS, it was interesting to note that almost all the TCS was removed in 60 minutes. PMS was reported to be more universal than both H_2O_2 and PS when coupled with transition metal in a homogenous reaction, especially at neutral pH levels [117]. PMS was also found to be a more effective oxidant than PS when coupled specifically with Fe(II) [151]. The result also agreed with previous studies, suggesting the Fe_3O_4 / H_2O_2 system is inefficient at neutral pH range [138, 140]. In light of this result, this study was focused on the removal of TCS in Fe_3O_4/PMS.

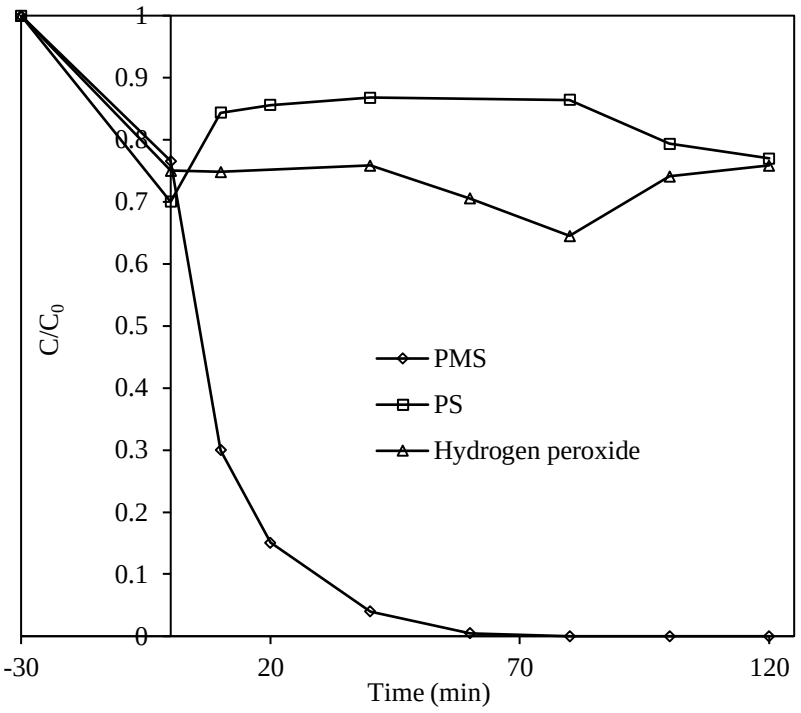

Figure 4-1 Effect of oxidants on the removal of TCS (Conditions: $[Fe_3O_4]_0$ = 0.75 g/L; $[H_2O_2]_0$ = $[PMS]_0$ = $[PS]_0$ = 0.75 mM; pH_i 6.0)

4.2 Adsorption of TCS

Since significant adsorption was observed in the proposed process, adsorption of TCS onto Fe_3O_4 under different conditions was investigated further. The effect of pH and Fe_3O_4 dosage on the adsorption of TCS onto Fe_3O_4 is shown in Figure 4-2. The solution pH has a significant effect on the adsorption. In general, the adsorption is quite stable from low to neutral pH range, then it gradually reduced at higher pH levels. The point of zero charge of Fe_3O_4 was reported to be 7.1 [152] while the pK_a of TCS is 8. Therefore at pH 8 or above, the negative surface charge of Fe_3O_4 will repel the phenolate form of TCS, resulting in the decreasing adsorption percentage as the pH increases beyond 8. In addition, at neutral pH, the adsorption generally increases with the increasing of Fe_3O_4 dosage.

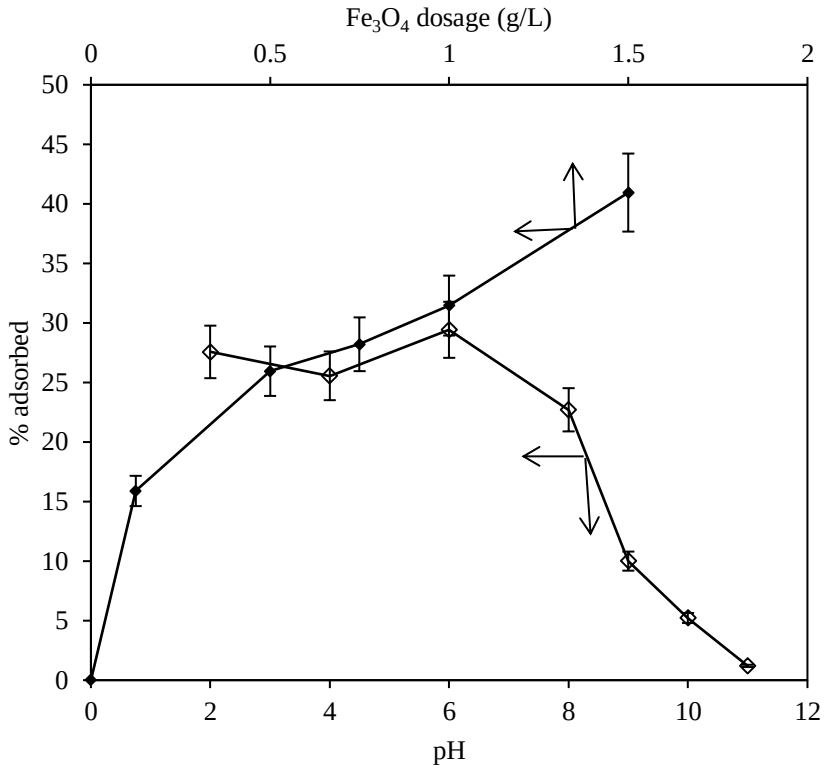

Figure 4-2 Percentage of TCS adsorbed by Fe_3O_4 at different pH (hollow; $[Fe_3O_4]_0$ = 0.25 g/L; $[TCS]_0$ = 0.03 mM) and Fe_3O_4 dosage (filled; $[TCS]_0$ = 0.03 mM; pH_i 6)

According to the observation, the adsorption/desorption of TCS onto Fe_3O_4 is a fast process. The equilibrium can be reached within the first few minutes of mixing. However, the bonding between TCS and Fe_3O_4 apparently is not very strong and the constant adsorption and desorption results in a mild fluctuation of concentration (±8%) after the equilibrium.

4.3 Effect of Fe_3O_4 dosage on TCS decomposition

The addition of PMS prompts the re-equilibration of the system as well as the activation of PMS by Fe_3O_4. After the formation of sulfate radicals, the oxidation of TCS and its intermediates is initiated.

The influence of Fe_3O_4 dosage on the degradation of TCS at 3 different initial pH levels (3.7, 6.0, and 9.0) was studied and the results are shown in Figure 4-3, in which the adsorption of TCS during sonication was excluded from the kinetic analysis. The degradation of TCS can be described by pseudo first-order kinetics for all tested dosages and the trend of observed decay rate constants is depicted in Figure 4-3d.

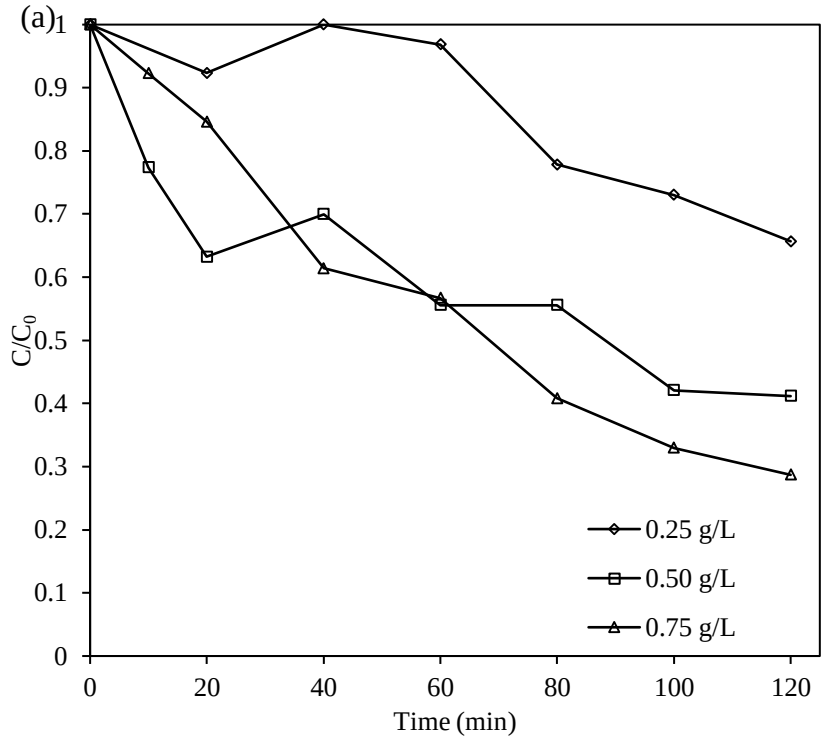

(b)

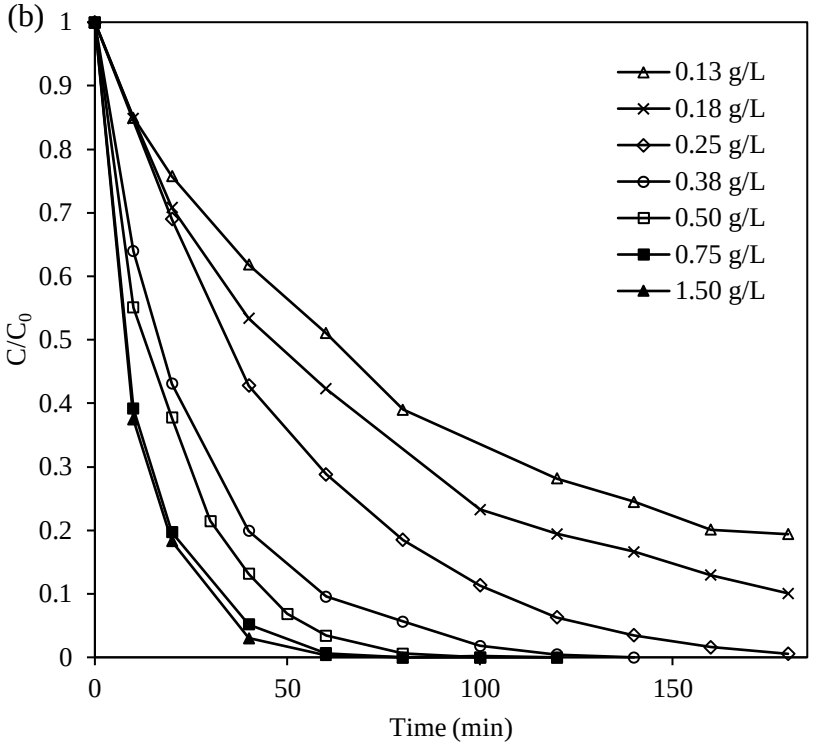
0.13 g/L
0.18 g/L
0.25 g/L
0.38 g/L
0.50 g/L
0.75 g/L
1.50 g/L
C/C0
Time (min)
0
0.1
0.2
0.3
0.4
0.5
0.6
0.7
0.8
0.9
1
0
50
100
150

(c)

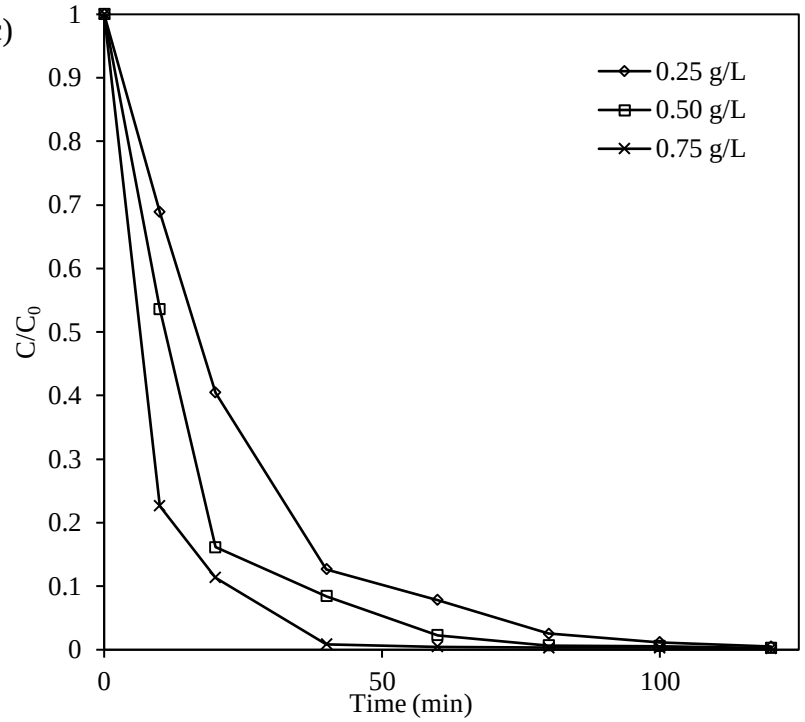
0.25 g/L
0.50 g/L
0.75 g/L
C/C0
Time (min)
0
0.1
0.2
0.3
0.4
0.5
0.6
0.7
0.8
0.9
1
0
50
100

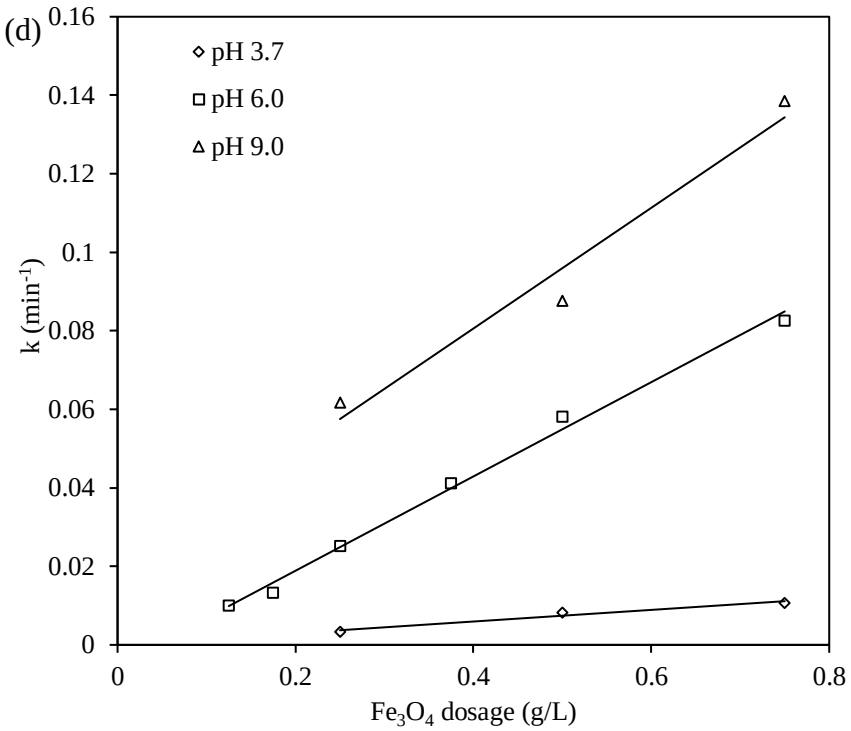

Figure 4-3 (a) TCS degradation at different initial Fe_3O_4 dosage at pH 3.7 (b) pH 6.0 (c) pH 9.0 (d) k vs Fe_3O_4 dosage at different pH. (Conditions: $[TCS]_0$ = 0.03 mM; [PMS] 0.75 mM; $[TCS]_0$:$[PMS]_0$ = 1:25)

The lowest rate constants were observed at pH 3.7, where the decay curves were unsteady because the oxidation performance is still low comparing to that of the adsorption and desorption. The curve fluctuation became insignificant however at higher pH levels when faster oxidation of TCS dominants the process and the effect of adsorption/desorption becomes trivial. At pH 9, a two-stage decay kinetics was observed, where a faster initial decay was followed by a slower reaction at about 20 minutes. This phenomenon can be explained by the change of pH throughout the reaction. The pH changes in the course were monitored and shown in Figure 4-4. As no buffer was used in this study, for the cases with initial pH of 8 (or above), significant pH drops from alkaline to neutral range were observed during the first 20 minutes (Figure 4-4), which led to a higher adsorption of TCS on the catalyst (as demonstrated

in Figure 4-2); however, such an (additional) adsorption was no longer available at the later stage of the process (the adsorption is more or less the same, if the pH is below 6), which resulted in a two-stage kinetics.

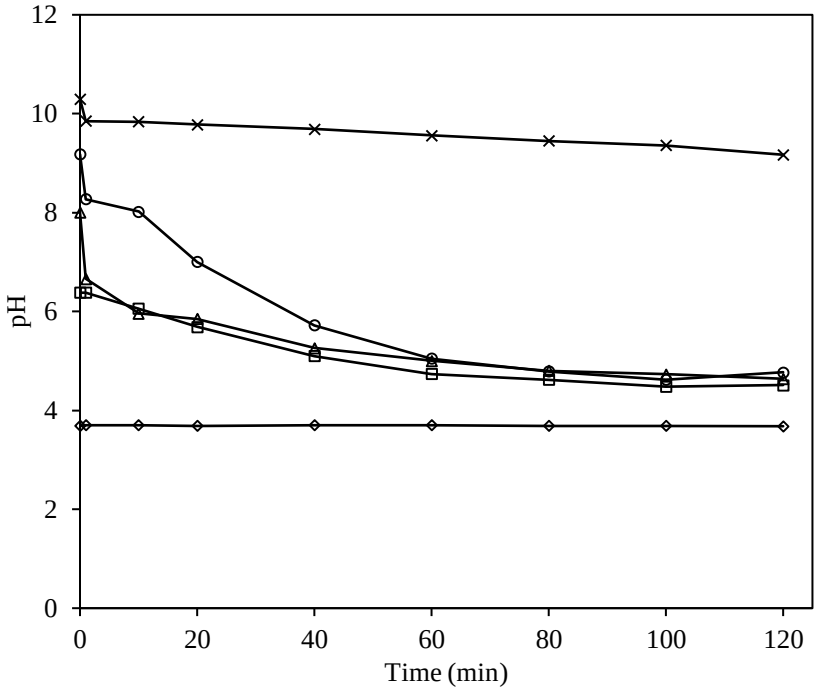

Figure 4-4 pH change as the reaction proceeds

The TCS decay rate constant increases linearly as the Fe_3O_4 dosage increases from 0.125 g/L to 0.75 g/L for all the tested pH levels from 3.7 to 9.0 as shown in Fig 4-3d. The increase in Fe_3O_4 dosage generally means an increase in the total adsorption sites and reaction sites available in the solution, and thus an increase in reaction rates. However, it was interesting to find that the further increase in Fe_3O_4 dosage beyond the above dosage to 1.5 g/L only results in a very slight increment in the rate constant (e.g. from 0.083 to 0.092 min^{-1} at pH 6.0, data not shown). This is attributed to the agglomeration of the fine Fe_3O_4 particles at higher dosage, which leads to the level off

of the total surface area. The number of reactive sites is therefore no longer linearly increased with the Fe_3O_4 dosage and so is the rate constant.

4.4 Effect of pH and PMS dosage on TCS removal

At pH 8 or above, an instant drop of pH was observed upon the addition of NaOH (for pH adjustment) (Figure 4-4). This indicates that hydroxyl ions were adsorbed quickly by Fe_3O_4 above its point of zero charge, and therefore lowered the solution pH. For the cases at initial pH 6 and above, the solution pH generally decreased during the process, which is because of the generation of organic acids as end oxidation products and the weaker buffer capacity at neutral pH ranges.

The initial pH is not only a critical factor on the treatment performance, but it will also affect the performance in using PMS. It was found that the PMS dosage had little effect for pH ranging from 3 to 5, but it became very active at pH 6 to 9 for the TCS removal (Figure 4-5). The increase of hydroxyl ions apparently aided the activation of PMS; however, it was interesting to note that when the initial pH increased to 10, the reaction rates significantly dropped to near zero. At this high pH level, the buffering capacity of the solution is high, so that the loss (adsorption) of hydroxyl ions onto Fe_3O_4 and the generation of organic acids during the reaction did not lower the solution pH (the pH remained above 9 throughout the reaction, see Figure 4-4). The low decay rate constant observed could be attributed to following reasons: a) at pH 10, the electrostatic repulsion between the negative charged Fe_3O_4 (PZC = 7.1) and TCS (pk_a = 8.0) restrains TCS from reaching the surface of Fe_3O_4; b) the adsorbed hydroxyl ions at the surface of Fe_3O_4 formed a thick barrier in repelling the PMS (pk_a = 9.4 [153]) and therefore

reduce the efficiency of radical formation; and c) the self-decomposition of PMS at high pH level (9 or above) was reported mainly through non-radical pathways [135, 151].

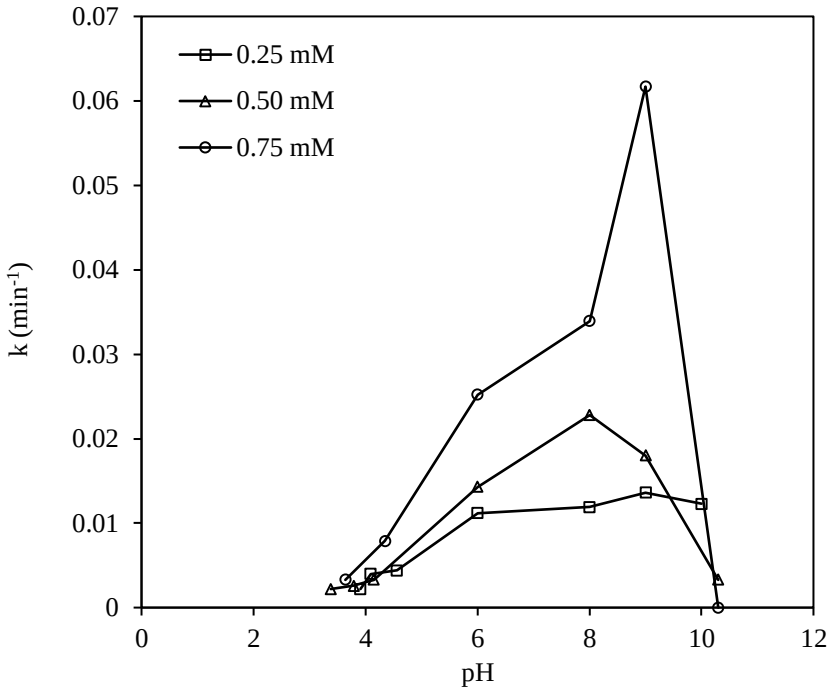

Figure 4-5 k vs. initial pH at different PMS dosage (Conditions: $[Fe_3O_4]_0$ = 0.25 g/L; $[TCS]_0$ = 0.03 mM)

Previous studies showed that when iron oxide used with H_2O_2, a low pH was often required to produce a significant removal of target compound, in which the production of hydroxyl radicals depends on the dissolution of Fe_3O_4 at acidic pH [136, 140]:

$$Fe_3O_4 + 8H^+ \rightarrow Fe^{2+} + 2Fe^{3+} + 4H_2O \qquad (4\text{-}1)$$

Therefore, a separate test was performed to investigate the effect of Fe_3O_4 dissolution on the removal of TCS and the results are shown in Figure 4-6. The rate constant is only slightly higher than reaction at pH 3.7 under same condition. It was found that, at pH 2, the soluble iron species would cumulate in water as the reaction proceeded while the

level of ferrous remained about the same because ferrous iron continues to be oxidized into ferric. For the other pH levels tested from 3.7 to 10.3, no obvious soluble iron species were detected (data not shown), suggesting the reaction is catalyzed by solid Fe_3O_4 rather than the soluble iron. In this study, because the optimum results are obtained in the neutral pH range (6-9), it is verified that the process is dominated by heterogeneous reactions.

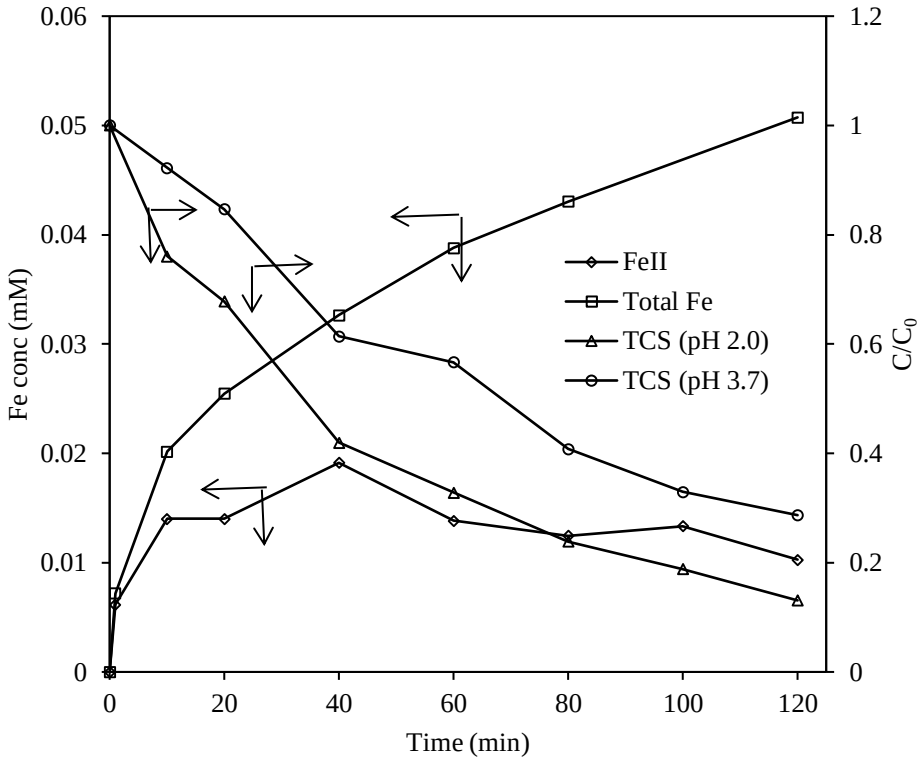

Figure 4-6 The degradation of TCS at pH 2.0 (Conditions: $[Fe_3O_4]_0$ = 0.75 g/L; $[PMS]_0$ = 0.75 mM; $[TCS]_0$ = 0.03 mM)

Both Fe(II) and Fe(III) in homogeneous reaction can activate PMS with Fe(II) being more efficient:

$$Fe(II) + HSO_5^- \rightarrow Fe(III) + SO_4^{\cdot -} + OH^- \quad (4\text{-}2)$$

$$Fe(III) + HSO_5^- \rightarrow Fe(II) + SO_5^{\cdot -} - + H^+ \quad (4\text{-}3)$$

The active sites on the Fe_3O_4 surface generally can be modeled as:

$$\equiv Fe - OH \quad (4\text{-}4)$$

In addition, the above site can also be reformulated into different forms depending on the solution pH:

$$\equiv Fe - OH + H^+ \leftrightarrows \equiv Fe\text{-}OH_2^+ \quad (4\text{-}5)$$

$$\equiv Fe - OH \leftrightarrows \equiv Fe - O^- + H^+ \quad (4\text{-}6)$$

The formation of inner-sphere complex among metal centers, TCS, and PMS is essential for the reaction to take place. Adsorbed TCS and PMS would react on the surface of the Fe_3O_4, giving rise to the formation of reaction intermediates/products and then regenerating the active sites. Acidic to neutral pH levels are more ideal than alkaline pH for the formation of complex between metal centers and TCS as verified from the adsorption profile in Figure 4-2. The PMS is negatively charge at all the tested pH levels, while TCS possesses with no charge or negative charge below or above its pK_a at 8, respectively. Figure 4-7 shows the schematic drawing of the charges of the components at different pH. The ratio of the positive form of the active site ($\equiv Fe\text{-}OH_2^+$) increases with the acidity and so does the electrostatic attraction between the positively charged active site and the negatively charged PMS, resulting in the increase of PMS adsorption at acid to neutral pH levels. However, at acid pH levels, the negatively charged PMS will compete, replace, or expel the non-charged TCS on the Fe_3O_4 surface. This becomes more critical at very low pH level, where a thick and highly protonated layer ($\equiv Fe\text{-}OH_2^+$) on the catalyst surface is likely formed. Such a heavily-charged layer attracts large quantity of PMS to the surface and blocks the TCS from the surface. The result is the domination of self-quenching sulfate radicals with the overdosed PMS. The

radicals therefore failed to react with TCS in the proximity effectively. This could explain the lower rate constant at pH 3.7 than that at neutral to weak alkaline pH ranging from 6-9.

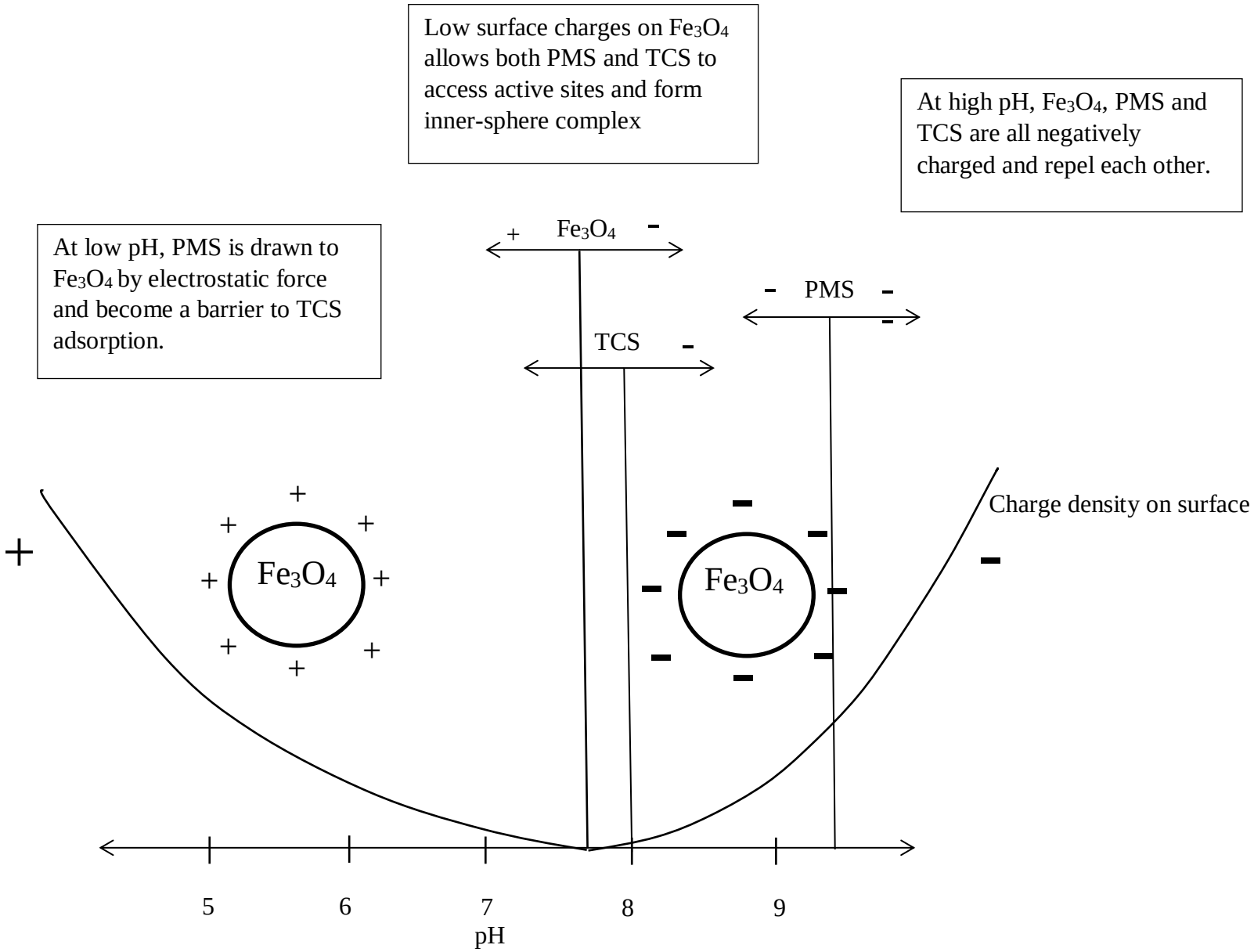

Figure 4-7 Schematic drawing showing the charges of the components at different pH

4.5 Effect of reactants ratio

From Figure 4-8, PMS at 0.75 mM, i.e. TCS/PMS = 1/25, is the optimum ratio regardless of the Fe_3O_4 dosage tested. The system would be overdosed when the PMS concentration was higher than 0.75 mM. This is likely due to the quenching of sulfate radicals by either Fe (II) or PMS:

$$Fe(II) + SO_4^{\cdot -} \rightarrow Fe(III) + SO_4^{2-} \quad (4\text{-}7)$$

$$HSO_5^- + SO_4^{\cdot -} \rightarrow SO_5^{\cdot -} + SO_4^{2-} + H^+ \quad (4\text{-}8)$$

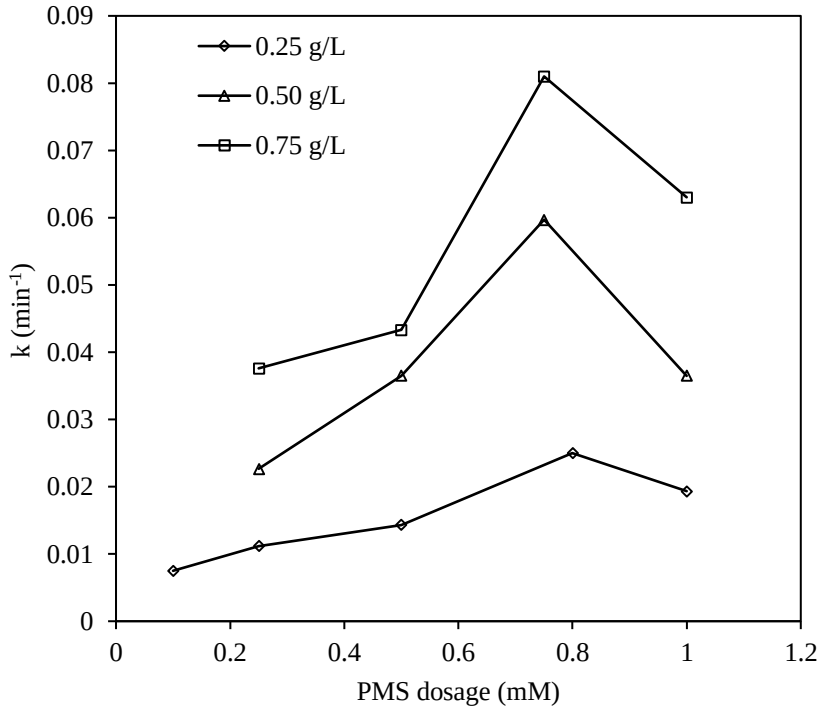

Figure 4-8 Decay rate constants at different PMS and Fe_3O_4 dosage (Conditions: $[TCS]_0$ = 0.03 mM; pH_i 6.0)

Since the PMS at 1.0 mM was overdosed and ferrous leaching was insignificant under these circumstances, the eq. 8 should be the main reason causing the rate retardation at high PMS dosages. In addition, it was found that 75% of PMS was remained in the solution after TCS was fully oxidized, while [PMS] kept decreasing for the continuing oxidation of the intermediates (Figure 4-9). This suggests PMS molecules outnumber the number of active sites on Fe_3O_4. As shown in Figure 4-3d, the increase of the Fe_3O_4 dosage can increase the reaction rate linearly within a proper range. However, overdosing the Fe_3O_4 can lead to catalyst agglomeration and the increment rate of total surface area for the active sites gradually reduced. Though the optimum TCS to PMS dosage was established at 1:25, within the tested Fe_3O_4 range (0.25 to 0.75 g/L), the ratio of active site on Fe_3O_4 to PMS should be a small fraction according to our observation.

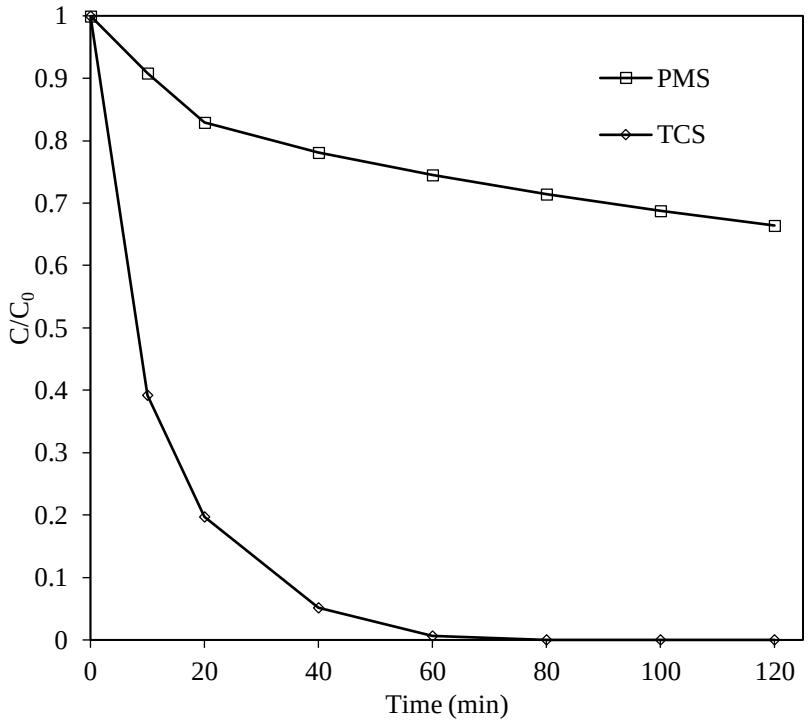

Figure 4-9 PMS and TCS degradation ($[TCS]_0$ = 0.03 mM; $[Fe_3O_4]_0$ = 0.75 g/L; $[PMS]_0$ = 0.75 mM; pH_i 6.0)

Figure 4-10 shows the magnetic hysteresis loop of Fe_3O_4 before and after uses. Both used and unused Fe_3O_4 exhibits good magnetic property and thus can easily be recovered by applying a magnetic field.

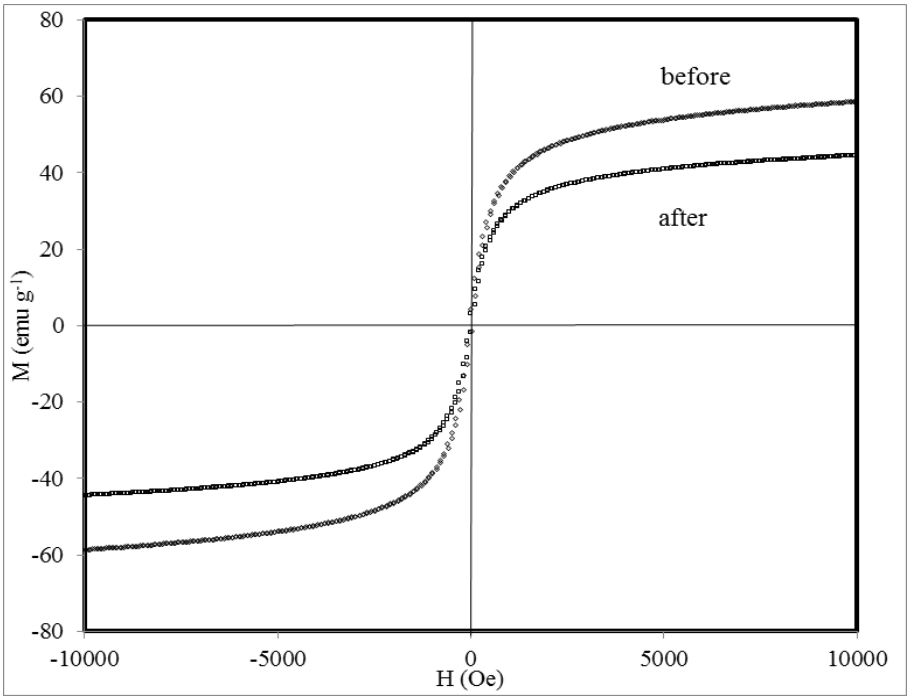

Figure 4-10 Magnetic hysteresis loop of Fe_3O_4

Chapter Five Degradation of Triclosan by $MnFe_2O_4$ with and without oxidants

5.1 Removal of TCS by $MnFe_2O_4$ alone

The degradation of TCS by $MnFe_2O_4$ alone at different pH is shown in Figure 5-1. At pH 4.3, 6.0 and 9.0, less than 15% TCS was removed by $MnFe_2O_4$ alone in 4 hours. However, when the pH dropped to 3.3 and further to 2.5, significant TCS removal was observed. The degradation of TCS follows pseudo-first order kinetics (R^2>0.99). Complete removal of TCS at pH 2.5 was achieved within 170 min. Ukrainczyk and McBride (1992) and Fan et al. (2010) found similar pH dependence in the treatment of phenols or phenolic wastewater by manganese oxides. [154, 155].

Tert-butanol and ethanol were used to investigate the reaction mechanism at pH 3.3 as the two alcohol reacts with sulfate radical and hydroxyl radicals at different rate. However, as it is obvious from Figure 5-2 that both have little effect on the reaction rate. The reaction was also unaffected by the addition of sodium chloride which indicates that ionic strength may not be a factor. N_2-protected experiment was performed to evaluate the effect of dissolved oxygen in the reaction medium and found that it did not affect the reaction rates. Thus, all subsequent experiments were performed without N_2-purging.

Many types of manganese oxides, including birnessite, manganite, hausmannite, and manganese dioxides were known to oxidize phenolic compounds [148, 155]. Zhang and

Huang (2003) have demonstrated that TCS can be oxidized by MnO_2 [105]. However, in the oxides that were used in those studies, manganese were mostly of 3+ and 4+ oxidation state. $MnFe_2O_4$ is a spinel ferrite and Mn occupying tetrahedral sites are usually of 2+ oxidation states. Therefore, XPS analysis is performed to shed lights on the oxidation state of Mn in the $MnFe_2O_4$ used in this study and the spectra of Fe 2p, Mn 2p and O 1s are shown in Figure 5-3. The characteristics and the peak location of Fe 2p fits the standard samples of Fe_2O_3, with the peaks of Fe $2p_{3/2}$ and Fe $2p_{1/2}$ at 710.86 and 724.19 eV respectively, and a satellite peak at 718.90 eV, which is well distinguished and do not overlap with Fe $2p_{3/2}$ or Fe $2p_{1/2}$ [156]. Hence, it can be concluded that Fe is mostly in 3+ oxidation state in the $MnFe_2O_4$ employed in this study. The O 1s spectra is resolved into two individual peaks at binding energy of 529.75 and 530.70 eV, which are assigned to surface lattice oxygen of metal oxides (M-O, denoted as O_I) and surface hydroxyl species (-OH, denoted as O_{II}) respectively [143]. The peaks of Mn $2p_{3/2}$ and Mn $2p_{1/2}$ are located at 642.00 and 653.63 eV respectively, which fits well with reference [143, 157]. Mn $2p_{3/2}$ was further resolved into two peaks at binding energy 641.73 and 643.40, which most likely represents Mn^{2+} and Mn^{3+} respectively, with the majority in 2+ oxidation state [143].

The effect of Mn(II) ions was tested and the result is shown in Figure 5-4. When 0.5 mM Mn(II) in form of $MnSO_4$ was added, k of the reactions dropped from 0.0168 min^{-1} to 0.0077 min^{-1}. The inhibiting effect of Mn (II) ions on the oxidation of phenols and TCS by manganese oxides was also observed by Ukrainczyk and McBride (1992), and Zhang and Huang (2003) [105, 155]. It was suggested that Mn^{2+} adsorbed strongly to active sites on manganese oxides and also Mn^{2+} is a reaction products and increases in its concentration slows the reaction.

Based on the experimental results presented above and literature on the oxidation of TCS and phenolic compounds by manganese oxides [105, 158], it can be proposed that the reaction mechanism proceeds as follows (Reaction 5-1 to 5-5):

TCS first forms a precursor complex with Mn(III) on the surface of $MnFe_2O_4$:

$$\equiv Mn(III) + ArOH \leftrightarrow \equiv Mn(III)\text{-}OAr \quad (5\text{-}1)$$

Electron is then transfer from the phenol moiety of TCS to Mn(III) and formation of a bound phenoxy radical:

$$\equiv Mn(III)\text{-}OAr \leftrightarrow \equiv Mn(II)\text{-}ArO^{\bullet} + H^{+} \quad (5\text{-}2)$$

It was then followed by the release of phenoxy radicals and Mn^{2+} from the surface:

$$\equiv Mn\text{-}ArO^{\bullet} \leftrightarrow \equiv Mn(II) + ArO^{\bullet} \quad (5\text{-}3)$$

$$\equiv Mn(II) \leftrightarrow Mn^{2+} \quad (5\text{-}4)$$

Phenoxy radical most likely then go through coupling and form dimers or polymers [105]:

$$ArO^{\bullet} + ArO^{\bullet} \rightarrow \text{quinones, dimers and polymeric oxidation} \quad (5\text{-}5)$$

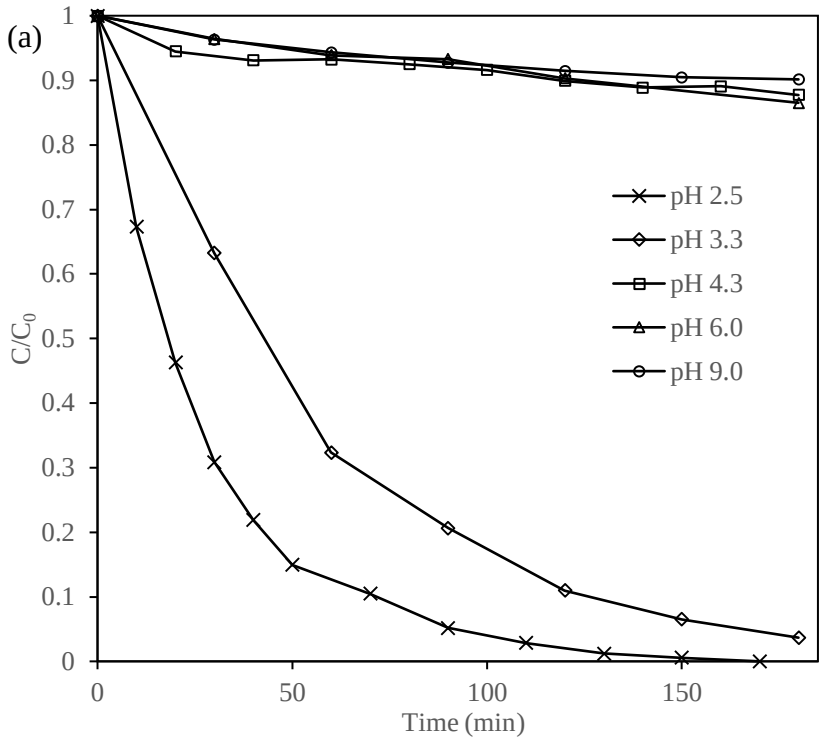
(a)
C/C0
Time (min)
pH 2.5
pH 3.3
pH 4.3
pH 6.0
pH 9.0

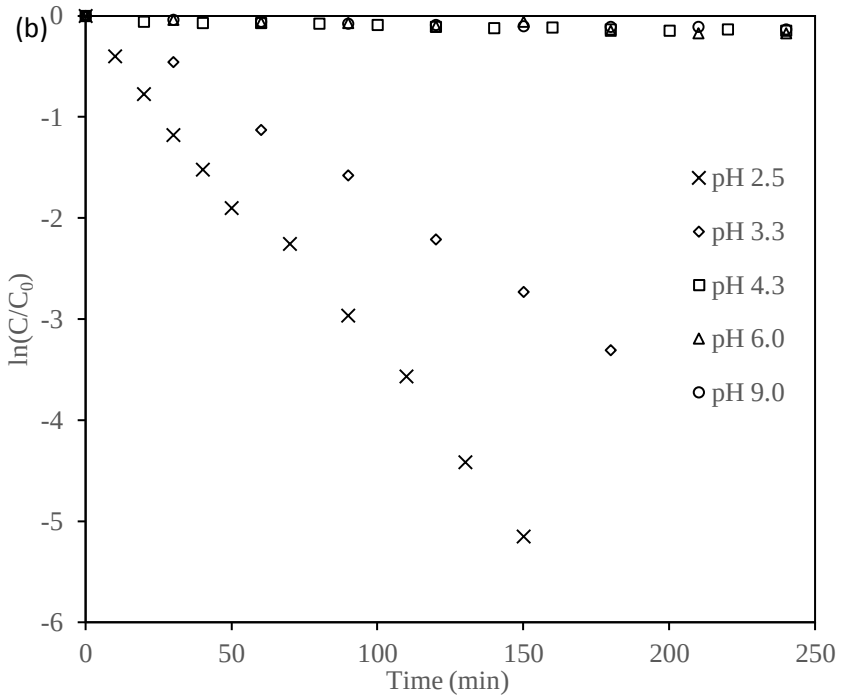
(b)
ln(C/C0)
Time (min)
pH 2.5
pH 3.3
pH 4.3
pH 6.0
pH 9.0

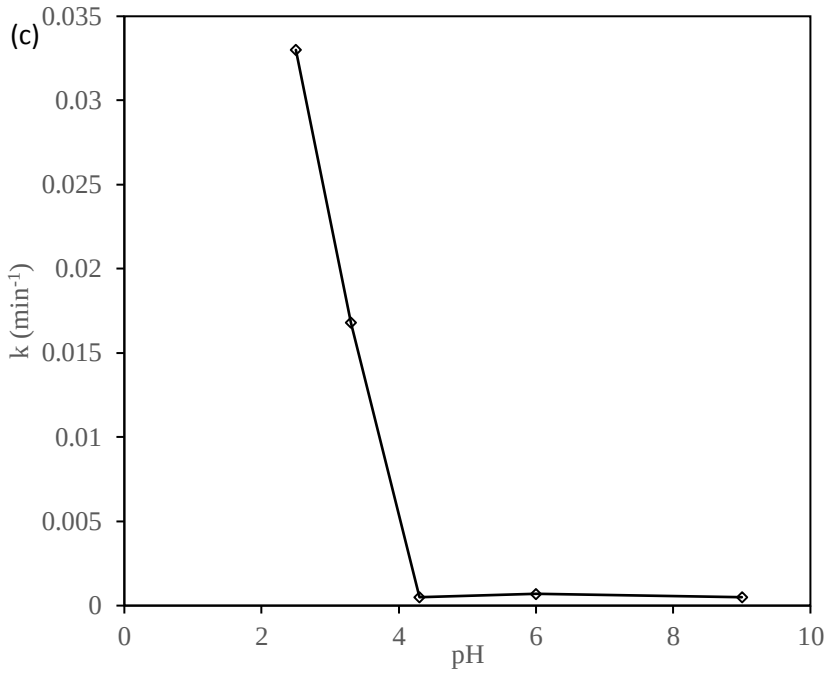

Figure 5-1 Degradation of TCS by $MnFe_2O_4$ alone (a) C/C_0 vs. time; (b) fitting of data to first-order kinetic model; (c) trend of k with the change in pH (conditions: $[MnFe_2O_4]_0$ = 0.25 g/L; $[TCS]_0$ = 0.03 mM)

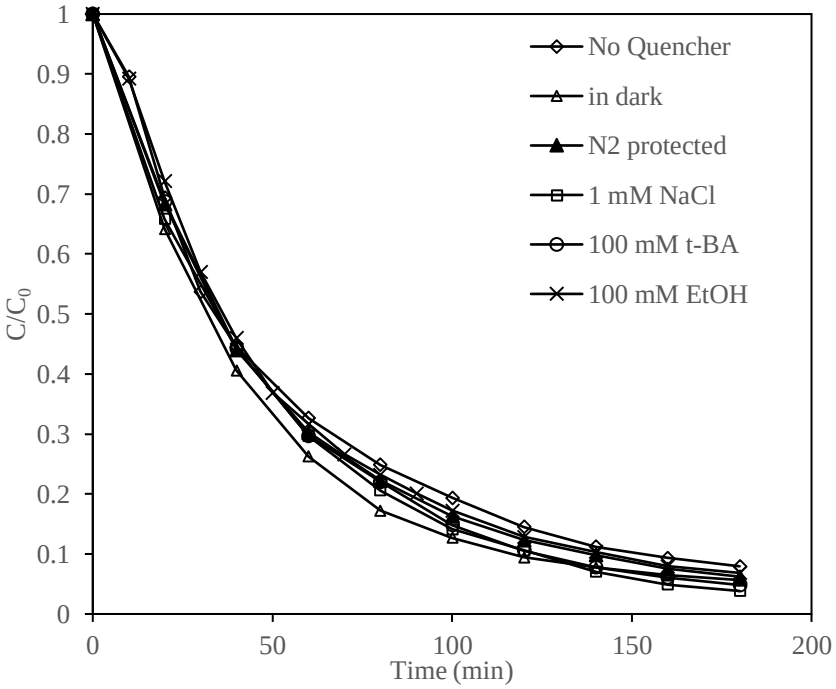

Figure 5-2 Effect of radical quencher, dissolved O_2, and NaCl (Conditions: $[MnFe_2O_4]_0$ = 0.25 g/L; $[TCS]_0$ = 0.03 mM; pH_i 3.3)

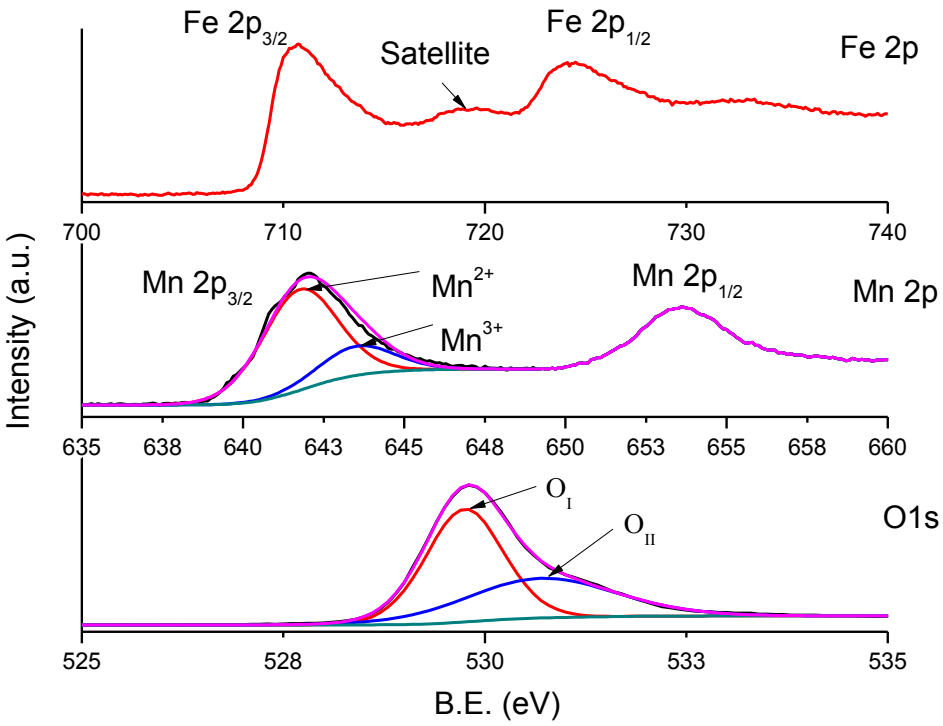

Figure 5-3 XPS spectra of unused $MnFe_2O_4$ (a) Fe 2p; (b) Mn 2p; (c) O 1s

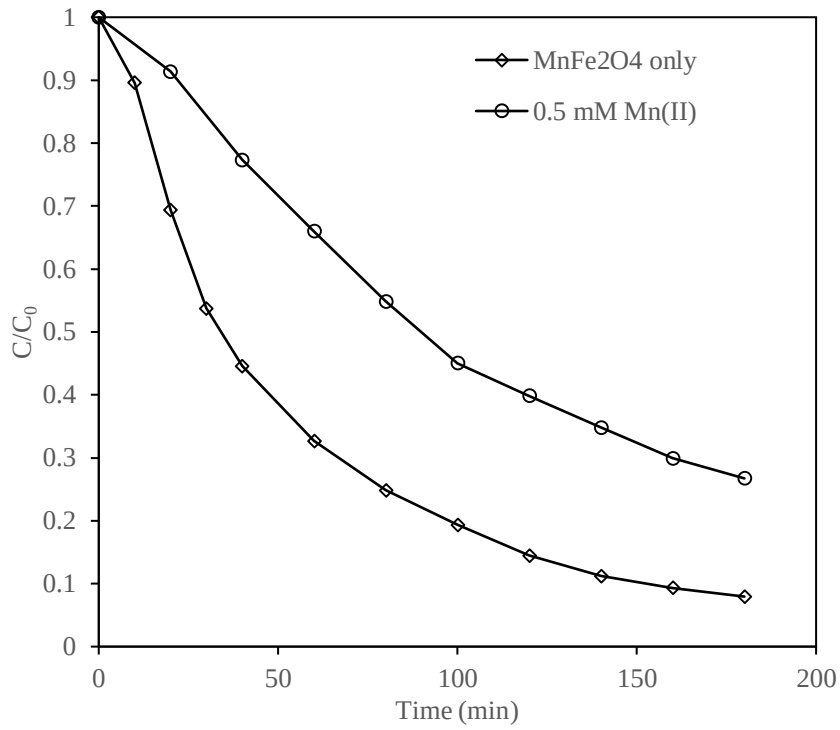

Figure 5-4 Effect of Mn(II) ions on the degradation of TCS by $MnFe_2O_4$ alone. (Conditions: [$MnFe_2O_4$] = 0.25 g/L; [Mn(II) = 0.5 mM; [TCS] = 0.03 mM; pH_i 3.3)

5.2 Effect of oxidant on the removal of TCS by $MnFe_2O_4$

Although as ions in homogenous reaction condition, manganese (II) interacts poorly with oxidants [117], manganese ferrite ($MnFe_2O_4$) has been used as Fenton or Fenton-like catalyst for the activation of hydrogen peroxide [147] and PMS [143, 159]. Various kinds of manganese oxides have also been used to activate PMS. In this study, three oxidants (H_2O_2, PMS and PS) were tested. At all the pH tested (pH 3.3, 7.0 and 9.0), $MnFe_2O_4$ is a poor activator of H_2O_2 as there was no significant removal of TCS for three hours (Figure 5-5). Previous study has shown that manganese containing ferrite can decompose H_2O_2; however, the ratio of Mn:Fe is critical for such reaction to take place. Costa et al. reported that $Fe_{2.47}Mn_{0.53}O_4$ could efficiently decompose H_2O_2, but the efficiency dropped by over 90% when $Fe_{2.79}Mn_{0.21}O_4$ was used [160]. The lack of activity in this study could be attributed to the ratio of Mn:Fe. It is interesting to note that at pH 3.3, H_2O_2 has an inhibiting effect on the removal of TCS by $MnFe_2O_4$ (Figure 5-6). It has previously been reported that Mn(III) are reduced to Mn(II) in the presence of H_2O_2 at low pH [161]. Mn(III) on $MnFe_2O_4$ surface could have reacted more rapidly with H_2O_2 than TCS. Therefore the inhibiting effect can be attributed to the decrease in Mn(III),which is believed to be the contributing party in the degradation of TCS [161].

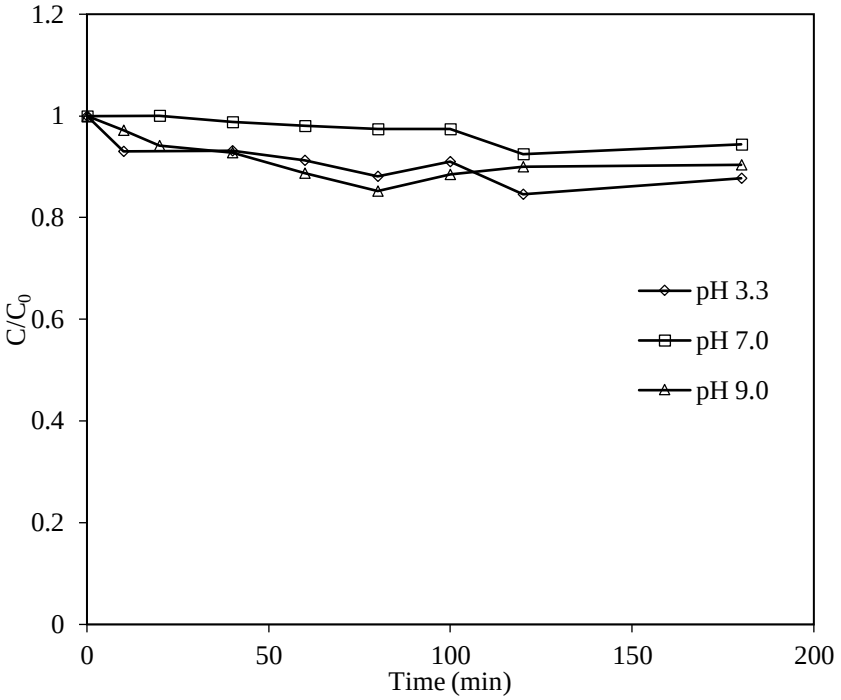

Figure 5-5 Effect of pH on the removal of TCS by $MnFe_2O_4/H_2O_2$ (Conditions: $[MnFe_2O_4]_0$ = 0.25 mM; $[H_2O_2]_0$ = 1.0 mM; $[TCS]_0$ = 0.03 mM)

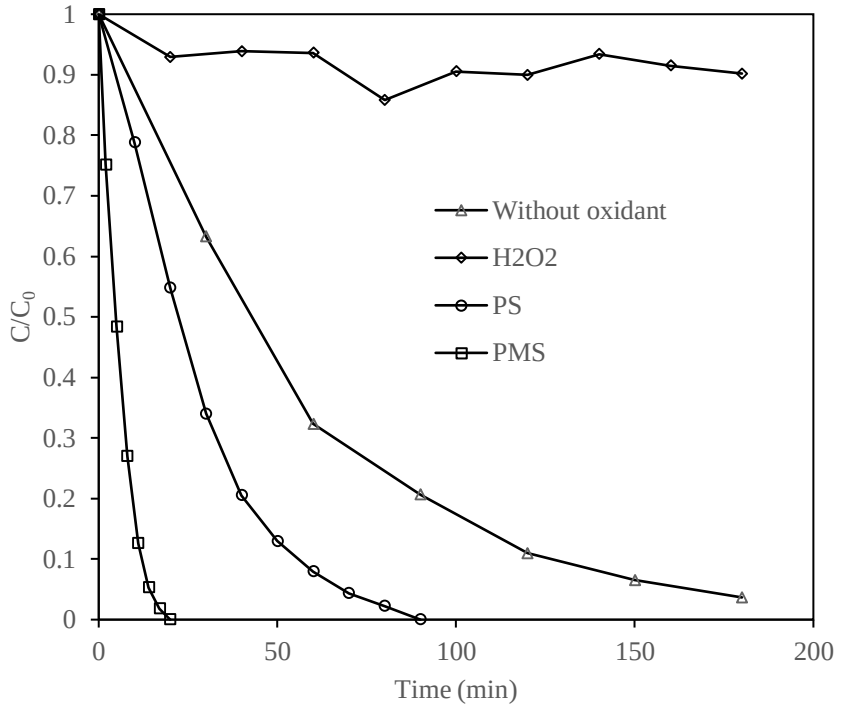

Figure 5-6 Effect of oxidant on the removal of TCS by $MnFe_2O_4$ at pH 3.3 (Condition: $[MnFe_2O_4]_0$ = 0.25 g/L; $[TCS]_0$ = 1.0 mM; pH 3.3)

On the other hand, PMS and PS enhance the degradation of TCS at all pH tested. The combination of $MnFe_2O_4$ and PMS yields the best performance in the removal of TCS at all pH tested. As for persulfate, activation is highly dependent on pH. The best condition for the activation of PS was found to be pH 3.2. $MnFe_2O_4$/PS and $MnFe_2O_4$/PMS will be discussed in detail in the following sections.

5.2.1 $MnFe_2O_4$/PS system

The removal of TCS by $MnFe_2O_4$/PS system was studied in greater detail in this section. The effect of initial pH, $MnFe_2O_4$ and PS dosage was investigated. The latter two was investigated at two pH level, pH 3 and 7 to evaluate the degradation of TCS with and without the combined effect of acid-altered $MnFe_2O_4$ and PS.

Effect of initial pH

The influence of pH on the removal of TCS by $MnFe_2O_4$/PS was investigated and the results are shown in Figure 5-7. The removal efficiency is highly dependent on the initial pH with the best performance at pH 3.3, where TCS was completely removed in 100 minutes. The efficiency decreases as the pH increases. At pH 9.0, only about 35% of the dosed TCS was removed after 4 hours.

It is interesting to note that the reaction rate order differs at different pH. Only reaction with an initial pH 3.3 follows pseudo first-order kinetics. At pH 4.3, 6.0 and 9.0, autocatalysis was observed (Figure 5-6). In other words, the system becomes more and more efficient in the degradation of TCS as the reaction proceeds.

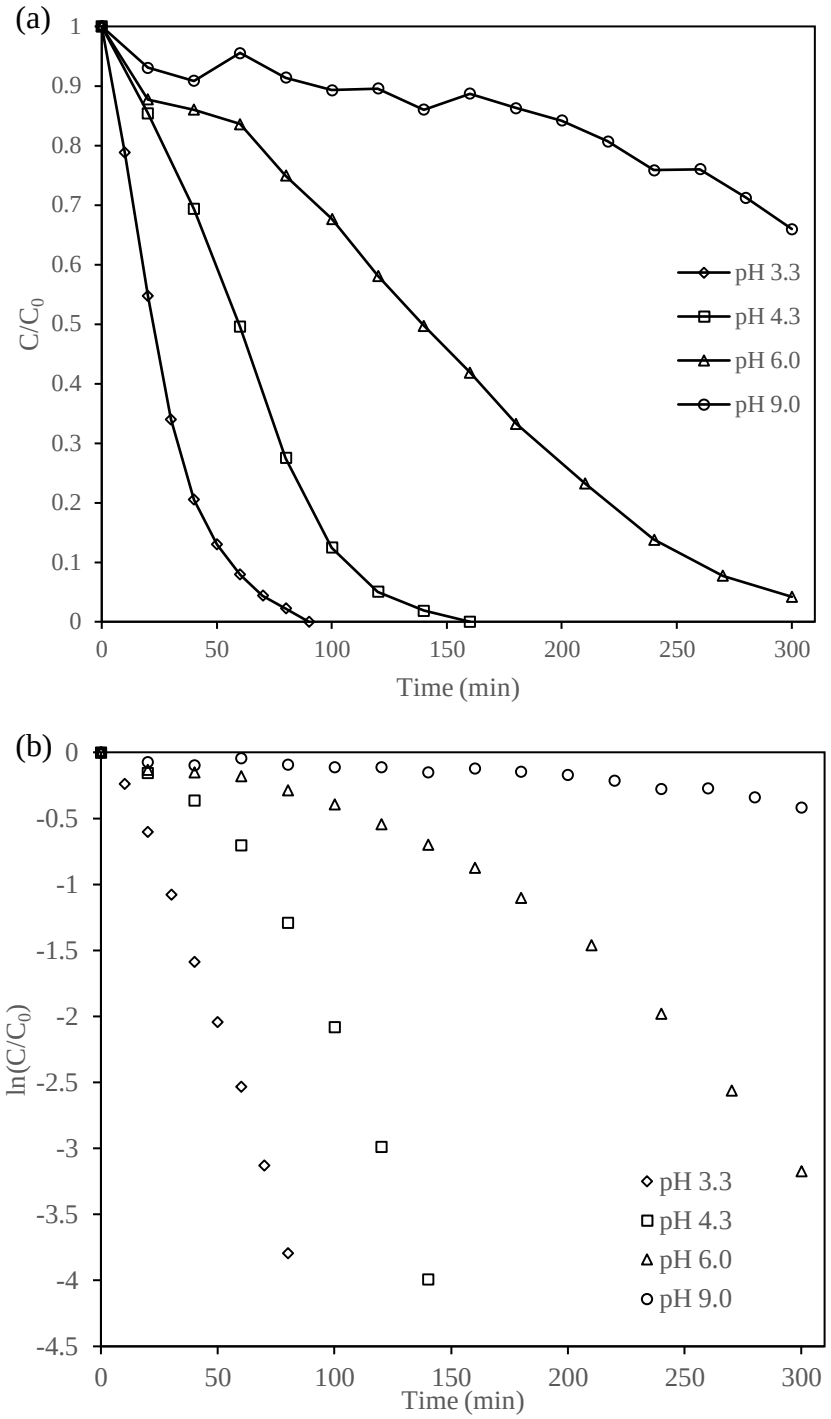

Figure 5-7 Effect of pH on the removal of TCS by $MnFe_2O_4$/PS (a) C/C_0 vs. time; (b) fitting of data to first-order kinetic model (Conditions: [$MnFe_2O_4$] = 0.25 g/L; PS = 1 mM)

Effect of $MnFe_2O_4$ and PS dosage at pH 3

Figure 5-8 and 5-9 show the effect of initial $MnFe_2O_4$ and PS dosage on the removal of TCS at pH 3. As discussed in the previous section, the degradation of TCS by $MnFe_2O_4$ /PS at pH 3 follows pseudo first-order kinetics. In all the dosage tested, a two-stage kinetics can be observed. The breakpoint time was found to be around 20 minutes. k of the first stage, denoted as k_1, increased from 0.0195 to 0.0531 min^{-1} as $MnFe_2O_4$ dosage increased from 0.13 to 0.50 g/L but decreased slightly to 0.042 g/L when it was further increased to 0.75 g/L. As for the second stage, k, denoted as k_2, increased steadily from 0.0245 to 0.1135 min^{-1} as $MnFe_2O_4$ dosage increased from 0.13 to 0.75 g/L. The gap between the first and the second stage kinetic constants widened as $MnFe_2O_4$ dosage increased.

Addition of 0.1 mM PS increases k_1 from 0.0168 to about 0.0300 min^{-1} but further increase in dosage did not improve k_1 further, while k_2 increased from 0.0168 to 0.0429 min^{-1} when 0.1 mM PS was added and then peaked at 0.0554 min^{-1} with the addition of 0.50 mM.

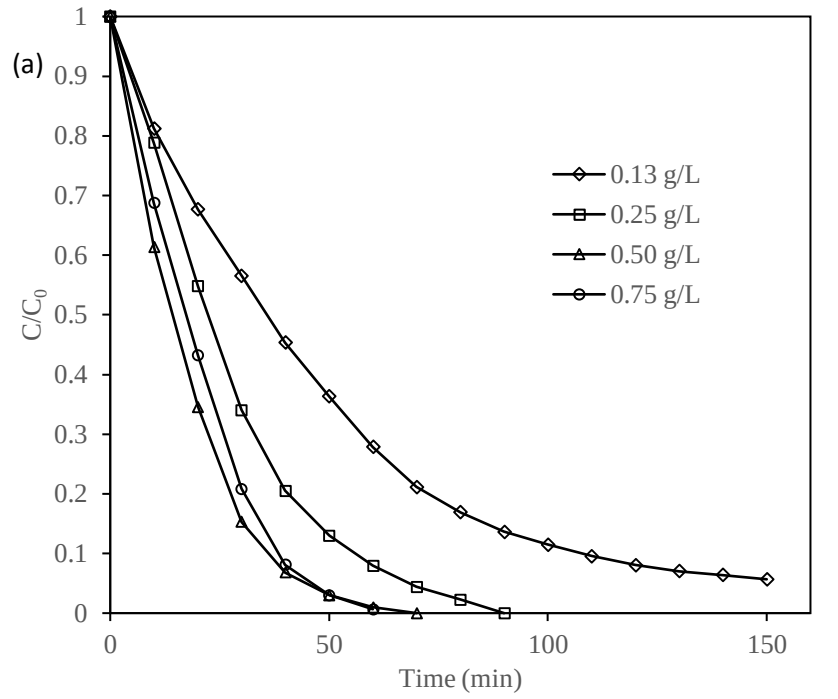
(a)
C/C0
Time (min)
0.13 g/L
0.25 g/L
0.50 g/L
0.75 g/L

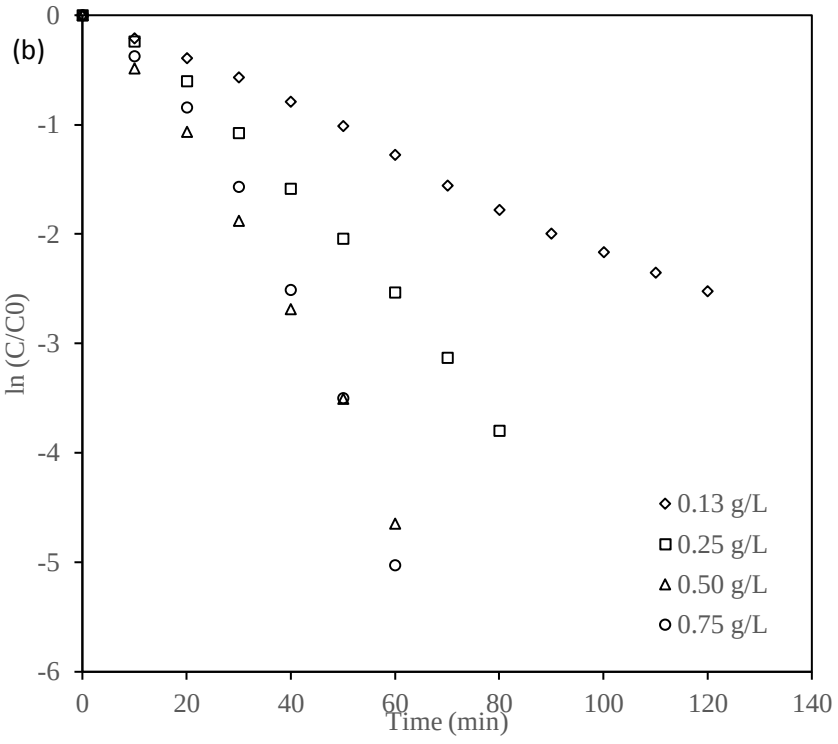
(b)
ln (C/C0)
Time (min)
0.13 g/L
0.25 g/L
0.50 g/L
0.75 g/L

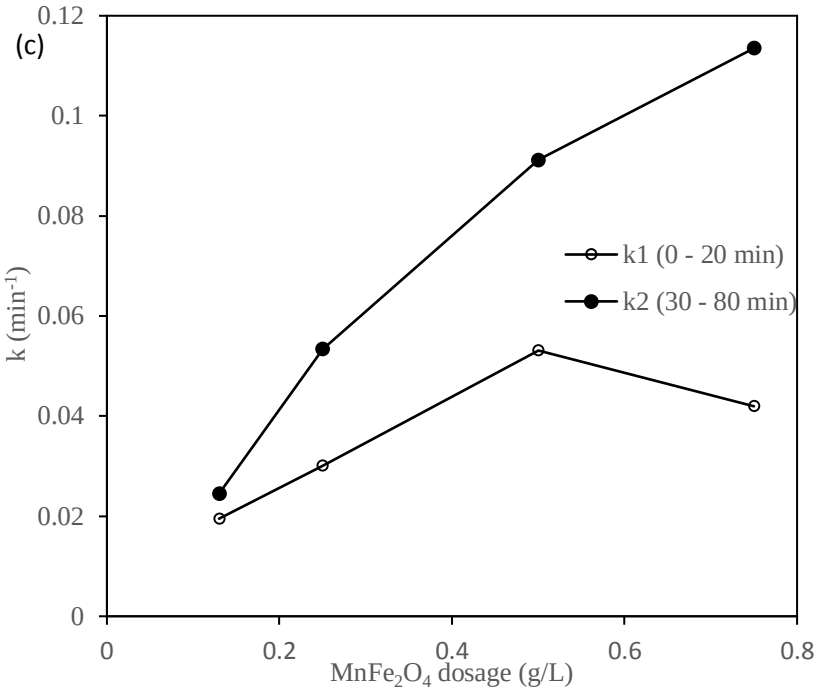

Figure 5-8 Effect of $MnFe_2O_4$ dosage on the removal of TCS at pH 3 (a) decay curve; (b) fitting of data to first-order kinetic model (c) trend of k with respect to initial $MnFe_2O_4$ dosage (Conditions: $[PS]_0$ = 1 mM; $[TCS]_0$ = 0.03 mM; pH 3)

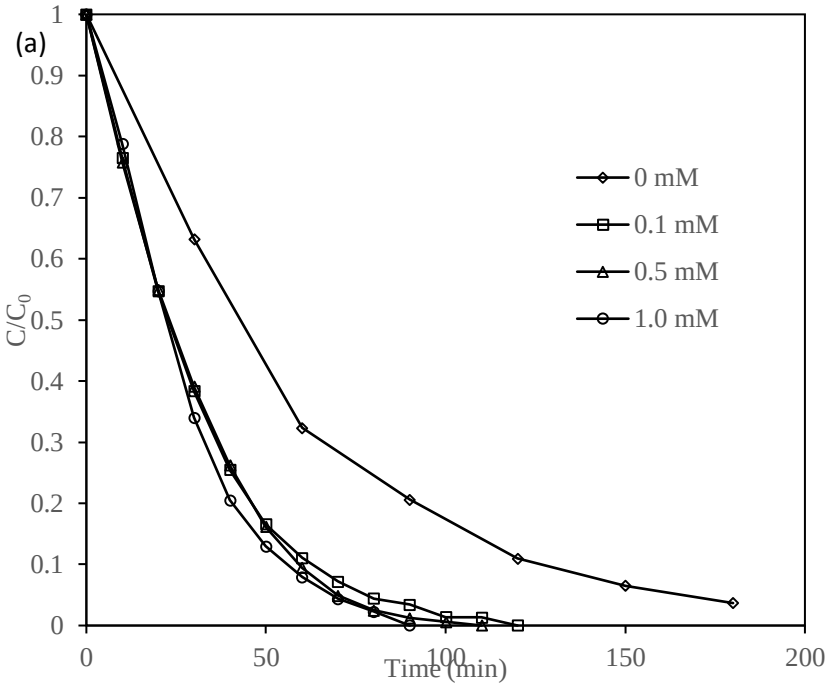

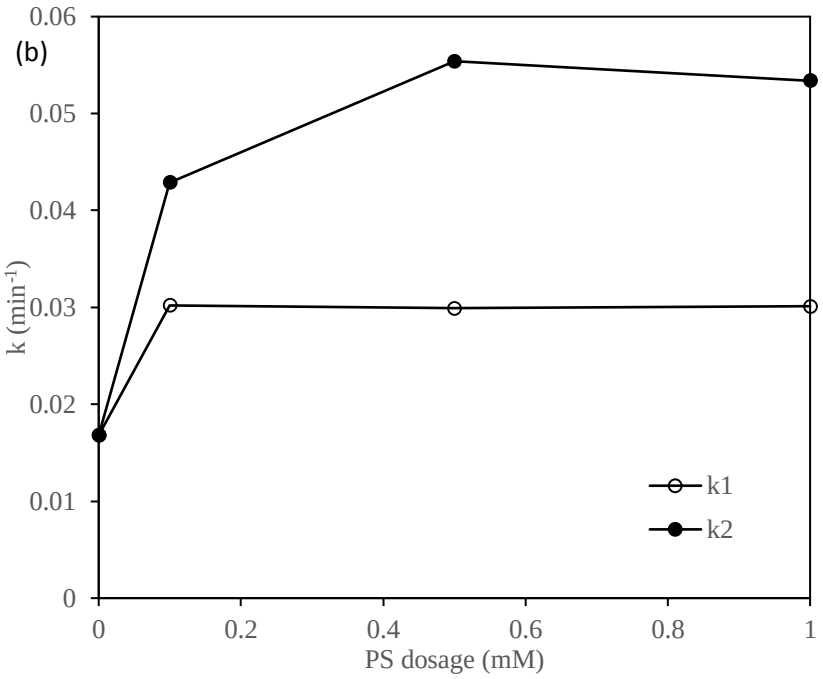

Figure 5-9 Effect of PS dosage on the removal of TCS at pH 3 (a) decay curve; (b) trend of k with respect to initial PS dosage (Conditions: $[MnFe_2O_4]_0$ = 0.25 g/L; $[TCS]_0$ = 0.03 mM; pH 3)

Effect of $MnFe_2O_4$ and PS dosage on the removal of TCS by $MnFe_2O_4$/PS at pH 4

Figure 5-10 shows the effect of initial PS dosage on the degradation of TCS by $MnFe_2O_4$/PS at pH 4. Since $MnFe_2O_4$ does not have the capacity to remove TCS at pH 4, the degradation observed here is therefore likely due to the effect of PS.

It should be noted from Figure 5-10b that the degradation of TCS by $MnFe_2O_4$/PS at pH 4 cannot be described by a conventional pseudo first-order kinetics; it is more like an autocatalytic reaction with the reaction rate increasing with time. A mathematical model is therefore proposed to describe the reaction trend as showed in equation 5-1:

$$y = \frac{ax}{1-bx} \quad (5\text{-}1)$$

Where, in this study, x is the reaction time, t (minutes); y is the treatment performance $\ln([TCS]/[TCS]_0)$; and a and b are characteristic constants. The above equation can be rearranged into a working linear equation as:

$$\frac{t}{\ln\frac{[TCS]}{[TCS]_0}} = \frac{1}{a} - \frac{b}{a}t \qquad (5\text{-}2)$$

Similar to that of many conventional multi-stage reaction kinetics of AOPs, after a short lag phase, a two-stage kinetics separated by a break point at time $t_{breakpoint}$, was also observed in this process at all the tested PS dosages; i.e. a lag phase without significant reaction followed by a mild TCS decay (Stage I) and then a faster TCS decay (Stage II). By fitting the observed laboratory data into equation 5-2 (without using the data in lag phase), it was found that the data fit well with the proposed model with linear regression coefficients (r^2) greater than 0.9706 (Figure 5-11). In addition, it was interesting to find that the natural logarithm of $t_{breakpoint,}$ (in minutes) and the duration of lag phase (i.e. the starting time of Stage I, $t_{lagphase,}$ (in minutes)) are both linearly correlated to the initial PS dosage by equations 5-3 and 5-4 with an r^2 of 0.9586 and 0.9680, respectively (Figure 5-12).

$$\ln t_{breakpoint} = -1.3508[PS]_0 + 5.6435 \qquad (5\text{-}3)$$

$$\ln t_{lagphase} = -2.0093[PS]_0 + 5.0897 \qquad (5\text{-}4)$$

Equations 5-3 and 5-4 indicate that the lag phase is shorter and the system takes less time to reach break point when more PS is used. This is due to the lack of oxidant to

activate the surface site on $MnFe_2O_4$, since $MnFe_2O_4$ by itself does not have the capacity to degrade TCS at pH 4.

As initial PS dosage increases, the position of the curves in Figure 5-11 becomes less negative on the $t/\ln(C/C_0)$ scale (y-axis) and approaches 0. This reflects that the system is becoming more and more efficient and the performance improves as more PS is added at the beginning of the process.

Two sets of kinetic constants can now be obtained from the linear curves as shown in Figure 5-11, in which a_1 and b_1 are the characteristic constants for Stage I while a_2 and b_2 are those for Stage II. To facilitate the prediction of the process, linear correlations between the characteristic constants and PS dosage were obtained by plotting 1/a vs ln $[PS]_0$ (Figure 5-13) and ln b vs. ln ln $[PS]_0$ (Figure 5-14), respectively. Then the constants a and b can be linearly correlated to the initial PS dosage by equation 5-5 to 5-8

$$\frac{1}{a_1} = 573.3\ ln[PS]_0 - 189.13 \quad (5\text{-}5)$$

$$\frac{1}{a_2} = 327.72 ln[PS]_0 - 106.54 \quad (5\text{-}6)$$

$$lnb_1 = 0.8315 ln[PS]_0 - 4.7887 \quad (5\text{-}7)$$

$$lnb_2 = 0.7147 ln[PS]_0 - 5.4635 \quad (5\text{-}8)$$

In addition to the mathematical correlation, the physical meaning of a is the initial reaction rate of Stage I (or right after the lag phase). It is worth noting that a_1 and a_2 are gradually converged as the initial PS dosage increased. In other words, the

reaction rate difference between Stage I and II is becoming smaller (or vague) as the initial PS keeps going up; eventually the system should be describable by a single-stage kinetics model.

The inverse of b, on the other hand, is the time when maximum reaction rate was reached and the concentration of TCS approaches 0, which offers a reference point to indicate the end of reaction, and can be used to determine a proper wastewater detention time and/or the size of the reactor in a real design.

By substituted equation 5-5 to 5-8 into 5-2, two equations for predicting the reaction rate using initial PS dosage were obtained (equation 5-9 and 5-10)

$$ln\frac{[TCS]}{[TCS]_0} = \frac{t}{(573.3\ln[PS]_0 - 189.13)*(1-e^{(0.8315\ln[PS]_0 - 4.7887)}t)} \quad \text{for } t_{lagphase} \leq t \leq t_{breakpoint} \tag{5-9}$$

$$ln\frac{[TCS]}{[TCS]_0} = \frac{t}{(327.72\ln[PS]_0 - 106.54)*(1-e^{(0.7147\ln[PS]_0 - 5.4635)}t)} \quad \text{for } t > t_{breakpoint} \tag{5-10}$$

Based on the above equations 5-9 and 5-10, predictions from the proposed models were compared to the experimental data, and as shown in Figure 5-15, the models can predict the reactions well within all the tested ranges.

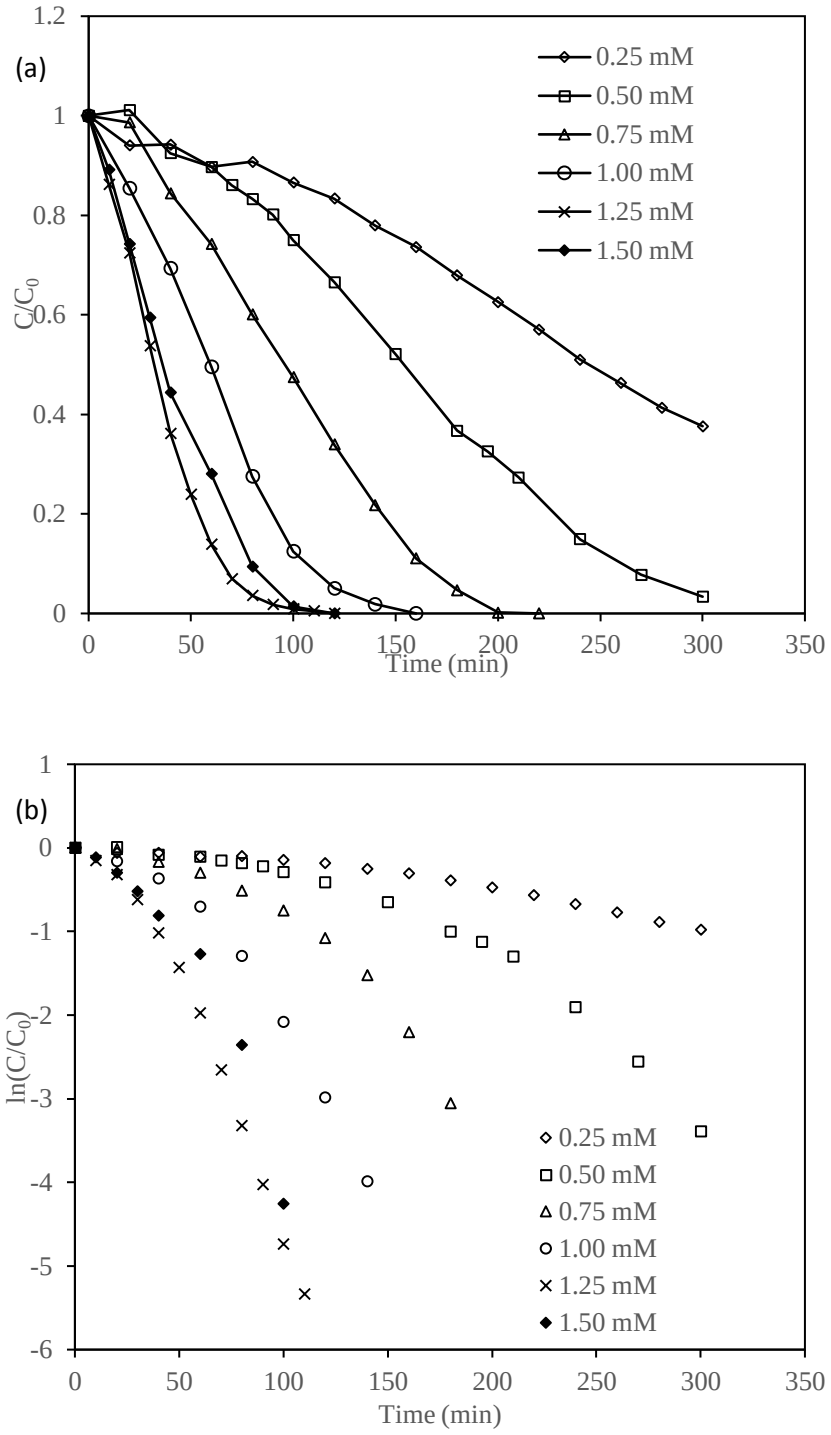

Figure 5-10 Effect of PS dosage on the removal of TCS at pH 4.3 (a) decay curve; (b) fitting of data into first-order kinetic model (Condition: $[MnFe_2O_4]_0$ = 0.25 g/L; $[TCS]_0$ = 0.03 mM; pH = 4.3)

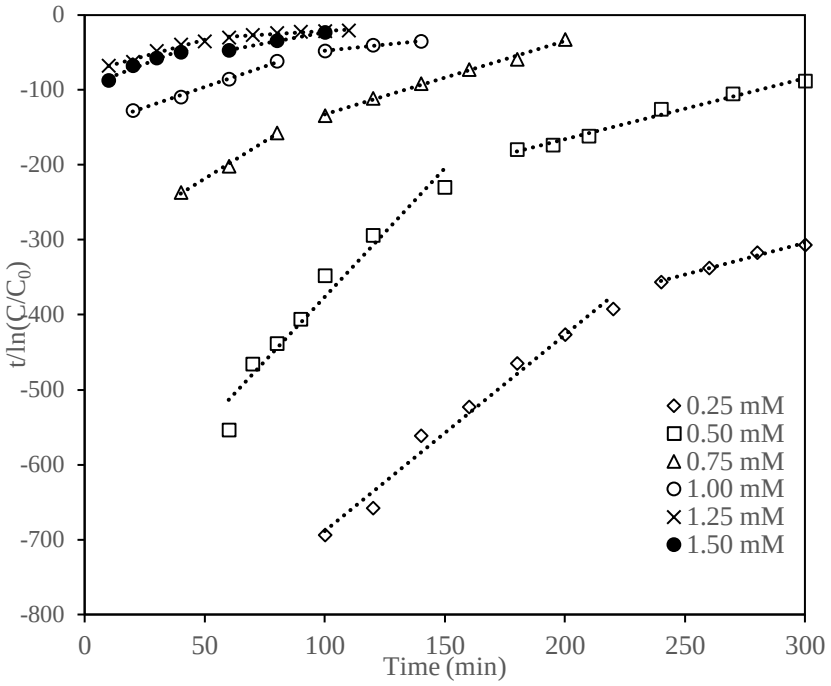

Figure 5-11 Fitting of data into linearized equation of proposed model

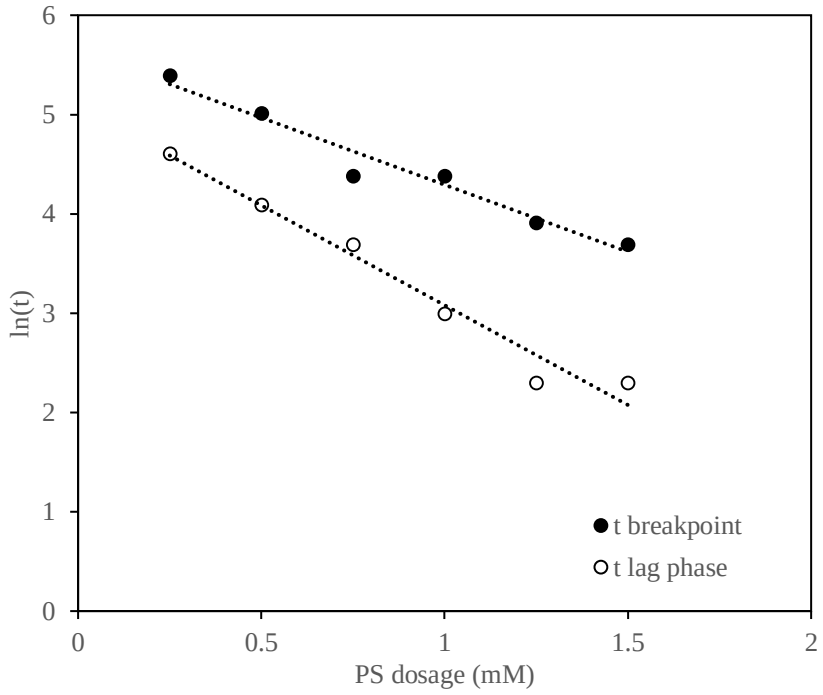

Figure 5-12 Correlation of $t_{breakpoint}$ and $t_{lagphase}$ with initial PS dosage

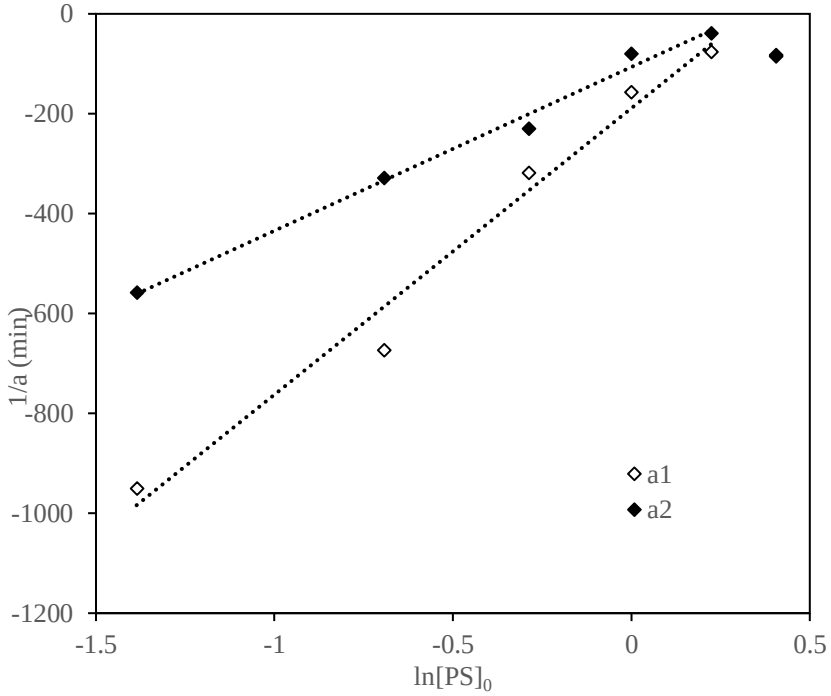

Figure 5-13 Correlation between a and initial PS dosage

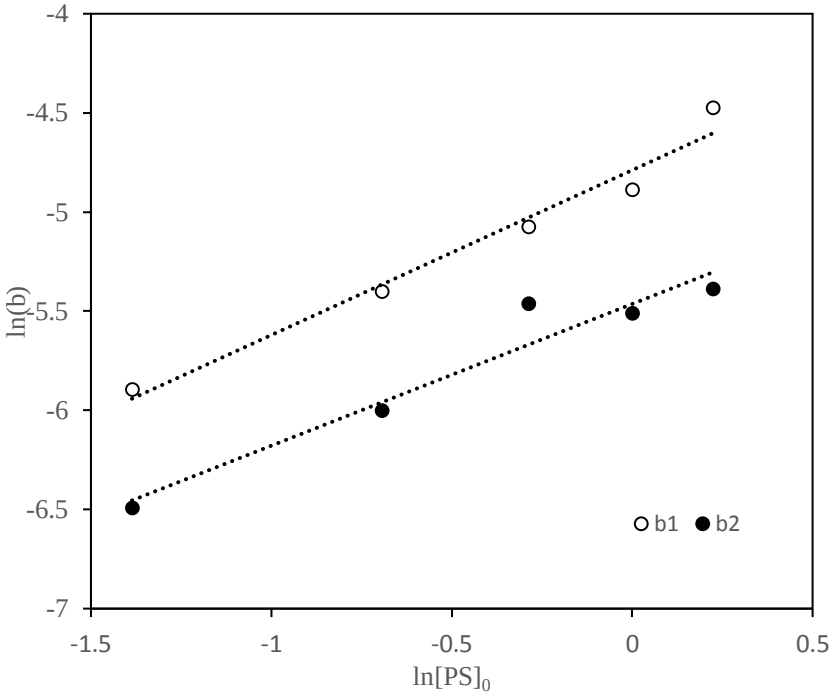

Figure 5-14 Correlation between b and initial PS dosage

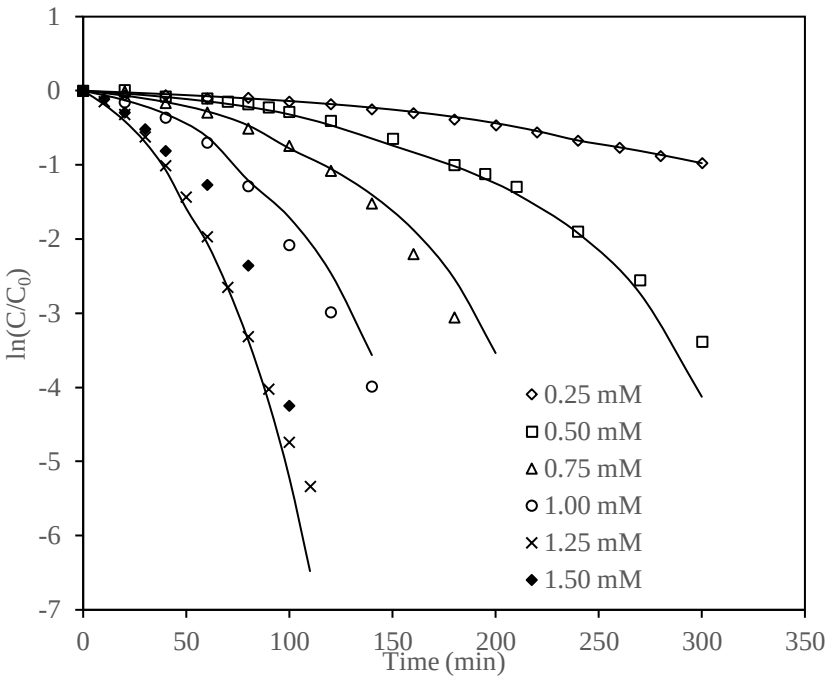

Figure 5-15 Comparison of model prediction with experimental data (mark: experimental data; line: model prediction)

The effect of initial $MnFe_2O_4$ dosage is shown in Figure 5-16. The data were fitted into equation 5-2 to obtain a and b. Figure 5-17 shows a comparison of the effect of $MnFe_2O_4$ and PS dosage on the initial rate of the removal of TCS at pH 4.0. It can be observed that increasing PS dosage from 0.25 mM to 1.5 mM greatly enhanced the degradation of TCS but the increasing $MnFe_2O_4$ dosage from 0.13 g/L to 0.75 g/L had little effect.

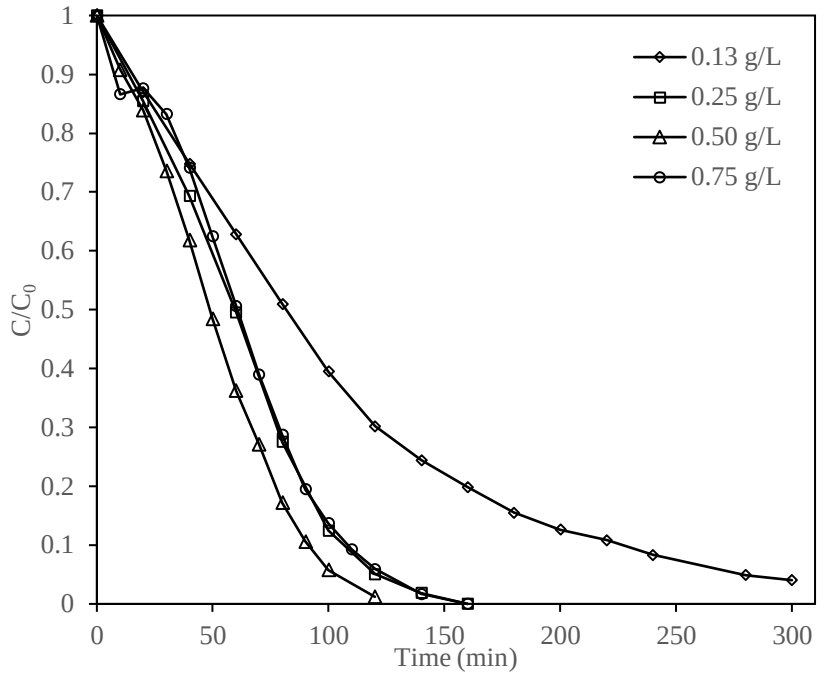

Figure 5-16 Effect of $MnFe_2O_4$ dosage on the degradation of TCS at pH 4 (Conditions: $[PS]_0$ = 1 mM; $[TCS]_0$ = 0.03 mM; pH 4.3)

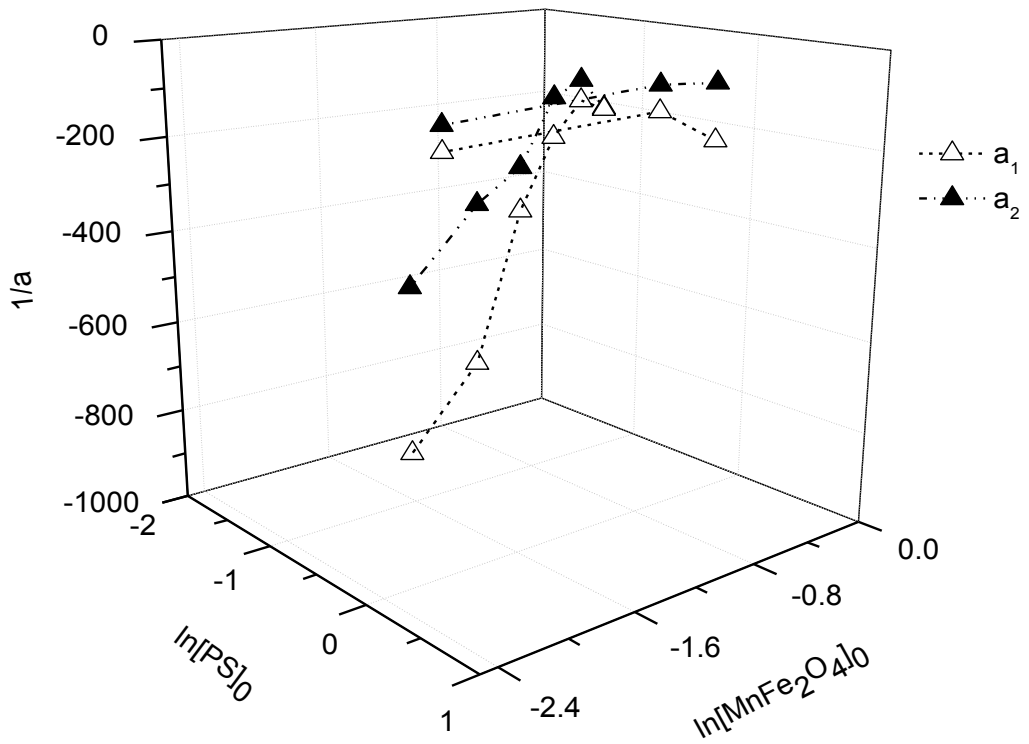

Figure 5-17 Trend of a with respect to initial PS and $MnFe_2O_4$ dosage (Conditions: pH_i 4.3)

5.2.2 $MnFe_2O_4$/PMS system

Effect of pH

Figure 5-18 shows the effect of pH on the degradation of TCS by $MnFe_2O_4$/PMS, which followed pseudo first-order kinetics ($r^2 > 0.97$). At all the pH tested, a lag phase can be observed at the beginning of the reaction (< 3 minutes) with reaction rate constants, $k_{lagphase}$, ranging from nearly 0 to 0.18 min^{-1}. The reaction rate constants for the phase following lag phase was termed k_1 in Figure 5-18. After the lag phase, all but pH 10.0 had only one phase. Two distinct phases can be observed for pH 10.0 after the lag phase, termed k_1 and k_2. This is similar to the autocatalytic reaction observed in $MnFe_2O_4$/PS system with the second phase (k_2 = 0.2075 min^{-1}) faster than the first (k_1 = 0.0907 min^{-1}). The trend of k with respect to pH for both phases are similar. k was lower at both ends of the pH range tested (pH 3.0, 3.8 and 10.0). $k_{lagphase}$ and k_1 increased from 0.0204 to 0.1577 min^{-1} and 0.1100 to 0.2999 min^{-1} respectively when pH increased from 3.0 to 5.0. However, when pH increases from 5.0 to 9.0, there were little changes in both $k_{lagphase}$ and k_1. $k_{lagphase}$ and k_1 at pH 10.0 were lower than that at pH 3.0 but k_2 was between k_1 of pH 3 and 5.

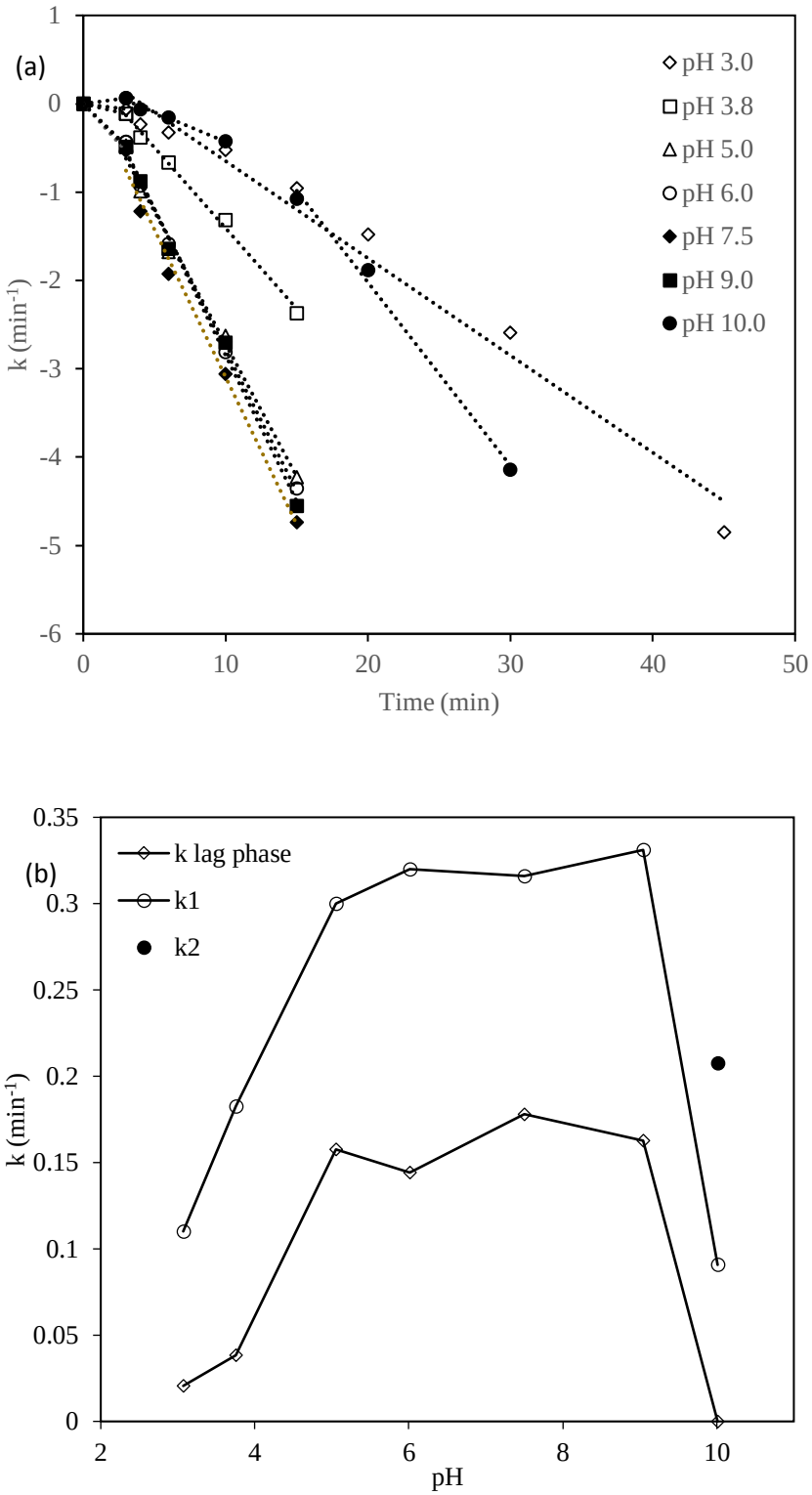

Figure 5-18 Effect of pH on the removal of TCS (a) First-order rate kinetics decay curve; (b) Trend of $k_{lagphase}$ and k_1 with respect to pH (Conditions: $[MnFe_2O_4]_0$ = 0.25 g/L; $[PMS]_0$ = 0.75 mM; $[TCS]_0$ = 0.03 mM)

Effect of initial $MnFe_2O_4$ and PMS dosage

Since neutral pH was optimal for the degradation of TCS by $MnFe_2O_4$ /PMS. The effect of initial $MnFe_2O_4$ and PMS dosage was investigated at pH 7 and the results are shown in Figure 5-19. Generally, k increases as initial $MnFe_2O_4$ dosage increases from 0.25 to 0.75 g/L. However, at all $MnFe_2O_4$ dosage tested, the increase in k was much less significant with increasing PMS dosage and the trend was similar. The k initially increased when PMS dosage increased from 0.13 to 0.25 mM but plateaued upon further addition of PMS (Figure 5-19). To determine whether the plateau was due to the depletion of oxidant or the lack of active sites, the changes in PMS concentration in aqueous phase during the reaction of 0.75 g/L $MnFe_2O_4$ with low (0.13 mM) and high (0.75 mM) PMS dosage was monitored and the results are shown in Figure 5-20. Only about 0.2 mM PMS out of the 0.75 mM initial dose was used while almost all of the 0.13 mM initial dosage was used up. Although a lag phase can be observed in the degradation of TCS, PMS degradation follows first-order kinetics without a lag phase. There was still excess of PMS when TCS was completely removed but the excess PMS was not efficiently utilized in further oxidation of intermediates as was evidenced by the extent of mineralization. Total organic carbon was measured and only 16% of the TCS was found to be mineralized (Figure 5-21).

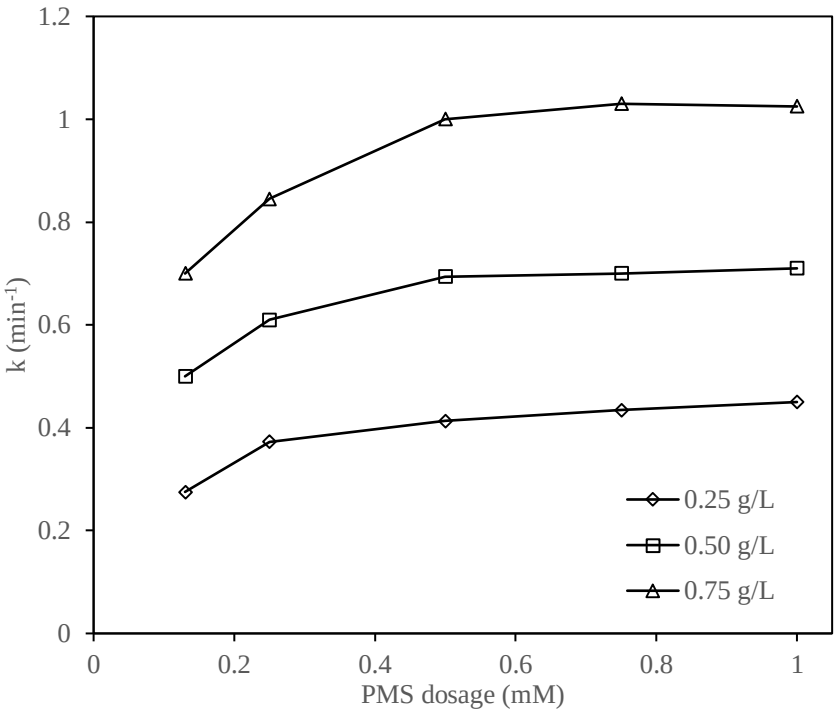

Figure 5-19 Trend of k with respect to initial PMS dosage at different initial $MnFe_2O_4$ dosage (Conditions: $[TCS]_0$ = 0.03 mM; pH 7)

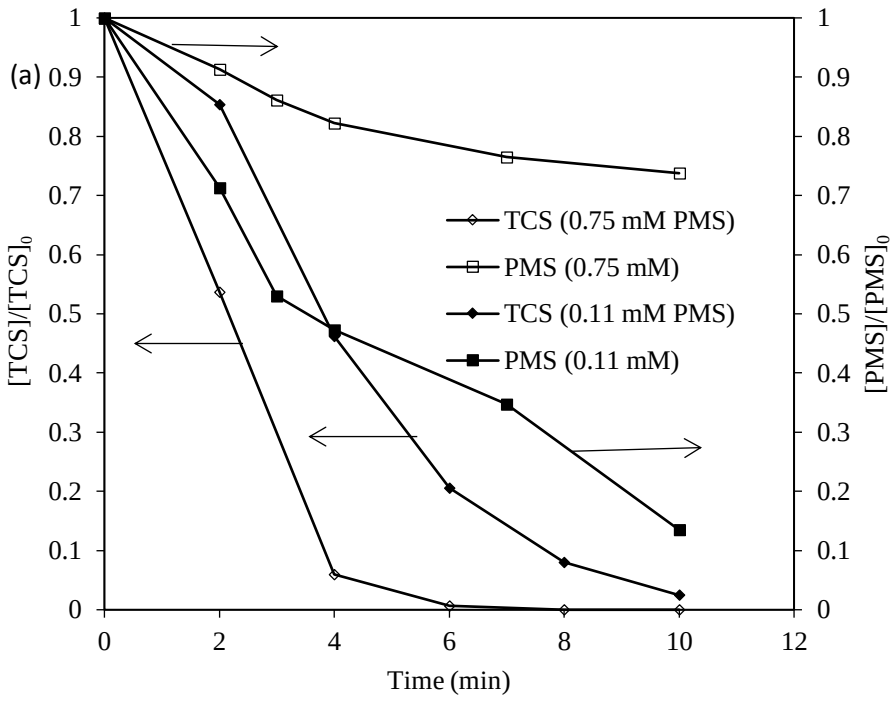

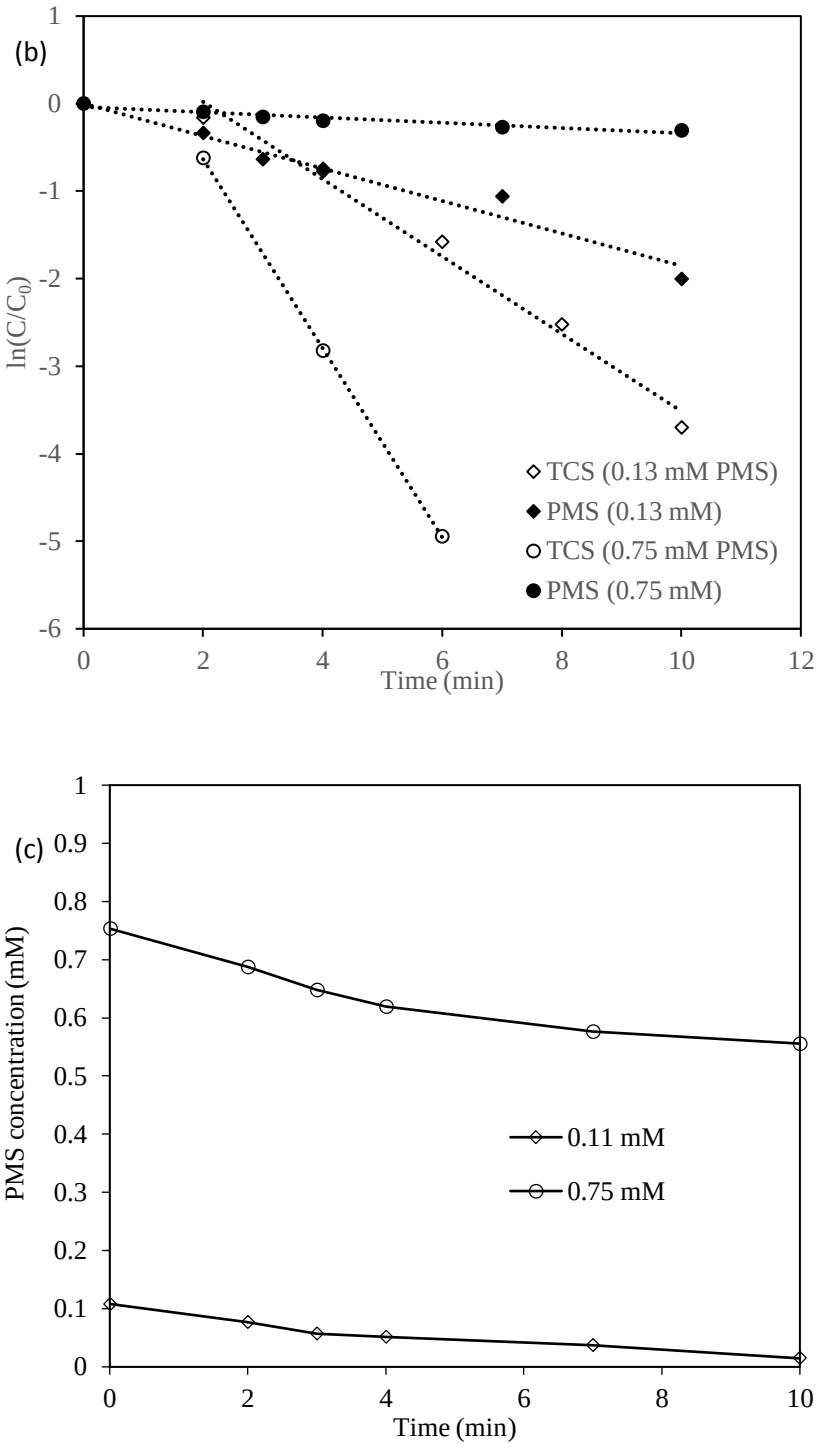

Figure 5-20 PMS degradation by $MnFe_2O_4$ at initial PMS dosage at 0.11 and 0.75 mM (Conditions: $[MnFe_2O_4]_0$ = 0.75 g/L; $[TCS]_0$ = 0.03 mM; pH 7)

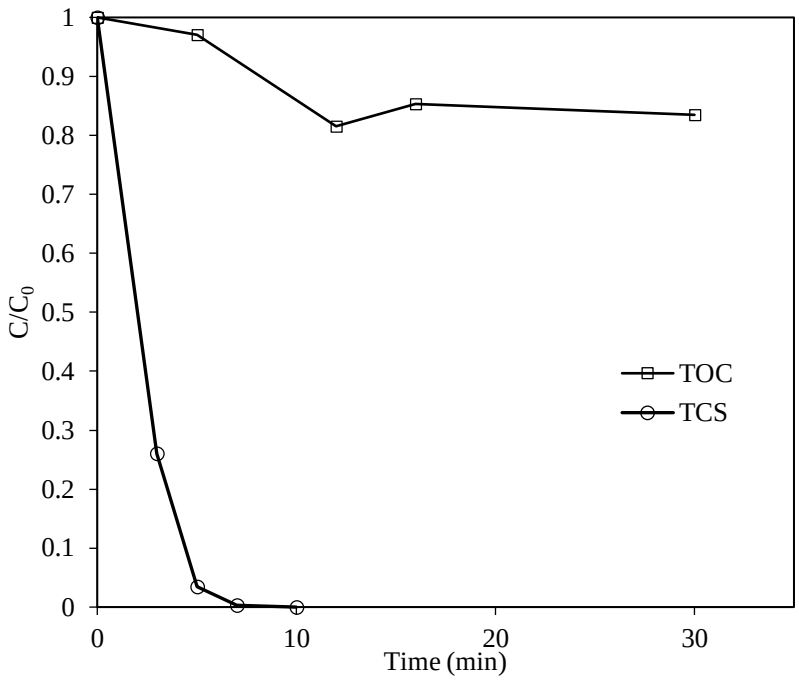

Figure 5-21 Total organic carbon measurement of TCS (Conditions: $[MnFe_2O_4]_0$ = 0.75 g/L; $[PMS]_0$ = 0.75mM; $[TCS]_0$ = 0.03 mM; pH_i 7)

Recyclability of $MnFe_2O_4$

Recyclability of catalysts is an important feature for heterogeneous system. Figure 5-22 shows the performance of $MnFe_2O_4$ in removing TCS in the presence of PMS at pH 7.0. It is interesting to note that the performance actually improved when $MnFe_2O_4$ was recycled in the second and third cycle and then plateaued afterwards. In light of this result, it is hypothesized that there were some changes in $MnFe_2O_4$ during the first cycle, which then contributed to the increase in both $k_{lagphase}$ and $k_{activated}$ in the subsequent phase. To test this theory, PMS was not added in the second cycle to test whether used $MnFe_2O_4$ alone could remove TCS. The results are shown in Figure 5-23. As mentioned previously unused $MnFe_2O_4$ had no effect on TCS at neutral pH. The results confirm that even without addition of PMS, TCS was completely removed in 20 minutes

comparing to 7 minutes in cycle 1. From Figure 5-23, it can be noted that the second cycle lacked a lag phase.

Figure 5-24 shows XPS analysis performed on the used and used $MnFe_2O_4$. There was little change in the oxidation state of Fe and Mn over 5 cycles but it can be observed from O 1s spectra that after the first cycle, an additional peak at binding energy of 533.6 eV appeared, which is a characteristic peak for C-O. After the fifth cycle, the peak become more prominent which reflects the accumulation of TCS or its transformed products on the surface of $MnFe_2O_4$. Figure 5-25 shows the magnetic hysteresis loop of $MnFe_2O_4$ before and after uses. Both used and unused $MnFe_2O_4$ exhibited good magnetic property and thus can easily be recovered by applying a magnetic field.

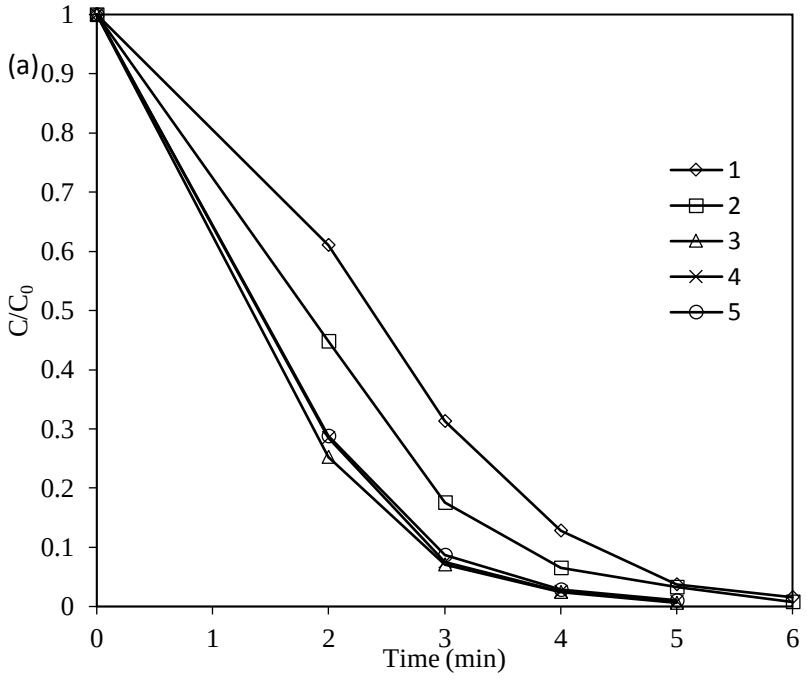

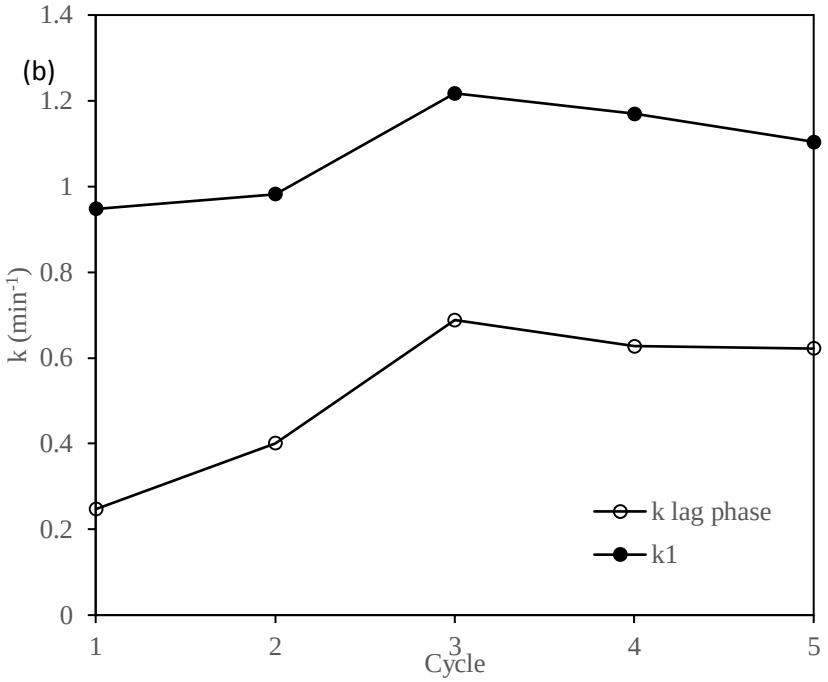

Figure 5-22 Recyclability of TCS (a) decay curve; (b) Trend of k with respect to number of cycle (Conditions: $[MnFe_2O_4]_0$ = 0.75 g/L; $[PMS]_0$ = 0.75 mM; pH_i 7)

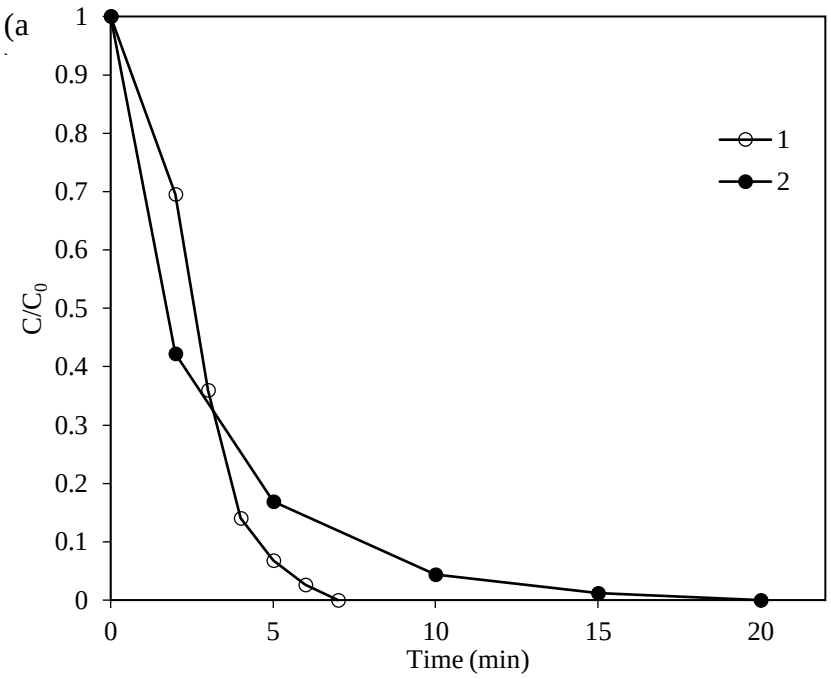

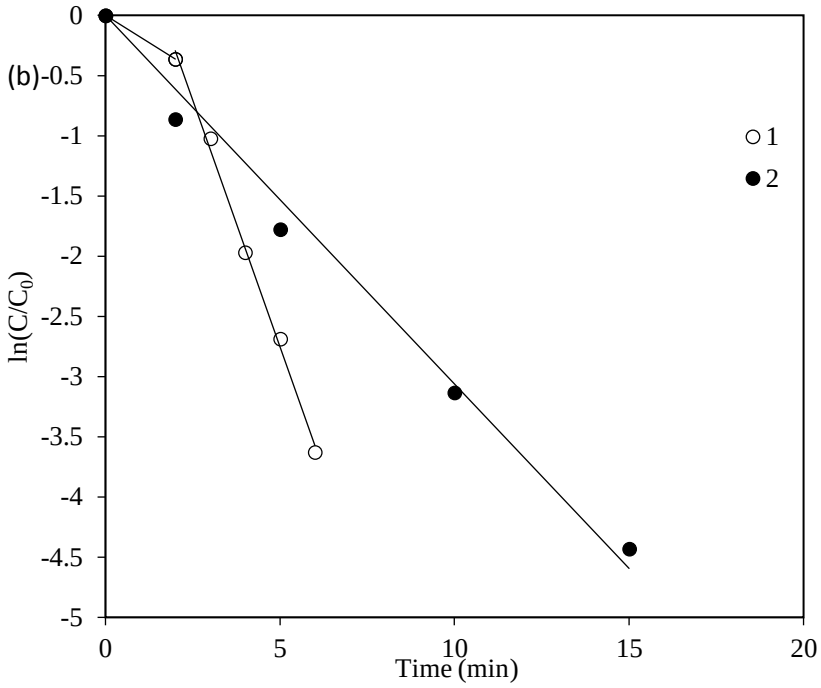

Figure 5-23 Recycle of $MnFe_2O_4$ without addition of PMS in the second cycle (Conditions: $[MnFe_2O_4]_0$ = 0.75 g/L; $[PMS]_0$ (1st cycle) = 0 mM; $[PMS]_0$ (2nd cycle) = 0.75 mM; pH_i 7)

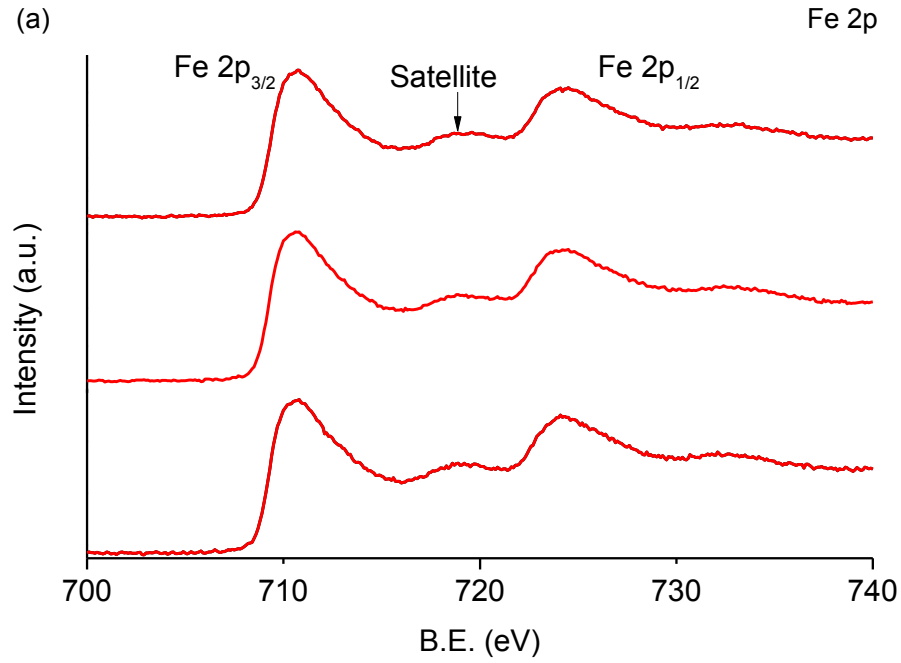

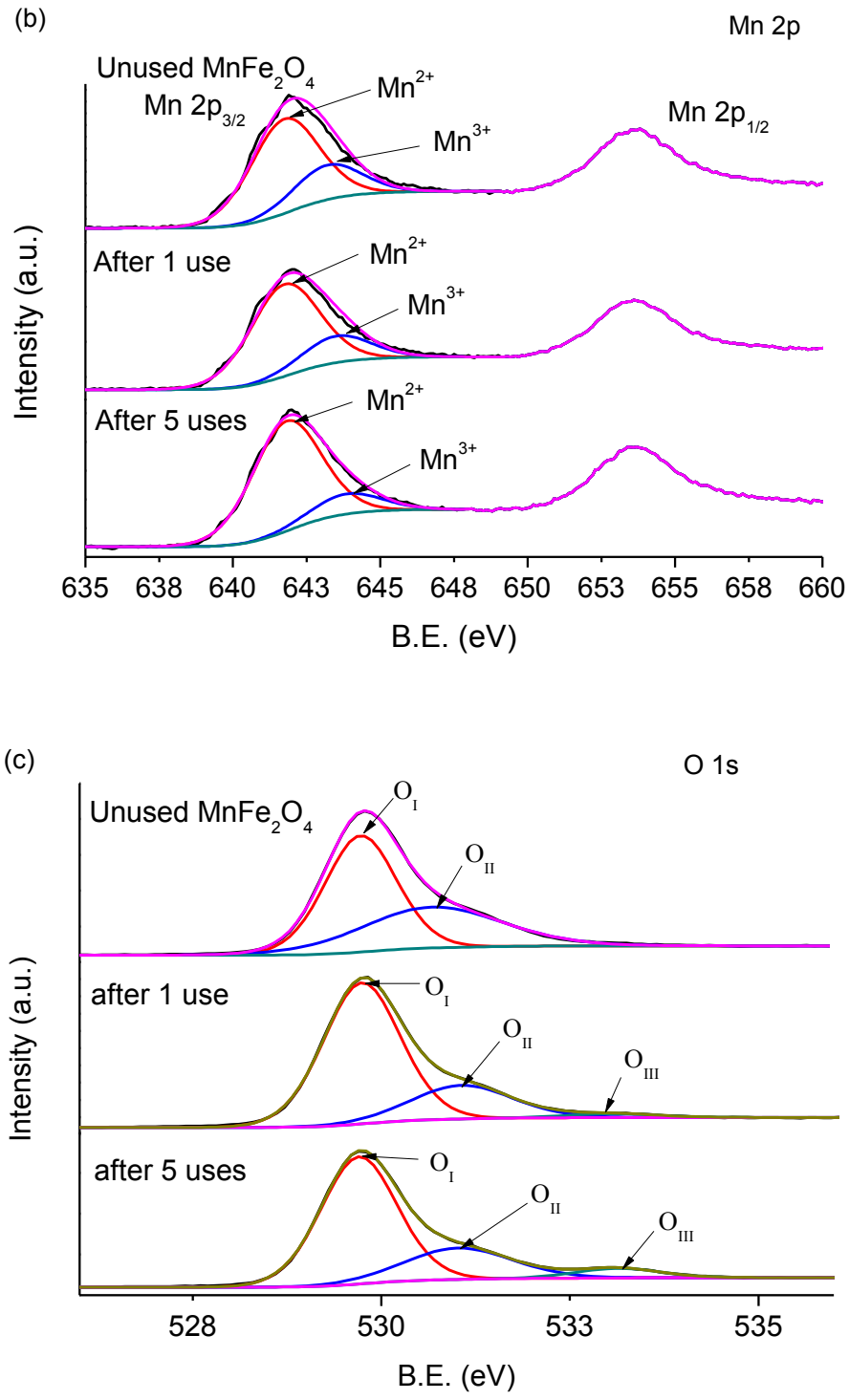

Figure 5-24 XPS spectra of unused and used $MnFe_2O_4$: (a) Fe 2p; (b) Mn 2p; (c) O 1s

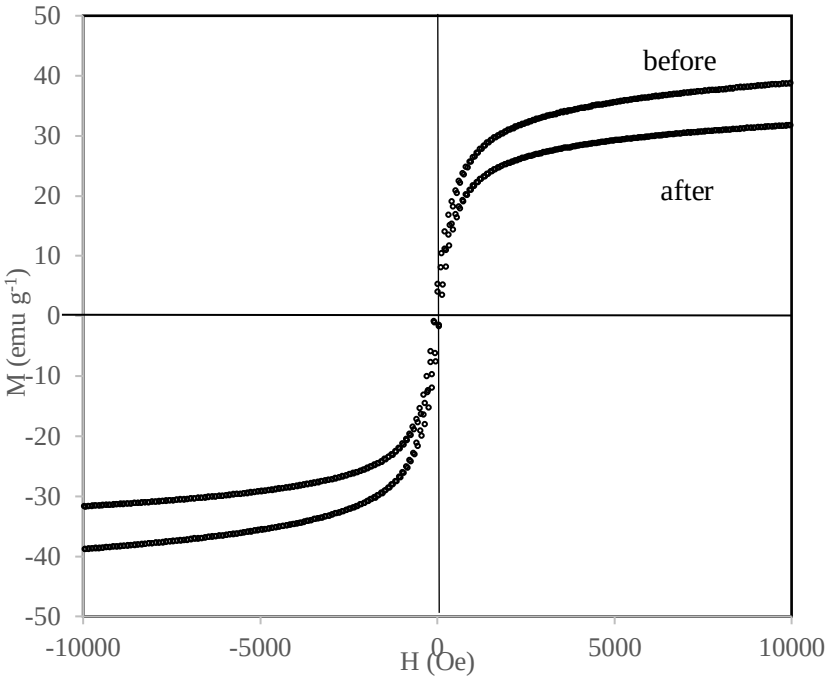

Figure 5-25 Magnetic hysteresis loop of $MnFe_2O_4$ before and after use

Effect of secondary effluent

In practical application, the matrix of the reaction medium is usually much more complicated. To evaluate the applicability of $MnFe_2O_4$/PMS system, secondary effluent was added to the TCS solution. Characteristics of the effluent were given in section 3.1. The lag phase was not quite affected but the activated phase was slowed by 48% (Figure 5-26) but TCS was still efficiently removed in 15 minutes. This could be due to the occupation of active sites by organic matters in the effluent or the reaction of radicals with ions to generate weaker radicals.

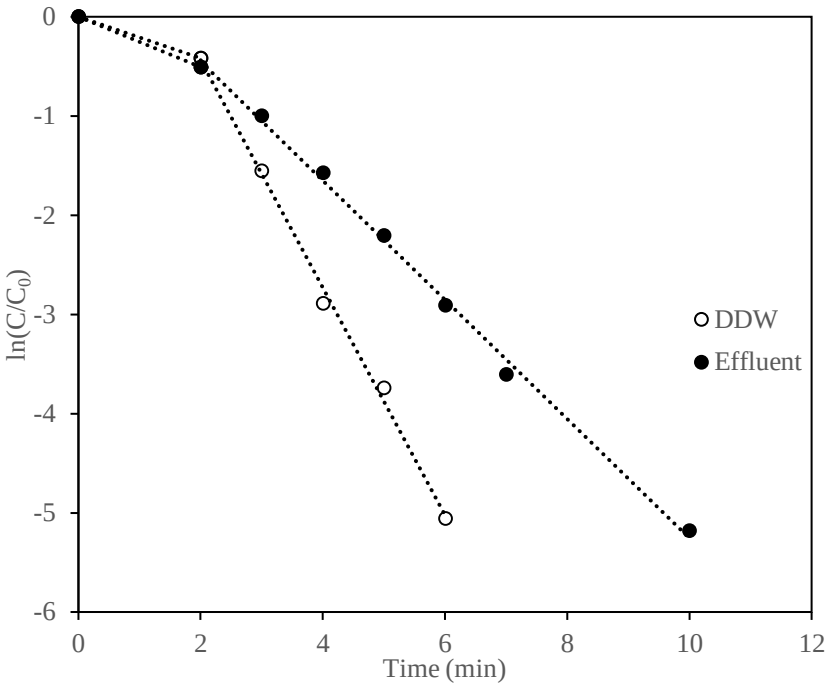

Figure 5-26 Effect of secondary effluent in the removal of TCS by $MnFe_2O_4$/PMS (Conditions: $[MnFe_2O_4]_0$ =0.75 g/L; $[PMS]_0$ = 0.75 mM; pH_i = 6.0)

Table 5-1 Reaction rate constants of the removal of TCS in DDW and Effluent matrix

	$k_{lagphase}$ (min^{-1})	k_1 (min^{-1})
DDW	0.2087	1.1464
Effluent	0.2532	0.6006

5.3 Toxicity Assessment utilizing mortality and vitality of A. salina

The toxicity of TCS and its degradation products was evaluated by studying their effect on Artemia salina (brine shrimp). The objective of the test was to determine whether the chemicals used in the treatment method and the degradation products generated posed threats to aquatic species.

The brine shrimp A. salina was chosen as target in this toxicity study for various reasons. First, it is a microplanktonic filter feeder that is often used as live food for other aquaculture organisms such as fish larvae [162]. The effect on this species could be biomagnified up the food chain. Second, the culture cost is low and the generation time is short. Besides, their sensitiveness towards environment also makes them popular test subjects in toxicity assessment of pollutants in aquatic environment [163-167].

The condition of the A. salina larvae after incubating with samples taken during the course of treatment was observed and quantified. Figure 5-28 shows the toxicity test results of the TCS treatment by $MnFe_2O_4$ alone at pH 3.3 while Figure 5-29 shows that by $MnFe_2O_4$/PMS at pH 7.0. At the beginning of the tests, all the larvae died upon exposure to TCS, which means that TCS at the concentration used in this study was acutely toxic to A. salina. When treated by $MnFe_2O_4$ alone, the mortality rate decreased and the vitality improved as TCS concentration decreases. All the larvae survived and were swimming when no TCS was detected. The intermediates generated during treatment did not appear to have posed significant toxicity to the brine shrimps nor affected the mobility of the species. However, when PMS is used, the survival rate dropped to below 40% even no TCS can be detected in the reactor and none of the brine shrimp tested were swimming in all the samples tested. Either the chemical used in the treatment process or the intermediates generated crippled the brine shrimps and notably influenced their survival.

Previous sections show that $MnFe_2O_4$/PMS trumps $MnFe_2O_4$ alone system in all the parameters studied. The addition of PMS significantly shortened the reaction time for

TCS degradation (from 4 hours to within 20 minutes) and allowed treatment to proceed effectively in a broader pH range. This study shows that the use of PMS has one major drawback. Although it is much more efficient, the treatment method could potentially disrupt the delicate balance of aquatic species and ecosystem in practical application. In view of this finding, a treatment method that could combine the advantages of both $MnFe_2O_4$ and $MnFe_2O_4$/PMS systems was considered and further explored.

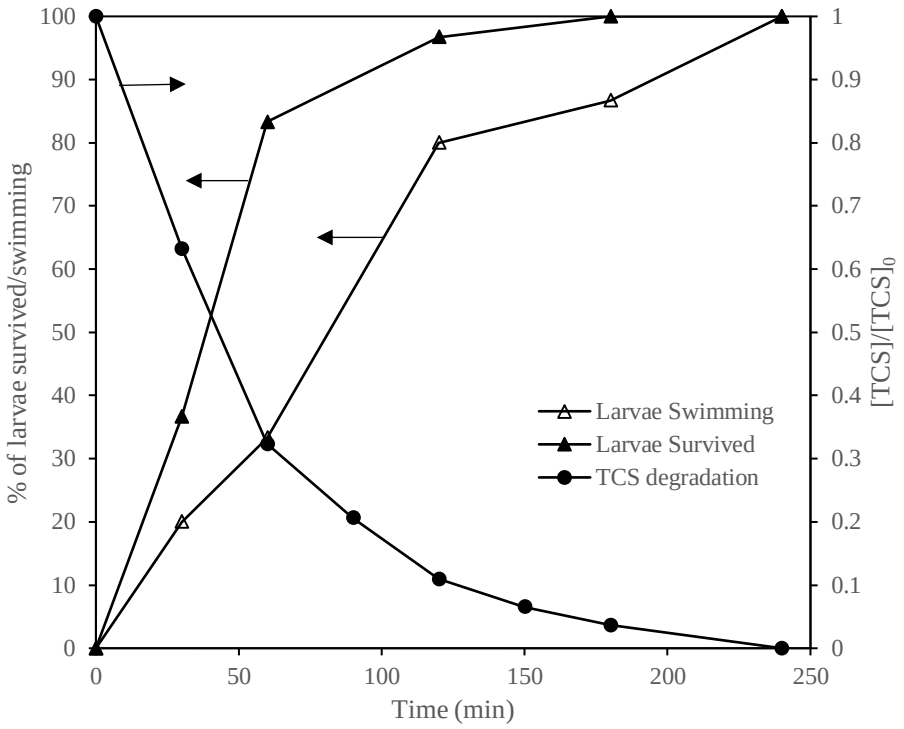

Figure 5-27 Effect of TCS and degradation products from the treatment using $MnFe_2O_4$ alone at pH 3.3 on the survival and vitality of A. salina

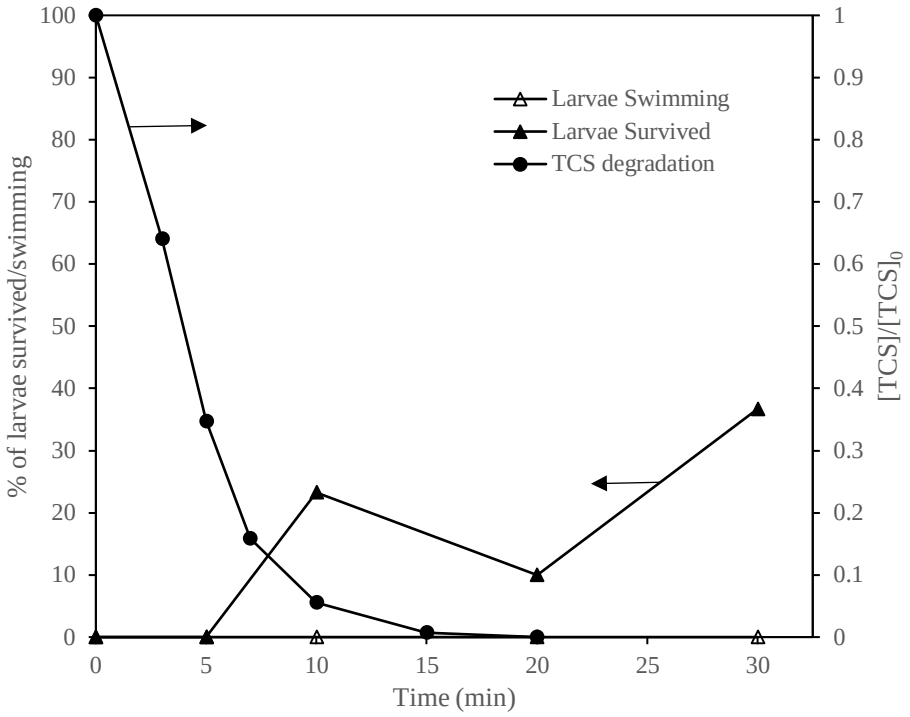

Figure 5-28 Effect of TCS and degradation products from the treatment using $MnFe_2O_4$/PMS at pH 7.0 on the survival and vitality of A. salina

5.4 Pre-activation of $MnFe_2O_4$ by acid, PS and PMS at pH 3 and 7

In section 5.2.2, it was found that PMS can alter the surface of $MnFe_2O_4$ and the resulting structure can remove TCS without the presence of any oxidant. It is hypothesized that PS and acid could also bring about such changes. Therefore, an experiment is designed to test (1) whether the altered $MnFe_2O_4$ can remove TCS in neutral condition, in which the original $MnFe_2O_4$ has no effect on TCS; (2) whether PS and acid can exert similar effect on $MnFe_2O_4$ as PMS does; and (3) the extent of activation by PS and PMS at pH 3 and 7. The new approach was to pre-treat $MnFe_2O_4$ with acid, PMS or PS and evaluate TCS degradation by the pretreated $MnFe_2O_4$ at neutral pH without additional oxidant.

The results from the toxicity test in the previous section also provide an incentive for exploring pre-activation of $MnFe_2O_4$ with acid or oxidants and eliminating *in situ* oxidants. It is desirable to take advantage of the superior performance brought about by oxidants and the low toxicity of $MnFe_2O_4$ alone system as compared to $MnFe_2O_4$/PMS as seen in section 5.3. Besides, concerns have been raised over the potential hazard of residual PMS in water and the byproducts of SR-AOP including the formation of ClO_3^- /BrO_3^-, halogenated disinfection byproducts[168], and sulfate anions [169]. These potential challenges can be alleviated by removing *in situ* PMS or PS.

Figure 5-29 shows the performance of five pre-treated $MnFe_2O_4$ on the removal of TCS at pH 7. It appears that changes that were made to the surface of $MnFe_2O_4$ were lasting. Even after being washed thoroughly, the used $MnFe_2O_4$ can still remove TCS by itself without addition of oxidants. Although acidic solution by itself can activate $MnFe_2O_4$, PMS was found to activate $MnFe_2O_4$ to the same extent whether the activation took place in acidic or neutral conditions. This corroborates the findings previously that removal of TCS by in-situ $MnFe_2O_4$/PMS system made more efficient use of PMS in neutral pH range than in low pH conditions. On the other hand, the activation of $MnFe_2O_4$ by PS was better at pH 3 than pH 7. The addition of PS to $MnFe_2O_4$ in acidic solution increased the subsequent removal of TCS at neutral pH from 53% to 72%, which, in other words, represented a 35% improvement. When activated at pH 7 by PS, $MnFe_2O_4$ was capable of removing 25% TCS at neutral pH. Generally, $MnFe_2O_4$ can be activated by acid, PS and PMS for the removal of TCS at neutral pH.

It is obvious from Figure 5-29 that PMS has superiority over PS and acid in the enhancing the performance of $MnFe_2O_4$ in TCS degradation in neutral pH. Although *in*

situ PMS still outperformed pre-activation by PMS, TCS degradation by $MnFe_2O_4$ at neutral pH range was made possible and was more efficient than degradation by $MnFe_2O_4$ alone at pH 3.3.

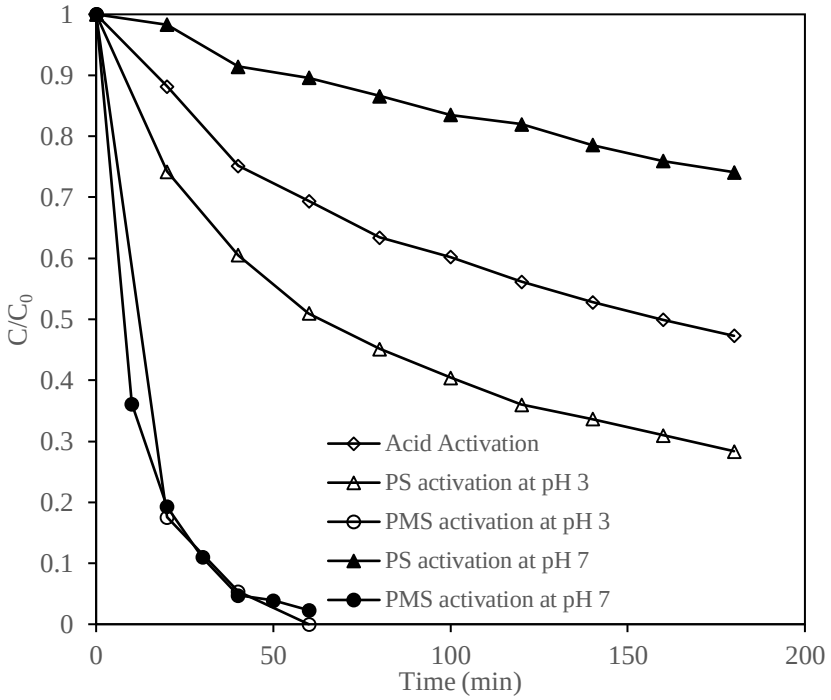

Figure 5-29 Degradation of TCS at neutral pH by $MnFe_2O_4$ activated by acid, PS, and PMS (Conditions: $[MnFe_2O_4]_0$ = 0.25 g/L; $[oxidant]_0$ = 1.0 mM; $[TCS]_0$ = 0.03 mM)

5.5 Reaction mechanism

According to literature, degradation of TCS by Mn-containing catalysts could proceed through two main pathways:

(1) Radical Pathway

In the presence of oxidants such as PMS and PS, surface-bound sulfate radical could be generated by the inner coordinated complex forming between Mn and Fe on the $MnFe_2O_4$ and oxidant [159]:

$$\equiv Mn(II)\text{-}OH^- + HSO_5^- \rightarrow \equiv Mn(III)\text{-}OH\text{-}OSO_3^- + OH^- \quad (5\text{-}6)$$

$$\equiv Mn(III)\text{-}OH\text{-}OSO_3^- \rightarrow \equiv Mn(II)\text{-}^-OH\text{-}\ (SO_4^{-\bullet}) \quad (5\text{-}7)$$

$$\equiv Mn(III)\text{-}OH^- + HSO_5^- \rightarrow \equiv Mn(II)\text{-}OOSO_3^{-\bullet} + H_2O \quad (5\text{-}8)$$

$$\equiv Fe(III)\text{-}OH^- + HSO_5^- \rightarrow \equiv Fe(II)\text{-}\ OOSO_3^{-\bullet} + H_2O \quad (5\text{-}9)$$

$$\equiv Fe(II)\text{-}OH^- + HSO_5^- \rightarrow \equiv Fe(III)\text{-}\ OH\text{-}\ (SO_4^{-\bullet})\ + OH^- \quad (5\text{-}10)$$

The bound sulfate radical could react with TCS, coupled with the catalyst or release into solution. SO_5^- radical was too weak for effective oxidation.

(2) Non-radical pathway (as described in Section 5.1 in this thesis)

TCS formed complex with Mn(III) on $MnFe_2O_4$ and electron transfers from Mn(III) to TCS to form phenoxy radicals, which was followed by the release of Mn^{2+} and phenoxy radicals (Reaction 5-1 to 5-5). Dimers and polymers were the likely resulting products of this pathway.

Based on the results in this chapter, non-radical pathway is likely the major player in the degradation of TCS by $MnFe_2O_4$ in the presence of PMS or PS whereas radical pathway plays a minor role. Observations leading to this conclusion are recapitulated as follows:

(1) After $MnFe_2O_4$ was exposed to PMS or PS, the performance of the catalyst alone without any oxidant in the degradation of TCS at neutral pH was greatly enhanced. In the absence of oxidant, the removal of TCS most likely proceeded

through non-radical pathway. With the continuous supply of oxidants, performance in terms of kinetics brought by this pathway would be expected to further improve.

(2) Most known effective sulfate and hydroxyl radicals quenchers (such as tert-butanol and ethanol) had no noticeable effect on the degradation rate even at high dosage.

(3) Autocatalysis observed for $MnFe_2O_4$ /PS system at pH 4 or above but not at pH 3 was likely due to the changes made on the surface of $MnFe_2O_4$ by PS. The catalyst subsequently became more efficient in removing TCS through non-radical pathway (Figure 5-10), while at pH 3, non-radical pathway was already available (Figure 5-1).

Chapter Six Conclusion

The removal of triclosan (TCS) by Fe_3O_4 was investigated. PMS was found to be a more effective oxidant (comparing to H_2O_2 and $K_2S_2O_8$) when used in combination with Fe_3O_4. The study was therefore focused on the use of Fe_3O_4/PMS for the TCS degradation. The adsorption of TCS onto Fe_3O_4 is a fast process and is strongly affected by the initial pH level and Fe_3O_4 dosage. About 26 – 30 % TCS was adsorbed at pH 2 – 6. When the pH further increased to 8 or above, significant decrease in TCS adsorption was observed due to the electrostatic repulsion between negatively charged Fe_3O_4 and TCS. The adsorption of TCS generally increases with Fe_3O_4 dosage (16% at 0.25 g/L to 35% at 1.5 g/L). The kinetics of TCS degradation and the effect of Fe_3O_4 dosage, PMS dosage and initial pH were studied. TCS removal is proportional to the Fe_3O_4 dosage at initial pH 3.7, 6.0 and 9.0 with the best performance at initial pH 9 and an optimum TCS to PMS ratio at 1:25. TCS was completely degraded from the solution in 2 hours. The effect of PMS dosage is more significant at the neutral pH range (6 – 9), in which the initial pH below 5 and above 10 yields low rate constants. The reaction rate depends strongly on the charges of Fe_3O_4, PMS and TCS at different pH. The process is dominated in heterogeneous rather than homogeneous phase, based on the observation of iron leaching.

The degradation of TCS by $MnFe_2O_4$ with and without oxidant was also studied. XPS analysis reveals that most of the manganese in $MnFe_2O_4$ were of 2+ oxidation state with a small portion of 3+ oxidation state, iron were of 3+ oxidation state. Without oxidant, significant removal of TCS by $MnFe_2O_4$ alone was only observed at pH 3.3 and below. At low pH, surface Mn(III) oxidizes TCS and releases Mn(II) ions. The addition of

Mn(II) slows the oxidation of TCS by $MnFe_2O_4$ through sorption to the surface active sites.

The effect of three different oxidants (H_2O_2, PMS and PS) were tested at acidic, neutral and basic conditions. The performance of the oxidants were in the following order: PMS > PS > H_2O_2. Although H_2O_2 was rapidly degraded, it was found to inhibit the oxidation of TCS by $MnFe_2O_4$ possibly through the reduction of Mn(III) to Mn(II).

The removal of TCS by $MnFe_2O_4$/PS at pH 3 follows pseudo first-order kinetics while autocatalytic degradation of TCS was observed at pH 4.3 and above. A mathematical model was developed for the autocatalytic degradation of TCS by $MnFe_2O_4$/PS at pH 4.3. Model prediction was found to be a good fit with the experimental data.

$MnFe_2O_4$ has excellent recyclability with performance improved for two successive cycles and plateaued in the following two. The O 1s peak from XPS analysis shows that with each successive cycle, there was an increase in C-O on the surface of $MnFe_2O_4$ but the oxidation state of Mn and Fe remains relatively the same. For an initial $MnFe_2O_4$ dosage of 0.75, only about 0.2 mM PMS was degraded for the complete removal of TCS even if much more initial PMS dosage was added.

Although PMS enhanced performance notably, the degradation of TCS by $MnFe_2O_4$ alone at pH 3.3 was less toxic for brine shrimp. Recycled $MnFe_2O_4$ was found to be superior to unused ones in the subsequent cycle whether oxidant is present or not. A

new experimental procedure was therefore proposed and it was found that by pre-treating $MnFe_2O_4$ with acid, PMS and PS, it can be used in the removal of TCS in neutral pH without *in situ* oxidant. $MnFe_2O_4$ can be pre-activated by acid, PMS and PS for its use in the removal of TCS in neutral pH without oxidant. Non-radical pathway is believed to be the major degradation mechanism while radical pathway is minor.

Bibliography

[1] L.M. McMurry, M. Oethinger, S.B. Levy, Triclosan targets lipid synthesis, Nature, 394 (1998) 531-532.

[2] R.U. Halden, D.H. Paull, Co-Occurrence of Triclocarban and Triclosan in U.S. Water Resources, Environmental Science & Technology, 39 (2005) 1420-1426.

[3] A.G. Asimakopoulos, N.S. Thomaidis, K. Kannan, Widespread occurrence of bisphenol A diglycidyl ethers, p-hydroxybenzoic acid esters (parabens), benzophenone type-UV filters, triclosan, and triclocarban in human urine from Athens, Greece, Science of The Total Environment, 470–471 (2014) 1243-1249.

[4] X. Li, G.-G. Ying, J.-L. Zhao, Z.-F. Chen, H.-J. Lai, H.-C. Su, 4-Nonylphenol, bisphenol-A and triclosan levels in human urine of children and students in China, and the effects of drinking these bottled materials on the levels, Environment International, 52 (2013) 81-86.

[5] A.M. Calafat, X. Ye, L.-Y. Wong, J.A. Reidy, L.L. Needham, Urinary Concentrations of Triclosan in the U.S. Population: 2003–2004, Environmental Health Perspectives, 116 (2008) 303-307.

[6] M. Allmyr, M. Adolfsson-Erici, M.S. McLachlan, G. Sandborgh-Englund, Triclosan in plasma and milk from Swedish nursing mothers and their exposure via personal care products, Science of The Total Environment, 372 (2006) 87-93.

[7] L.-M.L. Toms, M. Allmyr, J.F. Mueller, M. Adolfsson-Erici, M. McLachlan, J. Murby, F.A. Harden, Triclosan in individual human milk samples from Australia, Chemosphere, 85 (2011) 1682-1686.

[8] L.-Q. Wang, C.N. Falany, M.O. James, TRICLOSAN AS A SUBSTRATE AND INHIBITOR OF 3′-PHOSPHOADENOSINE 5′-PHOSPHOSULFATE-SULFOTRANSFERASE AND UDP-GLUCURONOSYL TRANSFERASE IN

HUMAN LIVER FRACTIONS, Drug Metabolism and Disposition, 32 (2004) 1162-1169.

[9] M.N. Jacobs, G.T. Nolan, S.R. Hood, Lignans, bacteriocides and organochlorine compounds activate the human pregnane X receptor (PXR), Toxicology and Applied Pharmacology, 209 (2005) 123-133.

[10] J. Chen, K.C. Ahn, N.A. Gee, S.J. Gee, B.D. Hammock, B.L. Lasley, Antiandrogenic properties of parabens and other phenolic containing small molecules in personal care products, Toxicology and Applied Pharmacology, 221 (2007) 278-284.

[11] A. Ki Chang, Z. Bin, C. Jinggang, G. Cherednichenko, E. Sanmarti, M.S. Denison, B. Lasley, I.N. Pessah, D. Kültz, D.P.Y. Chang, S.J. Gee, B.D. Hammock, In Vitro Biologic Activities of the Antimicrobials Triclocarban, Its Analogs, and Triclosan in Bioassay Screens: Receptor-Based Bioassay Screens, Environmental Health Perspectives, 116 (2008) 1203-1210.

[12] K.B. Paul, J.M. Hedge, M.J. DeVito, K.M. Crofton, Developmental triclosan exposure decreases maternal and neonatal thyroxine in rats, Environmental Toxicology and Chemistry, 29 (2010) 2840-2844.

[13] P.E.A. Rodríguez, M.S. Sanchez, Maternal Exposure to Triclosan Impairs Thyroid Homeostasis and Female Pubertal Development in Wistar Rat Offspring, Journal of Toxicology and Environmental Health, Part A, 73 (2010) 1678-1688.

[14] N. Veldhoen, R.C. Skirrow, H. Osachoff, H. Wigmore, D.J. Clapson, M.P. Gunderson, G. Van Aggelen, C.C. Helbing, The bactericidal agent triclosan modulates thyroid hormone-associated gene expression and disrupts postembryonic anuran development, Aquatic Toxicology, 80 (2006) 217-227.

[15] T. Geens, H. Neels, A. Covaci, Distribution of bisphenol-A, triclosan and n-nonylphenol in human adipose tissue, liver and brain, Chemosphere, 87 (2012) 796-802.

[16] K.M. Crofton, K.B. Paul, M.J. DeVito, J.M. Hedge, Short-term in vivo exposure to the water contaminant triclosan: Evidence for disruption of thyroxine, Environmental Toxicology and Pharmacology, 24 (2007) 194-197.

[17] L.M. Zorrilla, E.K. Gibson, S.C. Jeffay, K.M. Crofton, W.R. Setzer, R.L. Cooper, T.E. Stoker, The Effects of Triclosan on Puberty and Thyroid Hormones in Male Wistar Rats, Toxicological Sciences, 107 (2009) 56-64.

[18] T.E. Stoker, E.K. Gibson, L.M. Zorrilla, Triclosan Exposure Modulates Estrogen-Dependent Responses in the Female Wistar Rat, Toxicological Sciences, 117 (2010) 45-53.

[19] G. Cherednichenko, R. Zhang, R.A. Bannister, V. Timofeyev, N. Li, E.B. Fritsch, W. Feng, G.C. Barrientos, N.H. Schebb, B.D. Hammock, K.G. Beam, N. Chiamvimonvat, I.N. Pessah, Triclosan impairs excitation–contraction coupling and Ca2+ dynamics in striated muscle, Proceedings of the National Academy of Sciences, 109 (2012) 14158-14163.

[20] E.B. Fritsch, R.E. Connon, I. Werner, R.E. Davies, S. Beggel, W. Feng, I.N. Pessah, Triclosan Impairs Swimming Behavior and Alters Expression of Excitation-Contraction Coupling Proteins in Fathead Minnow (Pimephales promelas), Environmental Science & Technology, 47 (2013) 2008-2017.

[21] E.M.R. Clayton, M. Todd, J.B. Dowd, A.E. Aiello, The Impact of Bisphenol A and Triclosan on Immune Parameters in the U.S. Population, NHANES 2003-2006, Environmental Health Perspectives, 119 (2011) 390-396.

[22] G.-G. Ying, R.S. Kookana, Triclosan in wastewaters and biosolids from Australian wastewater treatment plants, Environment International, 33 (2007) 199-205.

[23] S. Kleywegt, V. Pileggi, P. Yang, C. Hao, X. Zhao, C. Rocks, S. Thach, P. Cheung, B. Whitehead, Pharmaceuticals, hormones and bisphenol A in untreated source and finished drinking water in Ontario, Canada — Occurrence and treatment efficiency, Science of The Total Environment, 409 (2011) 1481-1488.

[24] W. Hua, E.R. Bennett, R.J. Letcher, Triclosan in waste and surface waters from the upper Detroit River by liquid chromatography-electrospray-tandem quadrupole mass spectrometry, Environment International, 31 (2005) 621-630.

[25] M. Lv, Q. Sun, A. Hu, L. Hou, J. Li, X. Cai, C.-P. Yu, Pharmaceuticals and personal care products in a mesoscale subtropical watershed and their application as sewage markers, Journal of Hazardous Materials, 280 (2014) 696-705.

[26] Q. Bu, B. Wang, J. Huang, S. Deng, G. Yu, Pharmaceuticals and personal care products in the aquatic environment in China: A review, Journal of Hazardous Materials, 262 (2013) 189-211.

[27] Q. Sun, M. Lv, A. Hu, X. Yang, C.-P. Yu, Seasonal variation in the occurrence and removal of pharmaceuticals and personal care products in a wastewater treatment plant in Xiamen, China, Journal of Hazardous Materials, 277 (2014) 69-75.

[28] L. Wang, G.-G. Ying, F. Chen, L.-J. Zhang, J.-L. Zhao, H.-J. Lai, Z.-F. Chen, R. Tao, Monitoring of selected estrogenic compounds and estrogenic activity in surface water and sediment of the Yellow River in China using combined chemical and biological tools, Environmental Pollution, 165 (2012) 241-249.

[29] L. Wang, G.-G. Ying, J.-L. Zhao, S. Liu, B. Yang, L.-J. Zhou, R. Tao, H.-C. Su, Assessing estrogenic activity in surface water and sediment of the Liao River system in

northeast China using combined chemical and biological tools, Environmental Pollution, 159 (2011) 148-156.

[30] J. Gasperi, D. Geara, C. Lorgeoux, A. Bressy, S. Zedek, V. Rocher, A. El Samrani, G. Chebbo, R. Moilleron, First assessment of triclosan, triclocarban and paraben mass loads at a very large regional scale: Case of Paris conurbation (France), Science of The Total Environment, 493 (2014) 854-861.

[31] P. Pothitou, D. Voutsa, Endocrine disrupting compounds in municipal and industrial wastewater treatment plants in Northern Greece, Chemosphere, 73 (2008) 1716-1723.

[32] N.K. Stamatis, I.K. Konstantinou, Occurrence and removal of emerging pharmaceutical, personal care compounds and caffeine tracer in municipal sewage treatment plant in Western Greece, Journal of Environmental Science & Health, Part B -- Pesticides, Food Contaminants, & Agricultural Wastes, 48 (2013) 800-813.

[33] A.S. Stasinakis, G. Gatidou, D. Mamais, N.S. Thomaidis, T.D. Lekkas, Occurrence and fate of endocrine disrupters in Greek sewage treatment plants, Water Research, 42 (2008) 1796-1804.

[34] C.I. Kosma, D.A. Lambropoulou, T.A. Albanis, Investigation of PPCPs in wastewater treatment plants in Greece: Occurrence, removal and environmental risk assessment, Science of The Total Environment, 466–467 (2014) 421-438.

[35] I. Nishi, T. Kawakami, S. Onodera, Monitoring of Triclosan in the Surface Water of the Tone Canal, Japan, Bull Environ Contam Toxicol, 80 (2008) 163-166.

[36] T. Okumura, Y. Nishikawa, Gas chromatography—mass spectrometry determination of triclosans in water, sediment and fish samples via methylation with diazomethane, Analytica Chimica Acta, 325 (1996) 175-184.

[37] S.K. Behera, H.W. Kim, J.-E. Oh, H.-S. Park, Occurrence and removal of antibiotics, hormones and several other pharmaceuticals in wastewater treatment plants of the largest industrial city of Korea, Science of The Total Environment, 409 (2011) 4351-4360.

[38] S.D. Kim, J. Cho, I.S. Kim, B.J. Vanderford, S.A. Snyder, Occurrence and removal of pharmaceuticals and endocrine disruptors in South Korean surface, drinking, and waste waters, Water Research, 41 (2007) 1013-1021.

[39] J.L. Santos, I. Aparicio, M. Callejón, E. Alonso, Occurrence of pharmaceutically active compounds during 1-year period in wastewaters from four wastewater treatment plants in Seville (Spain), Journal of Hazardous Materials, 164 (2009) 1509-1516.

[40] R. Rosal, A. Rodríguez, J.A. Perdigón-Melón, A. Petre, E. García-Calvo, M.J. Gómez, A. Agüera, A.R. Fernández-Alba, Occurrence of emerging pollutants in urban wastewater and their removal through biological treatment followed by ozonation, Water Research, 44 (2010) 578-588.

[41] M. Pedrouzo, F. Borrull, R.M. Marcé, E. Pocurull, Ultra-high-performance liquid chromatography–tandem mass spectrometry for determining the presence of eleven personal care products in surface and wastewaters, Journal of Chromatography A, 1216 (2009) 6994-7000.

[42] G.C.C. Yang, C.-H. Yen, C.-L. Wang, Monitoring and removal of residual phthalate esters and pharmaceuticals in the drinking water of Kaohsiung City, Taiwan, Journal of Hazardous Materials, 277 (2014) 53-61.

[43] B. Petrie, E.J. McAdam, J.N. Lester, E. Cartmell, Obtaining process mass balances of pharmaceuticals and triclosan to determine their fate during wastewater treatment, Science of The Total Environment, 497–498 (2014) 553-560.

[44] K. Kumar, S.M. Priya, A. Peck, K. Sajwan, Mass Loadings of Triclosan and Triclocarbon from Four Wastewater Treatment Plants to Three Rivers and Landfill in Savannah, Georgia, USA, Arch Environ Contam Toxicol, 58 (2010) 275-285.

[45] N.A. Andrade, N. Lozano, L.L. McConnell, A. Torrents, C.P. Rice, M. Ramirez, Long-term trends of PBDEs, triclosan, and triclocarban in biosolids from a wastewater treatment plant in the Mid-Atlantic region of the US, Journal of Hazardous Materials, 282 (2015) 68-74.

[46] J. Heidler, R.U. Halden, Mass balance assessment of triclosan removal during conventional sewage treatment, Chemosphere, 66 (2007) 362-369.

[47] C.-P. Yu, K.-H. Chu, Occurrence of pharmaceuticals and personal care products along the West Prong Little Pigeon River in east Tennessee, USA, Chemosphere, 75 (2009) 1281-1286.

[48] P.M. Thomas, G.D. Foster, Tracking acidic pharmaceuticals, caffeine, and triclosan through the wastewater treatment process, Environmental Toxicology and Chemistry, 24 (2005) 25-30.

[49] H. Singer, S. Müller, C. Tixier, L. Pillonel, Triclosan: Occurrence and Fate of a Widely Used Biocide in the Aquatic Environment: Field Measurements in Wastewater Treatment Plants, Surface Waters, and Lake Sediments, Environmental Science & Technology, 36 (2002) 4998-5004.

[50] A. Lindström, I.J. Buerge, T. Poiger, P.-A. Bergqvist, M.D. Müller, H.-R. Buser, Occurrence and Environmental Behavior of the Bactericide Triclosan and Its Methyl Derivative in Surface Waters and in Wastewater, Environmental Science & Technology, 36 (2002) 2322-2329.

[51] R. Loos, R. Carvalho, D.C. António, S. Comero, G. Locoro, S. Tavazzi, B. Paracchini, M. Ghiani, T. Lettieri, L. Blaha, B. Jarosova, S. Voorspoels, K. Servaes, P.

Haglund, J. Fick, R.H. Lindberg, D. Schwesig, B.M. Gawlik, EU-wide monitoring survey on emerging polar organic contaminants in wastewater treatment plant effluents, Water Research, 47 (2013) 6475-6487.

[52] K. Bester, Triclosan in a sewage treatment process—balances and monitoring data, Water Research, 37 (2003) 3891-3896.

[53] P. Guerra, M. Kim, A. Shah, M. Alaee, S.A. Smyth, Occurrence and fate of antibiotic, analgesic/anti-inflammatory, and antifungal compounds in five wastewater treatment processes, Science of The Total Environment, 473–474 (2014) 235-243.

[54] N. Lozano, C.P. Rice, M. Ramirez, A. Torrents, Fate of Triclocarban, Triclosan and Methyltriclosan during wastewater and biosolids treatment processes, Water Research, 47 (2013) 4519-4527.

[55] USEPA, Targeted National Sewage Sludge Survey Statistical Analysis Report, in, United States Environmental Protection Agency, Office of Water, Washington DC, 2009.

[56] X. Chen, M.E. Casas, J.L. Nielsen, R. Wimmer, K. Bester, Identification of Triclosan-O-Sulfate and other transformation products of Triclosan formed by activated sludge, Science of The Total Environment, 505 (2015) 39-46.

[57] R. Addink, K. Olie, Mechanisms of Formation and Destruction of Polychlorinated Dibenzo-p-dioxins and Dibenzofurans in Heterogeneous Systems, Environmental Science & Technology, 29 (1995) 1425-1435.

[58] A. Kanetoshi, H. Ogawa, E. Katsura, H. Kaneshima, Chlorination of irgasan DP300 and formation of dioxins from its chlorinated derivatives, Journal of Chromatography A, 389 (1987) 139-153.

[59] J.M. Buth, M.R. Ross, K. McNeill, W.A. Arnold, Removal and formation of chlorinated triclosan derivatives in wastewater treatment plants using chlorine and UV disinfection, Chemosphere, 84 (2011) 1238-1243.

[60] S. Onodera, M. Ogawa, S. Suzuki, Chemical changes of organic compounds in chlorinated water : XIII. Gas chromatographic—mass spectrometric studies of the reactions of Irgasan DP 300 [5-chloro-2-(2,4-dichlorophenoxy_phenol] with chlorine in dilute aqueous solution, Journal of Chromatography A, 392 (1987) 267-275.

[61] P. Canosa, S. Morales, I. Rodríguez, E. Rubí, R. Cela, M. Gómez, Aquatic degradation of triclosan and formation of toxic chlorophenols in presence of low concentrations of free chlorine, Anal Bioanal Chem, 383 (2005) 1119-1126.

[62] K.L. Rule, V.R. Ebbett, P.J. Vikesland, Formation of Chloroform and Chlorinated Organics by Free-Chlorine-Mediated Oxidation of Triclosan, Environmental Science & Technology, 39 (2005) 3176-3185.

[63] D.C. McAvoy, B. Schatowitz, M. Jacob, A. Hauk, W.S. Eckhoff, Measurement of triclosan in wastewater treatment systems, Environmental Toxicology and Chemistry, 21 (2002) 1323-1329.

[64] T.J. Leiker, S.R. Abney, S.L. Goodbred, M.R. Rosen, Identification of methyl triclosan and halogenated analogues in male common carp (Cyprinus carpio) from Las Vegas Bay and semipermeable membrane devices from Las Vegas Wash, Nevada, Science of The Total Environment, 407 (2009) 2102-2114.

[65] K. Aranami, J.W. Readman, Photolytic degradation of triclosan in freshwater and seawater, Chemosphere, 66 (2007) 1052-1056.

[66] J.M. Buth, M. Grandbois, P.J. Vikesland, K. McNeill, W.A. Arnold, Aquatic photochemistry of chlorinated triclosan derivatives: Potential source of

polychlorodibenzo-P-dioxins, Environmental Toxicology and Chemistry, 28 (2009) 2555-2563.

[67] K. Inaba, T. Doi, N. Isobe, T. Yamamoto, Formation of bromo-substituted triclosan during chlorination by chlorine in the presence of trace levels of bromide, Water Research, 40 (2006) 2931-2937.

[68] P.J. Vikesland, E.M. Fiss, K.R. Wigginton, K. McNeill, W.A. Arnold, Halogenation of Bisphenol-A, Triclosan, and Phenols in Chlorinated Waters Containing Iodide, Environmental Science & Technology, 47 (2013) 6764-6772.

[69] J.-L. Zhao, G.-G. Ying, Y.-S. Liu, F. Chen, J.-F. Yang, L. Wang, Occurrence and risks of triclosan and triclocarban in the Pearl River system, South China: From source to the receiving environment, Journal of Hazardous Materials, 179 (2010) 215-222.

[70] M. Lv, Q. Sun, A. Hu, L. Hou, J. Li, X. Cai, C.-P. Yu, Pharmaceuticals and personal care products in a mesoscale subtropical watershed and their application as sewage markers, Journal of Hazardous Materials, 280 (2014) 696-705.

[71] M. Lv, Q. Sun, H. Xu, L. Lin, M. Chen, C.-P. Yu, Occurrence and fate of triclosan and triclocarban in a subtropical river and its estuary, Marine Pollution Bulletin, 88 (2014) 383-388.

[72] K. Bester, Fate of Triclosan and Triclosan-Methyl in Sewage TreatmentPlants and Surface Waters, Arch Environ Contam Toxicol, 49 (2005) 9-17.

[73] J.-L. Wu, N.P. Lam, D. Martens, A. Kettrup, Z. Cai, Triclosan determination in water related to wastewater treatment, Talanta, 72 (2007) 1650-1654.

[74] P. Gautam, J.S. Carsella, C.A. Kinney, Presence and transport of the antimicrobials triclocarban and triclosan in a wastewater-dominated stream and freshwater environment, Water Research, 48 (2014) 247-256.

[75] C. Tixier, H.P. Singer, S. Canonica, S.R. Müller, Phototransformation of Triclosan in Surface Waters: A Relevant Elimination Process for This Widely Used BiocideLaboratory Studies, Field Measurements, and Modeling, Environmental Science & Technology, 36 (2002) 3482-3489.

[76] D.E. Latch, J.L. Packer, W.A. Arnold, K. McNeill, Photochemical conversion of triclosan to 2,8-dichlorodibenzo-p-dioxin in aqueous solution, Journal of Photochemistry and Photobiology A: Chemistry, 158 (2003) 63-66.

[77] M. Mezcua, M.J. Gómez, I. Ferrer, A. Aguera, M.D. Hernando, A.R. Fernández-Alba, Evidence of 2,7/2,8-dibenzodichloro-p-dioxin as a photodegradation product of triclosan in water and wastewater samples, Analytica Chimica Acta, 524 (2004) 241-247.

[78] D.E. Latch, J.L. Packer, B.L. Stender, J. VanOverbeke, W.A. Arnold, K. McNeill, Aqueous photochemistry of triclosan: Formation of 2,4-dichlorophenol, 2,8-dichlorodibenzo-p-dioxin, and oligomerization products, Environmental Toxicology and Chemistry, 24 (2005) 517-525.

[79] X. Qiao, X. Zheng, Q. Xie, X. Yang, J. Xiao, W. Xue, J. Chen, Faster photodegradation rate and higher dioxin yield of triclosan induced by cationic surfactant CTAB, Journal of Hazardous Materials, 275 (2014) 210-214.

[80] A. Bianco, D. Fabbri, M. Minella, M. Brigante, G. Mailhot, V. Maurino, C. Minero, D. Vione, New insights into the environmental photochemistry of 5-chloro-2-(2,4-dichlorophenoxy)phenol (triclosan): Reconsidering the importance of indirect photoreactions, Water Research, 72 (2015) 271-280.

[81] M. Martínez-Zapata, C. Aristizábal, G. Peñuela, Photodegradation of the endocrine-disrupting chemicals 4n-nonylphenol and triclosan by simulated solar UV

irradiation in aqueous solutions with Fe(III) and in the absence/presence of humic acids, Journal of Photochemistry and Photobiology A: Chemistry, 251 (2013) 41-49.

[82] M.A. Coogan, R.E. Edziyie, T.W. La Point, B.J. Venables, Algal bioaccumulation of triclocarban, triclosan, and methyl-triclosan in a North Texas wastewater treatment plant receiving stream, Chemosphere, 67 (2007) 1911-1918.

[83] M.E. Balmer, T. Poiger, C. Droz, K. Romanin, P.-A. Bergqvist, M.D. Müller, H.-R. Buser, Occurrence of Methyl Triclosan, a Transformation Product of the Bactericide Triclosan, in Fish from Various Lakes in Switzerland, Environmental Science & Technology, 38 (2004) 390-395.

[84] N. Lozano, C.P. Rice, M. Ramirez, A. Torrents, Fate of triclosan in agricultural soils after biosolid applications, Chemosphere, 78 (2010) 760-766.

[85] G.-G. Ying, X.-Y. Yu, R.S. Kookana, Biological degradation of triclocarban and triclosan in a soil under aerobic and anaerobic conditions and comparison with environmental fate modelling, Environmental Pollution, 150 (2007) 300-305.

[86] C.A. Kinney, E.T. Furlong, D.W. Kolpin, M.R. Burkhardt, S.D. Zaugg, S.L. Werner, J.P. Bossio, M.J. Benotti, Bioaccumulation of Pharmaceuticals and Other Anthropogenic Waste Indicators in Earthworms from Agricultural Soil Amended With Biosolid or Swine Manure, Environmental Science & Technology, 42 (2008) 1863-1870.

[87] E. Butler, M.J. Whelan, R. Sakrabani, R. van Egmond, Fate of triclosan in field soils receiving sewage sludge, Environmental Pollution, 167 (2012) 101-109.

[88] J. Ding, M. Su, C. Wu, K. Lin, Transformation of triclosan to 2,8-dichlorodibenzo-p-dioxin by iron and manganese oxides under near dry conditions, Chemosphere, 133 (2015) 41-46.

[89] X. Peng, W. Ou, C. Wang, Z. Wang, Q. Huang, J. Jin, J. Tan, Occurrence and ecological potential of pharmaceuticals and personal care products in groundwater and reservoirs in the vicinity of municipal landfills in China, Science of The Total Environment, 490 (2014) 889-898.

[90] P.M. Buszka, D.J. Yeskis, D.W. Kolpin, E.T. Furlong, S.D. Zaugg, M.T. Meyer, Waste-Indicator and Pharmaceutical Compounds in Landfill-Leachate-Affected Ground Water near Elkhart, Indiana, 2000–2002, Bull Environ Contam Toxicol, 82 (2009) 653-659.

[91] A. Kanetoshi, H. Ogawa, E. Katsura, H. Kaneshima, T. Miura, Formation of polychlorinated dibenzo-p-dioxins upon combustion of commercial textile products containing 2,4,4′-trichloro-2′-hydroxydiphenyl ether (Irgasan® DP3000, Journal of Chromatography A, 442 (1988) 289-299.

[92] M. Munoz, Z.M. de Pedro, J.A. Casas, J.J. Rodriguez, Triclosan breakdown by Fenton-like oxidation, Chemical Engineering Journal, 198–199 (2012) 275-281.

[93] Z. Song, N. Wang, L. Zhu, A. Huang, X. Zhao, H. Tang, Efficient oxidative degradation of triclosan by using an enhanced Fenton-like process, Chemical Engineering Journal, 198–199 (2012) 379-387.

[94] P. Nfodzo, H. Choi, Triclosan decomposition by sulfate radicals: Effects of oxidant and metal doses, Chemical Engineering Journal, 174 (2011) 629-634.

[95] I. Sirés, N. Oturan, M.A. Oturan, R.M. Rodríguez, J.A. Garrido, E. Brillas, Electro-Fenton degradation of antimicrobials triclosan and triclocarban, Electrochimica Acta, 52 (2007) 5493-5503.

[96] H.-S. Son, J. Khim, K.-D. Zoh, Degradation of triclosan in the combined reaction of Fe2+ and UV-C: Comparison with the Fenton and photolytic reactions, Environmental Progress & Sustainable Energy, 29 (2010) 415-420.

[97] J.C. Yu, T.Y. Kwong, Q. Luo, Z. Cai, Photocatalytic oxidation of triclosan, Chemosphere, 65 (2006) 390-399.

[98] X. Chen, J. Richard, Y. Liu, E. Dopp, J. Tuerk, K. Bester, Ozonation products of triclosan in advanced wastewater treatment, Water Research, 46 (2012) 2247-2256.

[99] L. Sanchez-Prado, R. Barro, C. Garcia-Jares, M. Llompart, M. Lores, C. Petrakis, N. Kalogerakis, D. Mantzavinos, E. Psillakis, Sonochemical degradation of triclosan in water and wastewater, Ultrasonics Sonochemistry, 15 (2008) 689-694.

[100] Y.-Z. Ren, M. Franke, F. Anschuetz, B. Ondruschka, A. Ignaszak, P. Braeutigam, Sonoelectrochemical degradation of triclosan in water, Ultrasonics Sonochemistry, 21 (2014) 2020-2025.

[101] V. Bokare, K. Murugesan, Y.-M. Kim, J.-R. Jeon, E.-J. Kim, Y.S. Chang, Degradation of triclosan by an integrated nano-bio redox process, Bioresource Technology, 101 (2010) 6354-6360.

[102] Z. Zhang, X. Wang, Y. Xue, H. Li, W. Dong, Enhanced dechlorination of triclosan by hydrated electron reduction in aqueous solution, Chemical Engineering Journal, 263 (2015) 186-193.

[103] B. Yang, G.-G. Ying, J.-L. Zhao, L.-J. Zhang, Y.-X. Fang, L.D. Nghiem, Oxidation of triclosan by ferrate: Reaction kinetics, products identification and toxicity evaluation, Journal of Hazardous Materials, 186 (2011) 227-235.

[104] J. Jiang, S.-Y. Pang, J. Ma, Oxidation of Triclosan by Permanganate (Mn(VII)): Importance of Ligands and In Situ Formed Manganese Oxides, Environmental Science & Technology, 43 (2009) 8326-8331.

[105] H. Zhang, C.-H. Huang, Oxidative Transformation of Triclosan and Chlorophene by Manganese Oxides, Environmental Science & Technology, 37 (2003) 2421-2430.

[106] P. Neta, R.E. Huie, A.B. Ross, Rate Constants for Reactions of Inorganic Radicals in Aqueous Solution, Journal of Physical and Chemical Reference Data, 17 (1988) 1027-1284.

[107] P. Neta, V. Madhavan, H. Zemel, R.W. Fessenden, Rate constants and mechanism of reaction of so4·- with aromatic compounds, Journal of the American Chemical Society, 99 (1977) 163-164.

[108] M.G. Antoniou, A.A. de la Cruz, D.D. Dionysiou, Degradation of microcystin-LR using sulfate radicals generated through photolysis, thermolysis and e− transfer mechanisms, Applied Catalysis B: Environmental, 96 (2010) 290-298.

[109] E.G. Janzen, Y. Kotake, H. Randall D, Stabilities of hydroxyl radical spin adducts of PBN-type spin traps, Free Radical Biology and Medicine, 12 (1992) 169-173.

[110] T. Olmez-Hanci, I. Arslan-Alaton, Comparison of sulfate and hydroxyl radical based advanced oxidation of phenol, Chemical Engineering Journal, 224 (2013) 10-16.

[111] T.W. Chan, N.J.D. Graham, W. Chu, Degradation of iopromide by combined UV irradiation and peroxydisulfate, Journal of Hazardous Materials, 181 (2010) 508-513.

[112] M. Nie, Y. Yang, Z. Zhang, C. Yan, X. Wang, H. Li, W. Dong, Degradation of chloramphenicol by thermally activated persulfate in aqueous solution, Chemical Engineering Journal, 246 (2014) 373-382.

[113] K.-C. Huang, R.A. Couttenye, G.E. Hoag, Kinetics of heat-assisted persulfate oxidation of methyl tert-butyl ether (MTBE), Chemosphere, 49 (2002) 413-420.

[114] B. Neppolian, H. Jung, H. Choi, J.H. Lee, J.-W. Kang, Sonolytic degradation of methyl tert-butyl ether: the role of coupled fenton process and persulphate ion, Water Research, 36 (2002) 4699-4708.

[115] Q. Liu, Z. Zheng, X. Yang, X. Luo, J. Zhang, B. Zheng, Effect of factors on decolorization of azo dye methyl orange by oxone/natural sunlight in aqueous solution, Environ Sci Pollut Res, 19 (2011) 577-584.

[116] J. Criquet, N.K.V. Leitner, Degradation of acetic acid with sulfate radical generated by persulfate ions photolysis, Chemosphere, 77 (2009) 194-200.

[117] G.P. Anipsitakis, D.D. Dionysiou, Radical Generation by the Interaction of Transition Metals with Common Oxidants, Environmental Science & Technology, 38 (2004) 3705-3712.

[118] G.P. Anipsitakis, D.D. Dionysiou, M.A. Gonzalez, Cobalt-Mediated Activation of Peroxymonosulfate and Sulfate Radical Attack on Phenolic Compounds. Implications of Chloride Ions, Environmental Science & Technology, 40 (2005) 1000-1007.

[119] K.H. Chan, W. Chu, Degradation of atrazine by cobalt-mediated activation of peroxymonosulfate: Different cobalt counteranions in homogenous process and cobalt oxide catalysts in photolytic heterogeneous process, Water Research, 43 (2009) 2513-2521.

[120] C. Liang, C.J. Bruell, M.C. Marley, K.L. Sperry, Persulfate oxidation for in situ remediation of TCE. I. Activated by ferrous ion with and without a persulfate–thiosulfate redox couple, Chemosphere, 55 (2004) 1213-1223.

[121] Y.R. Wang, W. Chu, Degradation of a xanthene dye by Fe(II)-mediated activation of Oxone process, Journal of Hazardous Materials, 186 (2011) 1455-1461.

[122] X. Chen, J. Chen, X. Qiao, D. Wang, X. Cai, Performance of nano-Co3O4/peroxymonosulfate system: Kinetics and mechanism study using Acid Orange 7 as a model compound, Applied Catalysis B: Environmental, 80 (2008) 116-121.

[123] Q. Yang, H. Choi, S.R. Al-Abed, D.D. Dionysiou, Iron–cobalt mixed oxide nanocatalysts: Heterogeneous peroxymonosulfate activation, cobalt leaching, and ferromagnetic properties for environmental applications, Applied Catalysis B: Environmental, 88 (2009) 462-469.

[124] Y. Wang, H. Zhao, M. Li, J. Fan, G. Zhao, Magnetic ordered mesoporous copper ferrite as a heterogeneous Fenton catalyst for the degradation of imidacloprid, Applied Catalysis B: Environmental, 147 (2014) 534-545.

[125] Y.-H. Guan, J. Ma, Y.-M. Ren, Y.-L. Liu, J.-Y. Xiao, L.-q. Lin, C. Zhang, Efficient degradation of atrazine by magnetic porous copper ferrite catalyzed peroxymonosulfate oxidation via the formation of hydroxyl and sulfate radicals, Water Research, 47 (2013) 5431-5438.

[126] Y. Ding, L. Zhu, N. Wang, H. Tang, Sulfate radicals induced degradation of tetrabromobisphenol A with nanoscaled magnetic CuFe2O4 as a heterogeneous catalyst of peroxymonosulfate, Applied Catalysis B: Environmental, 129 (2013) 153-162.

[127] T. Zhang, H. Zhu, J.-P. Croué, Production of Sulfate Radical from Peroxymonosulfate Induced by a Magnetically Separable CuFe2O4 Spinel in Water: Efficiency, Stability, and Mechanism, Environmental Science & Technology, 47 (2013) 2784-2791.

[128] G.-D. Fang, D.D. Dionysiou, S.R. Al-Abed, D.-M. Zhou, Superoxide radical driving the activation of persulfate by magnetite nanoparticles: Implications for the degradation of PCBs, Applied Catalysis B: Environmental, 129 (2013) 325-332.

[129] F. Qi, W. Chu, B. Xu, Catalytic degradation of caffeine in aqueous solutions by cobalt-MCM41 activation of peroxymonosulfate, Applied Catalysis B: Environmental, 134–135 (2013) 324-332.

[130] F. Ji, C. Li, L. Deng, Performance of CuO/Oxone system: Heterogeneous catalytic oxidation of phenol at ambient conditions, Chemical Engineering Journal, 178 (2011) 239-243.

[131] A.L. Teel, M. Ahmad, R.J. Watts, Persulfate activation by naturally occurring trace minerals, Journal of Hazardous Materials, 196 (2011) 153-159.

[132] H. Liu, T.A. Bruton, F.M. Doyle, D.L. Sedlak, In Situ Chemical Oxidation of Contaminated Groundwater by Persulfate: Decomposition by Fe(III)- and Mn(IV)-Containing Oxides and Aquifer Materials, Environmental Science & Technology, 48 (2014) 10330-10336.

[133] M. Ahmad, A.L. Teel, R.J. Watts, Mechanism of Persulfate Activation by Phenols, Environmental Science & Technology, 47 (2013) 5864-5871.

[134] G. Fang, J. Gao, D.D. Dionysiou, C. Liu, D. Zhou, Activation of Persulfate by Quinones: Free Radical Reactions and Implication for the Degradation of PCBs, Environmental Science & Technology, 47 (2013) 4605-4611.

[135] D.L. Ball, J.O. Edwards, The Catalysis of the Decomposition of Caro's Acid, The Journal of Physical Chemistry, 62 (1958) 343-345.

[136] J. Zhang, J. Zhuang, L. Gao, Y. Zhang, N. Gu, J. Feng, D. Yang, J. Zhu, X. Yan, Decomposing phenol by the hidden talent of ferromagnetic nanoparticles, Chemosphere, 73 (2008) 1524-1528.

[137] X. Xue, K. Hanna, M. Abdelmoula, N. Deng, Adsorption and oxidation of PCP on the surface of magnetite: Kinetic experiments and spectroscopic investigations, Applied Catalysis B: Environmental, 89 (2009) 432-440.

[138] S. Zhang, X. Zhao, H. Niu, Y. Shi, Y. Cai, G. Jiang, Superparamagnetic Fe3O4 nanoparticles as catalysts for the catalytic oxidation of phenolic and aniline compounds, Journal of Hazardous Materials, 167 (2009) 560-566.

[139] S.-P. Sun, A.T. Lemley, p-Nitrophenol degradation by a heterogeneous Fenton-like reaction on nano-magnetite: Process optimization, kinetics, and degradation pathways, Journal of Molecular Catalysis A: Chemical, 349 (2011) 71-79.

[140] L. Xu, J. Wang, Fenton-like degradation of 2,4-dichlorophenol using Fe3O4 magnetic nanoparticles, Applied Catalysis B: Environmental, 123–124 (2012) 117-126.

[141] H. Yan, J. Zhang, C. You, Z. Song, B. Yu, Y. Shen, Influences of different synthesis conditions on properties of Fe3O4 nanoparticles, Materials Chemistry and Physics, 113 (2009) 46-52.

[142] S.-S. Lin, M.D. Gurol, Catalytic Decomposition of Hydrogen Peroxide on Iron Oxide: Kinetics, Mechanism, and Implications, Environmental Science & Technology, 32 (1998) 1417-1423.

[143] Y. Ren, L. Lin, J. Ma, J. Yang, J. Feng, Z. Fan, Sulfate radicals induced from peroxymonosulfate by magnetic ferrospinel MFe2O4 (M = Co, Cu, Mn, and Zn) as heterogeneous catalysts in the water, Applied Catalysis B: Environmental, 165 (2015) 572-578.

[144] S. Su, W. Guo, Y. Leng, C. Yi, Z. Ma, Heterogeneous activation of Oxone by CoxFe3−xO4 nanocatalysts for degradation of rhodamine B, Journal of Hazardous Materials, 244–245 (2013) 736-742.

[145] J. Yan, M. Lei, L. Zhu, M.N. Anjum, J. Zou, H. Tang, Degradation of sulfamonomethoxine with Fe3O4 magnetic nanoparticles as heterogeneous activator of persulfate, Journal of Hazardous Materials, 186 (2011) 1398-1404.

[146] C. Tan, N. Gao, Y. Deng, J. Deng, S. Zhou, J. Li, X. Xin, Radical induced degradation of acetaminophen with Fe3O4 magnetic nanoparticles as heterogeneous activator of peroxymonosulfate, Journal of Hazardous Materials, 276 (2014) 452-460.

[147] L. Zhang, Y. Wu, Sol-Gel Synthesized Magnetic Spinel Ferrite Nanoparticles as Novel Catalyst for Oxidative Degradation of Methyl Orange, Journal of Nanomaterials, 2013 (2013) 6.

[148] A.T. Stone, Reductive Dissolution of Manganese(III/Iv) Oxides by Substituted Phenols, Environmental Science & Technology, 21 (1987) 979-988.

[149] D.R. Kester, I.W. Duedall, D.N. Connors, R.M. Pytkowicz, PREPARATION OF ARTIFICIAL SEAWATER1, Limnology and Oceanography, 12 (1967) 176-179.

[150] I.M. Kolthoff, E.M. Carr, Volumetric Determination of Persulfate in Presence of Organic Substances, Analytical Chemistry, 25 (1953) 298-301.

[151] A. Rastogi, S.R. Al-Abed, D.D. Dionysiou, Sulfate radical-based ferrous–peroxymonosulfate oxidative system for PCBs degradation in aqueous and sediment systems, Applied Catalysis B: Environmental, 85 (2009) 171-179.

[152] R.M. Cornell, U. Schwertmann, Surface Chemistry and Colloidal Stability, in: The Iron Oxides, Wiley-VCH Verlag GmbH & Co. KGaA, 2004, pp. 221-252.

[153] Y.-H. Guan, J. Ma, X.-C. Li, J.-Y. Fang, L.-W. Chen, Influence of pH on the Formation of Sulfate and Hydroxyl Radicals in the UV/Peroxymonosulfate System, Environmental Science & Technology, 45 (2011) 9308-9314.

[154] C. Fan, A. Lu, Y. Li, C. Wang, Pretreatment of actual high-strength phenolic wastewater by manganese oxide method, Chemical Engineering Journal, 160 (2010) 20-26.

[155] L. Ukrainczyk, M.B. McBride, Oxidation of phenol in acidic aqueous suspensions of manganese oxides, Clays and Clay Minerals, 40 (1992) 157-166.

[156] T. Yamashita, P. Hayes, Analysis of XPS spectra of Fe2+ and Fe3+ ions in oxide materials, Applied Surface Science, 254 (2008) 2441-2449.

[157] T. Şimşek, S. Akansel, Ş. Özcan, A. Ceylan, Synthesis of MnFe2O4 nanocrystals by wet-milling under atmospheric conditions, Ceramics International, 40 (2014) 7953-7956.

[158] H.J. Ulrich, A.T. Stone, The oxidation of chlorophenols adsorbed to manganese oxide surfaces, Environmental Science & Technology, 23 (1989) 421-428.

[159] Y. Yao, Y. Cai, F. Lu, F. Wei, X. Wang, S. Wang, Magnetic recoverable MnFe2O4 and MnFe2O4-graphene hybrid as heterogeneous catalysts of peroxymonosulfate activation for efficient degradation of aqueous organic pollutants, Journal of Hazardous Materials, 270 (2014) 61-70.

[160] R.C.C. Costa, M.F.F. Lelis, L.C.A. Oliveira, J.D. Fabris, J.D. Ardisson, R.R.V.A. Rios, C.N. Silva, R.M. Lago, Novel active heterogeneous Fenton system based on Fe3−xMxO4 (Fe, Co, Mn, Ni): The role of M2+ species on the reactivity towards H2O2 reactions, Journal of Hazardous Materials, 129 (2006) 171-178.

[161] F. Jacobsen, J. Holcman, K. Sehested, Oxidation of manganese(II) by ozone and reduction of manganese(III) by hydrogen peroxide in acidic solution, International Journal of Chemical Kinetics, 30 (1998) 207-214.

[162] V. Kokkali, I. Katramados, J.D. Newman, Monitoring the Effect of Metal Ions on the Mobility of Artemia salina Nauplii, Biosensors, 1 (2011) 36.

[163] i.A.P. Krishnakumar P.K., Geetha Sasikumar, Bhat G.S., Toxicity Evaluation of Treated Refinery Effluent using brine Shrimp (Artemia salina) Egg and Larval Bioassay, Fishery Technology, 44 (2007) 85-92.

[164] O.O.O. Awolola G.V., Solanke A., Dosumu O.O., Shuiab A.O., Toxicity assessment of natural and chemical coagulants using brine shrimp (Artemia salina) bioassay, International Journal of Biological and Chemical Sciences, 4 (2010) 633-641.

[165] M.J. Costello, K. Fretwell, P. Read, Toxicity of sewage sludge to Crangon crangon and Artemia salina, with reference to other marine Crustacea, Aquat. Living Resour., 6 (1993) 351-356.

[166] J.C.C. da Silva, J.A.R. Teodoro, R.J.d.C.F. Afonso, S.F. Aquino, R. Augusti, Photolysis and photocatalysis of ibuprofen in aqueous medium: characterization of by-products via liquid chromatography coupled to high-resolution mass spectrometry and assessment of their toxicities against Artemia Salina, Journal of Mass Spectrometry, 49 (2014) 145-153.

[167] M.M. Milhem, A.S. Al-Hiyasat, H. Darmani, Toxicity Testing of Restorative Dental Materials Using Brine Shrimp Larvae (Artemia salina), Journal of Applied Oral Science, 16 (2008) 297-301.

[168] K. Liu, J. Lu, Y. Ji, Formation of brominated disinfection by-products and bromate in cobalt catalyzed peroxymonosulfate oxidation of phenol, Water Research, 84 (2015) 1-7.

[169] W.-D. Oh, Z. Dong, T.-T. Lim, Generation of sulfate radical through heterogeneous catalysis for organic contaminants removal: Current development, challenges and prospects, Applied Catalysis B: Environmental, 194 (2016) 169-201.